

TACTILE SPATIAL ACUITY FROM CHILDHOOD INTO
ADULTHOOD

TACTILE SPATIAL ACUITY FROM CHILDHOOD INTO
ADULTHOOD: AN EXPERIMENTAL, COMPUTATIONAL &
THEORETICAL EXPLORATION.

By RYAN MICHAEL PETERS Hon. B.A.

A Thesis Submitted to the School of Graduate Studies in Partial
Fulfillment of the Requirements for the Degree Doctor of
Philosophy

McMaster University © Copyright by Ryan M. Peters
July 2013

McMaster University
DOCTOR OF PHILOSOPHY (2013)
Hamilton, Ontario
(Psychology)

TITLE: Tactile spatial acuity from childhood into adulthood.

AUTHOR: Ryan M. Peters, Hon. B.A. (McMaster University)

SUPERVISOR: Dr. Daniel Goldreich

NUMBER OF PAGES: xii, 129

Abstract

Measurement of human tactile spatial acuity – the ability to perceive the fine spatial structure of surfaces contacting our fingertips – provides a valuable tool for probing both the peripheral and central nervous system. However, measures of tactile spatial acuity have long been plagued by a prodigious amount of variability present between individuals in their sense of touch. Previously proposed sources of variability include sex, and age; here we propose a novel source of variability – fingertip size. Building upon anatomical research, we hypothesize that mechanoreceptors are more sparsely distributed in larger fingers.

In this thesis, I provide empirical and theoretical support for the hypothesis that fingertip growth from childhood into adulthood sets up an apparent sex difference in human tactile spatial acuity during young adulthood (Chapter 2), and also predicts changes in acuity more strongly than does age over development (Chapter 3). To further understand how fingertip size could limit an individual's tactile spatial acuity, we develop an ideal observer model using neurophysiological data collected by other labs (Chapter 4).

In summary, this research provides support for a novel source of variability in the sense of touch: one that parsimoniously explains an apparent sex difference, and helps clarify the source of changes in tactile spatial acuity occurring with age during childhood.

Preface

This thesis is composed of five chapters. Chapter 1 introduces the reader to relevant background information, and places the empirical and theoretical work discussed later in the thesis within the context of the tactile research field. Chapters 2 and 3 are empirical studies; one is published in the *Journal of Neuroscience*¹ (Chapter 2), and the other is a recently submitted manuscript (Chapter 3). Chapter 2 is included in this thesis with permission from the *Journal of Neuroscience*. Chapter 4 presents computational modelling of the empirical results described in Chapters 2 and 3. Lastly, Chapter 5 reviews our findings and discusses the implications of this research.

This research was supported by a Natural Sciences and Engineering Research Council of Canada (NSERC) Discovery Grant awarded to Dr. Daniel Goldreich. This research was also supported through a graduate stipend (years 1 to 4) from the Department of Psychology, Neuroscience & Behaviour, and Ontario Graduate Scholarships (years 3 & 4).

¹ Peters, R.M., Hackeman, E., & Goldreich, D. (2009). Diminutive Digits Discern Delicate Details: Fingertip size and the Sex Difference in Tactile Spatial Acuity. *The Journal of Neuroscience*. 29(50): 15756-15761.

Declaration of Academic Achievement

Chapter 2.

My graduate advisor, Dr. Daniel Goldreich, and an undergraduate thesis student, Erik Hackeman, designed the experiment and collected the initial portion of the data. Upon joining the laboratory, I helped design the fingertip measurement protocols, collected the remainder of the data, and was involved in all aspects of preparing the manuscript (e.g., statistical analyses and writing).

Chapter 3.

I was involved in all aspects of the research: experimental design, programming, data collection, statistical analyses, and writing. Dr. Daniel Goldreich also contributed to the experimental design, programming, statistical analysis, and writing. I conducted all sensory testing, and collected a large portion of the fingertip measurements. Several undergraduate students in the lab, namely, Onkar Marway, Steven Botts, Danielle Allen, James Hu, Philip Staibano, Ashley Beaulieu, and Sophia Piro assisted with collection of the remaining fingertip measurements.

Chapter 4.

I was involved in all aspects of the modelling presented within this chapter: programming, numerical simulations, figures, statistical analysis, and writing. Dr. Daniel Goldreich contributed to the programming and helped edit the manuscript.

Acknowledgements

Above all, I would like to express the utmost gratitude towards my graduate supervisor, mentor, and friend, Dr. Daniel Goldreich. His guidance and wisdom has left an enduring impact on me as a person, and also on the way I communicate, conduct, and critically think about science. Dr. Goldreich saw my potential 6 years ago when he took me on as an undergraduate thesis student, and he continues to help me launch a successful career in science today. I would also like to sincerely thank the other two members of my supervisory committee, Dr. Deda Gillespie, and Dr. Paul Faure, whose thoughtful feedback and support has been instrumental to my professional development.

I would also like to thank my lab-mates in the Tactile Research Lab, Dr. Michael Wong, Andy Bhattacharjee, Luxi Li, and particularly Jonathan Tong, for their friendship and guidance during my time as a graduate student. Over the years, our office has hosted many of the most fascinating, hilarious, and meaningful discussions I have ever had. I wish you all the greatest success in your future endeavours, whichever paths you go down!

Finally, I would like to thank my parents Scott and Michelle, brother Josh, and sister Sarah, as well as other close family and friends for their continued love and support. This work is lovingly dedicated to my wife Stacey, whose encouragement and devotion has sustained me through the years.

Table of Contents

CHAPTER 1	1
<hr/>	
GENERAL INTRODUCTION	
1.1 Human tactile spatial acuity: a historical perspective	1
1.2 The two point limen – Ernst H. Weber	2
1.3 Non-human primate neurophysiology – Vernon B. Mountcastle	2
1.4 Human microneurography – Åke B. Vallbo & Rolland S. Johansson	4
1.5 The grating orientation task: replacement for the flawed two-point task – Kenneth O. Johnson, Robert W. VanBoven & John R. Phillips	5
1.6 Previously reported sources of variability between individuals	8
1.7 Fingertip size as a proxy for receptor density	10
1.8 Overview of studies	11
1.9 References	14
CHAPTER 2	21
<hr/>	
2.1 Preface	21
2.2 Abstract	22
2.3 Introduction	22
2.4 Methods	22
2.5 Results	23

2.6 Discussion	24
2.7 References	26
CHAPTER 3	28
3.1 Preface	28
3.2 Abstract	29
3.3 Introduction	30
3.4 Methods	32
3.5 Results	41
3.6 Discussion	44
3.7 References	51
3.8 Table and Figure Legends	56
3.9 Table and Figures	59
CHAPTER 4	64
4.1 Preface	64
4.2 Abstract	65
4.3 Introduction	66
4.4 Methods	69
4.5 Results	82
4.6 Discussion	88
4.7 References	95

4.8 Figure Legends	102
4.9 Figures	105
CHAPTER 5	109
<hr/>	
GENERAL DISCUSSION	
5.1 Summary of studies	109
5.2 The neural basis of human tactile spatial acuity	110
5.2.1 Peripheral factors limiting acuity	110
5.2.2 Central factors limiting acuity	113
5.3 Implications & Future Directions	117
5.4 Conclusion	119
5.5 References	120

List of Figures and Tables

CHAPTER 1

Figure 1. The grating orientation task	7
---	---

CHAPTER 2

Figure 1. Perceptual data and finger size	23
--	----

Figure 2. Multivariate Bayesian analysis	24
---	----

Figure 3. Finger surface microstructure	25
--	----

Figure 4. Proposed receptor anatomy and effect of finger size	25
--	----

CHAPTER 3

Table 1. Participants who qualified for the study (n = 100), by age and sex	59
--	----

Table 2. GBF criterion value sensitivity analysis for multiple regressions between different fingertip metrics together with age (independent variables) and log tactile thresholds (dependent variable)	59
---	----

Figure 1. Bayesian adaptive procedure for threshold groove width estimation	60
--	----

Figure 2. GBF disqualification analysis and comparison between psychophysical testing protocols	61
--	----

Figure 3. Fingertip growth from childhood into adulthood	62
---	----

Figure 4. Tactile spatial acuity as a function of the six fingertip metrics	62
--	----

Figure 5. Tactile spatial acuity from childhood into adulthood	63
---	----

CHAPTER 4

Figure 1. Stimulus encoding models	105
Figure 2. The effect of fingertip size on tactile spatial acuity, from childhood into young adulthood	106
Figure 3. Decoder One – Peripheral afferent responses	106
Figure 4. Decoder Two – Peripheral afferent responses	107
Figure 5. Decoder Three – Peripheral afferent responses	107
Figure 6. Decoder One – S1 responses	108

List of all Abbreviations and Symbols

ABBREVIATIONS

TAPS	Tactile Automated Passive-Finger Stimulator
2-IFC	Two-Interval (Two-Alternative) Forced-Choice
CNS	Central Nervous System
GOT	Grating Orientation Task
SA	Slowly-Adapting
RA	Rapidly-Adapting
S1	Primary Somatosensory Cortex
S2	Secondary Somatosensory Cortex
V1	Primary Visual Cortex
RF	Receptive Field
MI	Modulation Index
GW	Groove Width
PDF	Probability Distribution Function
GBF	Guessing Bayes Factor

SYMBOLS

Ψ	Psychometric Function
a	X-position of the Psychometric Function
b	Slope of the Psychometric Function
δ	Participant Lapse Rate
ρ	Density (# of neurons/mm ²)
ε	Strain Component (Continuum Mechanics Model)
λ	Wavelength of Sinusoidal Factor (Gabor Filter)
θ	Orientation (Gabor Filter)
φ	Phase Offset (Gabor Filter and Grating Stimulus)
σ	Standard Deviation of the Gaussian Envelope (Gabor Filter)
γ	Spatial Aspect Ratio (Gabor Filter)

Chapter 1

General introduction

1.1 Human tactile spatial acuity: a historical perspective

Dexterous manipulation of tools is at the heart of human civilization – the stone mason's trowel, the surgeon's blade, the violinist's bow. Our ability to resolve the spatial structure of objects we touch – our so-called tactile spatial acuity – is intimately linked with manual dexterity. This has been demonstrated physiologically by anaesthetizing mechanoreceptive afferents in the skin (Westling & Johansson, 1984), and psychophysically by the close correlation between tactile spatial acuity and manual dexterity within the same individuals (Tremblay et al., 2003; Bleyenheuft et al., 2010)¹. Because superior tactile acuity appears to bestow superior dexterity, it is vital that we understand the source(s) of variability in the sense of touch across the lifespan.

In what follows, I provide the reader with some historical perspective on the measurement of tactile spatial acuity, and introduce them to the key concepts necessary for understanding the research presented later in this thesis. To help guide the reader, I begin this introduction by chronologically reviewing the work of some of the foremost researchers in the tactile field.

¹Note that, although Bleyenheuft et al., (2010) reported there was no relationship between tactile spatial acuity and manual dexterity, we suggest that they did not use the most-appropriate statistical analysis. Upon re-analyzing their dataset (extracted using GraphClick v3.0) with a partial correlation between tactile thresholds and dexterity scores, controlling for age, we found that their data in fact show a strong relationship between tactile spatial acuity and manual dexterity ($\rho = -0.555$; $p < 10^{-7}$); thus, children with lower tactile thresholds also had higher manual dexterity scores.

1.2 The two point limen – Ernst H. Weber

The measurement of human tactile spatial acuity has benefited from nearly two centuries of experimental and clinical research. The earliest experimental work came from German physiologist Ernst Weber (1795 – 1878). In his book, *De Tactu* (1834; translated by Ross, 1978), Weber describes experiments where he measured the separation between two points of contact where they began feeling like just a single point (the *two point limen*), as well as the ability to perceive the orientation of two points with respect to the tested body part. Weber (1834) made several important observations about how tactile experiments should be conducted. He recommended that measurements be repeated and collected from many participants. He also cautioned experimenters to use care when applying tactile stimuli, ensuring that the two points are identical in material, shape, and temperature, and that the two points are applied to the skin simultaneously, with identical application force. While Weber's early guidelines for measuring tactile spatial acuity are still generally followed today, refinements have been made to the way tactile spatial acuity is measured.

1.3 Non-human primate neurophysiology – Vernon B. Mountcastle

Methodological improvements were brought about by advancement in our understanding of the neural basis of tactile spatial acuity, owing primarily to combined psychophysical and neurophysiological research conducted around the mid 20th century. Much of our understanding derives from the work of American neurophysiologist Vernon Mountcastle and colleagues working with non-human

primates. The innovative approach they took towards understanding the neural basis of tactile perception was to combine peripheral and cortical single-unit recordings in non-human primates, with perceptual performance measures from humans and awake-behaving non-human primates. Mountcastle and colleagues provided comprehensive evidence for distinct afferent sub-modalities, each maximally sensitive to a particular frequency bandwidth and other properties of tactile stimulation (Talbot et al., 1968; Mountcastle et al., 1972; LaMotte & Mountcastle, 1975). They also characterized the response of neurons in primary somatosensory cortex to 5-300 Hz vibrotactile stimulation (Mountcastle et al., 1969), as well as the reliance of vibrotactile perception on different cortical areas (LaMotte & Mountcastle, 1979).

Mountcastle is further credited with the discovery of the columnar organization of the neocortex, a breakthrough he made while recording extracellularly from the somatosensory cortices of cats (Mountcastle, 1957; Mountcastle et al., 1957; Mountcastle, 1997). David Hubel and Torsten Wiesel later elaborated upon Mountcastle's work in their Nobel prize winning description of ocular dominance, and the functional organization of cat primary visual cortex (Hubel & Wiesel 1959, Hubel & Wiesel, 1962). Hubel originally sought a post-doctoral fellowship with Vernon Mountcastle, but the timing was awkward due to the remodelling of Mountcastle's lab; somewhat fortuitously, Hubel then joined Wiesel in Steven Kuffler's lab and began investigating cat visual cortex (Hubel, 1981).

1.4 Human microneurography – Åke B. Vallbo & Roland S. Johansson

Around the same time as Mountcastle's early work, Swedish neurophysiologists Karl-Erik Hagbarth and Åke Vallbo developed a method for recording from human peripheral afferents: a technique called human microneurography (Hagbarth & Vallbo, 1967). In a series of pioneering experiments (Vallbo & Hagbarth, 1968; Knibestöl & Vallbo, 1970; Vallbo & Johansson, 1978; Johansson, 1978; Johansson & Vallbo, 1980; Johansson et al., 1980; Johansson & Vallbo, 1983; Vallbo & Johansson 1984), Vallbo and his student, Roland Johansson, recorded percutaneously (in awake humans) from the four different classes of afferents innervating the human hand, and provided the first, and still only empirically based estimates of their innervation densities (Johansson & Vallbo, 1979) – values to which I will return in Chapter 4. In a fascinating experiment, Vallbo et al., (1984) even performed micro-stimulation of peripheral afferents, which caused the illusory perception of a tactile stimulus delivered to the skin. With this technique, Vallbo et al., (1984) demonstrated that afferent receptive fields mapped by mechanical stimulation of the skin corresponded well to the perceived region of illusory tactile stimulation during micro-stimulation (the “projected field”), suggesting that human perception might have access to the information of individual afferents.

Given the emerging neurophysiological data, researchers knew which afferents were primarily involved in spatially discriminating statically indented points used in the classic two-point task, they knew that differences in application

force between the points would affect afferent response magnitudes, and they knew the approximate spacing of tactile afferents innervating the human hand. With these newfound insights into the neural basis of tactile perception, it became apparent that the traditional method of measuring tactile spatial acuity was flawed.

1.5 The grating orientation task: replacement for the flawed two-point task – Kenneth O. Johnson, Robert W. VanBoven & John R. Phillips

Though several variants of the task exist, many clinical and some experimental researchers measure tactile spatial acuity using the classic two-point task, where the participant discriminates whether the skin was contacted by one point, or two points of variable separation. Using the classic two-point task, researchers often find thresholds far below that which the underlying afferent spacing should allow; in fact, on the fingertip, two points can often be distinguished from one point, even when the two points have zero separation. Additionally, classic two-point threshold estimates from the same individual are highly variable across repeated testing blocks (Van Boven & Johnson 1994b; Craig & Johnson, 2000), impeding the assessment of an individual's true tactile spatial acuity.

A substantial improvement to the way tactile spatial acuity is measured was the introduction of a novel sensory task (Figure 1). The neural representation of square-wave gratings indented into the skin was thoroughly investigated in a series of papers in the early-80s (Johnson & Phillips, 1981; Phillips & Johnson 1981a; 1981b), and in the mid-90s, Van Boven and Johnson (1994a; 1994b),

provided empirical support for a new test of tactile spatial acuity: the grating orientation task. This task requires participants to discriminate the orientation of square-wave gratings indented into the skin; the spatial period of the gratings is decreased to increase task difficulty. The gratings are presented with their grooves aligned either parallel or perpendicular to the long axis of the tested body part (e.g., fingertip or lip), and the participant reports the perceived orientation.

Johnson, Van Boven, and Phillips – developers and namesakes of the commercially available “J.V.P. Domes” (Stoelting Co.) commonly used to administer the task today – showed that, not only did the grating orientation task correlate more closely than the classic two-point task with the re-innervation of skin following peripheral nerve injury (Van Boven & Johnson, 1994a), it also provided a less-variable estimate of tactile spatial acuity; threshold estimates using the grating orientation task were more consistent across testing blocks, and better-correlated with the underlying receptor density of the tested body part (Van Boven & Johnson, 1994b). Both of these studies, along with more recent research (Craig & Johnson, 2000; Tong et al., Submitted), suggest that the grating orientation task provides a more rigorous measure of tactile spatial acuity than the classic two-point task.

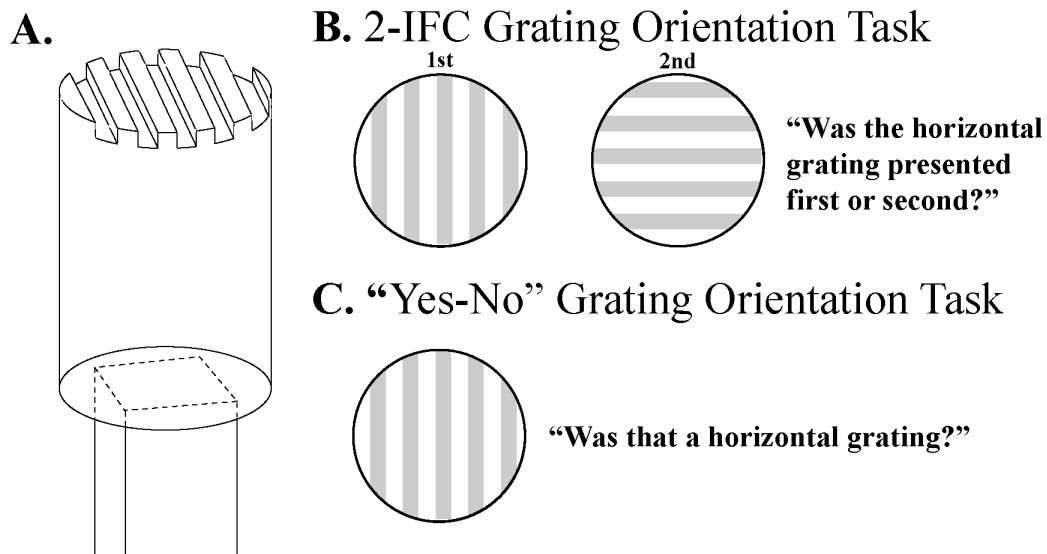


Figure 1. The grating orientation task. **A.** 3D schematic of a grating used in TAPS (Goldreich et al., 2009). **B.** Two-Interval Forced Choice (2-IFC) version, where participants indicate which interval contained the horizontal (or vertical) grating. **C.** “Yes-No” version, where participants indicate the grating orientation (single interval).

The grating orientation task also gets around another criticism of the classic two-point task: the *magnitude cue* (Vega-Bermudez & Johnson, 1999; Craig & Johnson, 2000; Tong et al., Submitted). The classic two-point task suffers from the existence of a non-spatial cue, resulting from the fact that two points directly apposed to one another feel qualitatively different than one point; in fact, due to skin mechanics, indenting two closely spaced points evokes fewer spikes in the peripheral afferent population than does indenting a single point at equal indentation (Vega-Bermudez & Johnson, 1999). Thus, rather than being forced to attend to the spatial conformation of the stimulus, participants can base their judgments on a difference in the *magnitude* of the evoked response (i.e., they can

perform the task just based on the total number of evoked spikes, rather than the spatial structure of the point stimuli). The grating orientation task avoids the *magnitude cue* by always having the participant discriminate gratings with equal groove width (and therefore, equal groove number), but orthogonal orientation; the participant is forced to attend to the spatial configuration of the gratings.

In this thesis, we use the gold-standard grating orientation task to investigate potential sources of variability in the human sense of touch. We took Weber's (1834) advice, both in conducting psychophysical testing on large sample sizes, and in using fully-automated testing equipment (Goldreich et al., 2009) to ensure that the stimuli were applied with precise control over stimulus velocity, duration, stability, and application force. We show, for the first time, that a major source of variability between individuals in their tactile spatial acuity is the size of one's fingertip, linking perception with physical differences in the organ of touch.

1.6 Previously reported sources of variability between individuals

Since its inception in the mid-90s, the grating orientation task has been used by a wide variety of researchers, investigating a wide variety of questions. From research into neurological disorders (Grant et al., 1999; 2005; Wingert et al., 2008), to the development of tactile spatial acuity in children, and its relation to manual dexterity (Tremblay et al., 2003; Bleyenheuft et al., 2006; 2010), to tactile perceptual learning (Sathian & Zangaladze, 1997; Wong et al., 2013), and the enhanced tactile acuity of blind individuals (Goldreich & Kanics, 2003; Wong et al., 2011) – the grating orientation task has proven very useful. One finding this

entire body of research agrees upon is that tactile spatial acuity varies between individuals, for reasons that are largely unknown.

One factor that has been reported to influence tactile spatial acuity is an individual's sex. Several studies report that tactile spatial acuity differs between the sexes, with women tending to outperform men on average (Van Boven et al., 2000; Goldreich & Kanics, 2003; Goldreich & Kanics, 2006). We found this difference between the sexes intriguing; although it is small, it is statistically significant, and using our automated equipment to administer the grating orientation task in two different studies, we found the sex difference to be identical in magnitude (Goldreich & Kanics, 2003; Peters et al., 2009 – effect size = 0.18 mm).

By far the most apparent, and commonly-reported source of variability is a decline in tactile spatial acuity during healthy aging (Van Boven et al., 2000; Goldreich & Kanics, 2003; Tremblay et al., 2003; Goldreich & Kanics, 2006), which has been attributed to the gradual loss of tactile receptors across the lifespan (Bruce, 1980). Although the effect of age is quite clear later in life, relatively few studies have investigated the effect of age in developing children, and there is a disagreement between the only two studies that have. Using the grating orientation task Bleyenheuft et al. (2006; 2010) found that there was an improvement in tactile spatial acuity, until roughly the age of 10, when performance saturated to young adult levels. With a less-commonly used test of tactile spatial acuity (the “gap detection task”, where the participant discriminates

between the presence or absence of a gap of variable width in an edge that is indented into the fingertip), Stevens and Choo (1996) showed evidence to the contrary: young children outperformed adults.

1.7 Fingertip size as a proxy for receptor density

As mentioned above, a small but consistent sex difference in tactile spatial acuity had been reported previously (Van Boven et al., 2000; Goldreich & Kanics, 2003; Goldreich & Kanics, 2006), with females having finer resolution for spatial details pressed against their skin; this sex difference received little attention in the literature, and its cause was previously unknown. We reasoned that a sex difference in tactile spatial acuity could be of central origin, peripheral origin, or possibly a combination of both, and we set out to determine the source.

We decided to explore the possibility that what appeared to be a sex difference to previous researchers, was due in fact to a simple physical difference in the touch-organs of the different sexes: their physical size. Anatomical studies suggest that receptor number is conserved across individuals, and that those with smaller fingers have denser receptor arrays at their fingertips (Bolton et al., 1966; Dillon et al., 2001; Nolano et al., 2003). We reasoned that women, who have smaller fingers on average due to human sexual dimorphism, might have greater receptor density on average, and thus, finer tactile acuity. Intuitively, a measure of spatial acuity should be limited by sensory receptor density – just as greater numbers of pixels per inch provides a clearer visual display, the tactile *neural image* supplied to the CNS by the afferent population response should become

clearer if receptor density is higher. As alluring as sex differences are in popular psychology, in Chapter 2, we provide evidence that the sex difference in tactile spatial acuity is fully accounted for by an effect of fingertip size. Men with small fingertips have the acuity of women with large fingertips – there is nothing special about people's sex *per se* in determining their tactile spatial acuity.

With respect to the effect of age during development, neither of the previous studies investigating this question (Stevens & Choo, 1996; Bleyenheuft et al., 2006; 2010) took into account a variable that is concomitantly changing with age, namely, fingertip size, which we had shown significantly predicts tactile spatial acuity in young adults (Chapter 2). Due to the disagreement in the literature regarding the effect of age during childhood, and a relative dearth of research on the topic in general, we decided re-investigate development of tactile spatial acuity from childhood into adulthood (Chapter 3). We show that fingertip size is better than age at predicting changes in acuity over development.

1.8 Overview of studies

We set out to explore a potential link between tactile spatial acuity (perception), and physical differences in the peripheral somatosensory apparatus. The research presented in this thesis provides support for fingertip size as a novel source of variation in the tactile perception of different individuals.

In the first study (Chapter 2), we used the grating orientation task to test the fingertip size hypothesis in a large sample ($n = 100$) of undergraduate students. In addition to measuring each individual's tactile spatial acuity on the

dominant index fingertip, we also optically imaged the fingertip, and digitally measured its surface area. Our results demonstrate that fingertip surface area significantly predicts tactile spatial acuity, and when included in statistical analyses, completely and parsimoniously accounts for the sex difference that had previously been reported in the literature (Van Boven et al., 2000; Goldreich & Kanics, 2003; Goldreich & Kanics, 2006).

In the second study (Chapter 3), we again used the grating orientation task; however, this time we investigated the development of tactile spatial acuity from childhood into adulthood ($n = 116$). Following our previous work, we coupled tactile threshold estimates with measurements of physical properties of each child's fingertip. Our results demonstrate that fingertip size predicted better than age the development of tactile spatial acuity from childhood into adulthood, a novel finding, and one that clarifies the previously debated effect of age on tactile spatial acuity in childhood.

In a companion modelling project (Chapter 4), we used a Bayesian ideal observer model to investigate the effect of fingertip size on a theoretical basis. The model has two major components: a stimulus *encoding* component, which simulates the population response of peripheral or cortical neurons, and a stimulus *decoding* component, which uses probability theory to infer grating orientation from stimulus-epoch spike counts, and optimally performs the grating orientation task. Results of this modelling demonstrate that the fingertip surface area effect we observed empirically in children and young adults (Peters et al., 2009; Peters

& Goldreich, Submitted) emerges from the model only when certain sub-optimal assumptions are made by the ideal observer. We further speculate on the plausibility of such assumptions in real-world human perception.

Taken together, the results of this research favour the hypothesis that fingertip size – which likely reflects an individual's underlying receptor density – provides a physical limit on tactile spatial acuity in humans.

1.9 References

- Bleyenheuft Y, Cols C, Arnould C, & Thonnard JL (2006). Age-related changes in tactile spatial resolution from 6 to 16 years old. *Somatosensory and Motor Research*. 23: 83–87.
- Bleyenheuft Y, Wilmotte P & Thonnard JL (2010). Relationship between tactile spatial resolution and digital dexterity during childhood. *Somatosensory and Motor Research*. 27: 9–14.
- Bolton CF, Winkelmann RK & Dyck PJ (1966). A quantitative study of Meissner's corpuscles in man. *Neurology*. 16: 1–9.
- Bruce MF, (1980). The relation of tactile thresholds to histology in the fingers of elderly people. *Journal of Neurology, Neurosurgery, and Psychiatry*. 43: 730–734.
- Craig JC & Johnson KO (2000). The two-point threshold: not a measure of tactile spatial resolution. *Current Directions in Psychological Science*. 9: 29–32.
- Dillon YK, Haynes J & Henneberg M (2001). The relationship of the number of Meissner's corpuscles to dermatoglyphic characters and finger size. *Journal of Anatomy*. 199: 577–584.
- Goldreich D & Kanics IM (2003). Tactile acuity is enhanced in blindness. *The Journal of Neuroscience*. 23: 3439–3445.
- Goldreich D & Kanics IM (2006). Performance of blind and sighted humans on a tactile grating detection task. *Perception and Psychophysics*. 68: 1363–

1371.

- Goldreich D, Wong M, Peters RM & Kanics IM (2009). A tactile automated passive-finger Stimulator (TAPS). *Journal of Visualized Experiments*. 28: doi: 10.3791/1374.
- Grant AC, Zangaladze A, Thiagarajah MC & Sathian K (1999). Tactile perception in developmental dyslexia: a psychophysical study using gratings. *Neuropsychologia*. 37: 1201–1211.
- Grant AC, Henry TR, Fernandez R, Hill MA & Sathian K (2005). Somatosensory processing is impaired in temporal lobe epilepsy. *Epilepsia*. 46: 534–539.
- Hagbarth KE & Vallbo ÅB (1967). Mechanoreceptor activity recorded percutaneously with semi-microelectrodes in human peripheral nerves. *Acta Physiologica Scandinavica*. 69: 121–122.
- Hubel DH & Wiesel TN (1959). Receptive fields of single neurones in the cat's striate cortex. *Journal of Physiology*. 148: 574–591.
- Hubel DH & Wiesel TN (1962). Receptive fields, binocular interaction and functional architecture in the cat's visual cortex. *Journal of Physiology*. 160: 106–154.
- Hubel DH (1981). Evolution of ideas on the primary visual cortex, 1955-1978: a biased historical account. *Nobel lecture, December 8, 1981*.
- Johansson RS (1978). Tactile sensibility in the human hand: receptive field characteristics of mechanoreceptive units in the glabrous skin area. *Journal of Physiology*. 281: 101–123.

- Johansson RS & Vallbo ÅB (1979). Tactile sensibility in the human hand: relative and absolute densities of the four types of mechanoreceptive units in glabrous skin. *Journal of Physiology*. 286: 283–300.
- Johansson RS, Vallbo ÅB & Westling G (1980). Thresholds of mechanosensitive afferents in the human hand as measured with Von Frey hairs. *Brain Research*. 184: 343–351.
- Johansson RS & Vallbo ÅB (1980). Spatial properties of the population of mechanoreceptive units in the glabrous skin of the human hand. *Brain Research*. 184: 353–366.
- Johansson RS, Vallbo ÅB (1983). Tactile sensory coding in the glabrous skin of the human hand. *Trends in Neuroscience*. 6: 27–32.
- Knibestöl M & Vallbo ÅB (1970). Single unit analysis of mechanoreceptor activity from the human glabrous skin. *Acta Physiologica Scandinavica*. 80: 178–195.
- LaMotte RH & Mountcastle VB (1975). Capacities of human and monkeys to discriminate vibratory stimuli of different frequency and amplitude: a correlation between neural events and psychological measurements. *Journal of Neurophysiology*. 38: 539–559.
- LaMotte RH & Mountcastle VB (1979). Disorders in somesthesia following lesions of parietal lobe. *Journal of Neurophysiology*. 42: 400–419.
- Mountcastle VB, Davies PW & Berman AL (1957). Response properties of neurons of cat's somatic sensory cortex to peripheral stimuli. *Journal of*

Neurophysiology. 20: 374–407.

Mountcastle VB (1957). Modality and topographic properties of single neurons of cat's somatic sensory cortex. *Journal of Neurophysiology*. 20: 408–434.

Mountcastle VB, Talbot WH, Sakata H & Hyvärinen J (1969). Cortical neuronal mechanisms in flutter-vibration studied in unanesthetized monkeys: neuronal periodicity and frequency discrimination. *Journal of Neurophysiology*. 32: 452–484.

Mountcastle VB, LaMotte RH & Carli G (1972). Detection thresholds for stimuli in humans and monkeys: comparison with threshold events in mechanoreceptive afferent nerve fibers innervating the monkey hand. *Journal of Neurophysiology*. 35: 122–136.

Mountcastle VB (1997). The columnar organization of the neocortex. *Brain*. 120: 701–722.

Nolano M, Provitera V, Crisci C, Stancanelli A, Wendelschafer-Crabb G, Kennedy WR & Santoro L (2003). Quantification of myelinated endings and mechanoreceptors in human digital skin. *Annals of Neurology*. 54: 197–205.

Peters RM & Goldreich D (Submitted). The development of tactile spatial acuity from childhood into adulthood.

Peters RM, Hackman E & Goldreich D (2009). Diminutive digits discern delicate details: fingertip size and the sex difference in tactile spatial acuity. *The Journal of Neuroscience*. 29: 15756–15761.

- Johnson KO & Phillips JR (1981). Tactile spatial resolution. I. Two-point discrimination, gap detection, grating resolution, and letter recognition. *Journal of Neurophysiology*. 46: 1177–1191.
- Phillips JR & Johnson KO (1981a). Tactile spatial resolution. II. Neural representation of bars, edges, and gratings in monkey primary afferents. *Journal of Neurophysiology*. 46: 1192–1203.
- Phillips JR & Johnson KO (1981b). Tactile spatial resolution. III. A continuum mechanics model of skin predicting mechanoreceptor responses to bars, edges, and gratings. *Journal of Neurophysiology*. 46: 1204–1225.
- Ross HE (1978). Weber, De tactu. In: “The sense of touch”. *Academic Press for Experimental Psychology Society, London*.
- Sathian K & Zangaladze A (1997). Tactile learning is task specific but transfers between fingers. *Perception & Psychophysics*. 59: 119–128.
- Stevens JC & Choo KK (1996). Spatial acuity of the body surface over the life span. *Somatosensory and Motor Research*. 13: 153–166.
- Talbot WH, Darian-Smith I, Kornhuber HH & Mountcastle VB (1968). The sense of flutter-vibration: comparison of the human capacity with response patterns of mechanoreceptive afferents from the monkey hand. *Journal of Neurophysiology*. 31: 301–334.
- Tong J, Mao O, & Goldreich D (Submitted). Two-point orientation discrimination: a valid measure of tactile spatial acuity to replace the flawed

two-point limen.

- Tremblay F, Wong K, Sanderson R & Coté L (2003). Tactile spatial acuity in elderly persons: assessment with grating domes and relationship to manual dexterity. *Somatosensory & Motor Research*. 20: 127–132.
- Vallbo ÅB & Hagbarth KE (1968). Activity from skin mechanoreceptors recorded percutaneously in awake human subjects. *Experimental Neurology*. 21: 270–289.
- Vallbo ÅB & Johansson RS (1978). The tactile sensory innervation of the glabrous skin of the human hand. In: “Active touch, the mechanism of recognition of objects by manipulation”, edited by Gordon G, *Pergamon Press Ltd.* (Oxford). 29–54.
- Vallbo ÅB & Johansson RS (1984). Properties of cutaneous mechanoreceptors in the human hand related to touch sensation. *Human Neurobiology*. 3: 3–14.
- Vallbo ÅB, Olsson KÅ, Westberg KG & Clark FJ (1984). Microstimulation of single tactile afferents from the human hand: sensory attributes related to unit type and properties of receptive fields. *Brain*. 107: 727–749.
- Van Boven RW, Hamilton RH, Kauffman T, Keenan JP & Pascual-Leone A (2000). Tactile spatial resolution in blind Braille readers. *Neurology*. 45: 2230–2236.
- Van Boven RW & Johnson KO (1994a). A psychophysical study of the mechanisms of sensory recovery following nerve injury in humans. *Brain*. 117: 149–167.

- Van Boven RW & Johnson KO (1994b). The limit of tactile spatial resolution in humans: grating orientation discrimination at the lip, tongue, and finger. *Neurology*. 44: 2361–2366
- Vega-Bermudez F, Johnson KO (1999). Surround suppression in the responses of primate SA1 and RA mechanoreceptive afferents mapped with a probe array. *Journal of Neurophysiology*. 81: 2711–2719.
- Weber, E. H. (1834). De tactu. *Koehler, Leipzig*.
- Westling G & Johansson RS (1984). Factors influencing the force control during precision grip. *Experimental Brain Research*. 53: 277–284.
- Wingert JR, Burton H, Sinclair RJ, Brunstrom JE & Damiano DL (2008). Tactile sensory abilities in cerebral palsy: deficits in roughness and object discrimination. *Developmental Medical Child Neurology*. 50: 832–838.
- Wong M, Gnanakumaran V & Goldreich D (2011). Tactile spatial acuity enhancement in blindness: evidence for experience-dependent mechanisms. *The Journal of Neuroscience*. 31: 7028–7037.
- Wong M, Peters RM, Goldreich D (2013). A physical constraint on perceptual learning: Tactile spatial acuity improves with training to a limit set by finger size. *The Journal of Neuroscience*. 33: 9345–9352.

Chapter 2

2.1 Preface

In this study, we wished to elucidate the source of a sex difference in tactile spatial acuity that we and others had found previously. Using the grating orientation task, we measured the tactile acuity of 100 undergraduate participants, and coupled this with surface area measurements of each participant's dominant index fingertip.

Our results strongly favoured the hypothesis that fingertip size predicts tactile spatial acuity and fully accounts for the sex difference in tactile spatial acuity. In light of anatomical research, we suggest that fingertip size sets a person's afferent innervation density, and thus, the ability to perceive fine spatial details. This result provides a novel and parsimonious explanation for a significant proportion of variability between individuals in their sense of touch.

Brief Communications

Diminutive Digits Discern Delicate Details: Fingertip Size and the Sex Difference in Tactile Spatial Acuity

Ryan M. Peters,¹ Erik Hackeman,² and Daniel Goldreich^{1,2}

¹Department of Psychology, Neuroscience & Behaviour, McMaster University, Hamilton, Ontario L8S 4K1, Canada, and ²Department of Occupational Therapy, Duquesne University, Pittsburgh, Pennsylvania 15282

We have observed that passive tactile spatial acuity, the ability to resolve the spatial structure of surfaces pressed upon the skin, differs subtly but consistently between the sexes, with women able to perceive finer surface detail than men. Eschewing complex central explanations, we hypothesized that this sex difference in somatosensory perception might result from simple physical differences between the fingers of women and men. To investigate, we tested 50 women and 50 men on a tactile grating orientation task and measured the surface area of the participants' index fingertips. In subsets of participants, we additionally measured finger skin compliance and optically imaged the fingerprint microstructure to count sweat pores. We show here that tactile perception improves with decreasing finger size, and that this correlation fully explains the better perception of women, who on average have smaller fingers than men. Indeed, when sex and finger size are both considered in statistical analyses, only finger size predicts tactile acuity. Thus, a man and a woman with fingers of equal size will, on average, enjoy equal tactile acuity. We further show that sweat pores, and presumably the Merkel receptors beneath them, are packed more densely in smaller fingers.

Introduction

The ability to resolve patterned surfaces pressed upon the stationary fingertip differs between the sexes, according to recent studies, with women able to perceive finer surface detail than men (Van Boven et al., 2000; Goldreich and Kanics, 2003, 2006). For instance, Goldreich and Kanics (2003) tested 43 blind and 47 sighted participants on a tactile grating orientation task. The blind participants significantly outperformed their sighted peers, and within both the blind and sighted groups, women significantly outperformed men. A recently concluded grating orientation study with a new group of 28 blind and 57 sighted participants has again shown this result (M. Wong, V. Gnanakumaran, D. Goldreich, unpublished observations).

Why do women outperform men on tests of tactile spatial acuity? Eschewing more complex explanations, we hypothesized that the superior tactile perception of women might result from physical differences between the fingers of women and men. We considered two hypotheses: (1) If women's fingers are more compliant than those of men (Woodward, 1993), a force-controlled stimulus would indent more deeply into women's fingers, perhaps resulting in superior perception, and (2) as women's fingers are smaller than men's (Dillon et al., 2001), Merkel receptor den-

sity might be higher in women's fingers, again resulting in superior perception.

The following reasoning led us to the second hypothesis: Merkel cells, activated by static skin displacement, are thought to mediate tactile spatial perception (Iggo and Muir, 1969; Ogawa, 1996; Johnson, 2001). These receptors are difficult to visualize anatomically (Boulais and Misery, 2007), and their density with respect to finger size is unknown. However, Meissner corpuscles, activated by low-frequency skin vibration and easily visualized anatomically, are more densely distributed in smaller fingers (Bolton et al., 1966; Dillon et al., 2001; Nolano et al., 2003). Indeed, homologous fingers in different individuals probably have the same number of Meissner corpuscles (Bolton et al., 1966; Dillon et al., 2001). If Merkel cells, like Meissner corpuscles, are more densely packed in smaller fingers, then presumably the fingers of women would be endowed with greater spatial resolving power than those of men.

Here we show that tactile perception indeed correlates with finger size, and that this effect fully explains the superior tactile spatial acuity of women compared to men.

Materials and Methods

Participants. One hundred undergraduate participants (50 women, 50 men; 18–27 years old), were recruited from Duquesne University ($n = 48$) and McMaster University ($n = 52$). The study protocol was approved by the review boards of both universities. Entrance criteria ensured that participants had no index finger cuts, scars, or calluses, and that they were (by self-report) free from nervous system disorders, dyslexia, and diabetes. Two participants (one male, one female) were unable to complete the majority of testing blocks, so their data were omitted from analysis. The finger scan from a third participant (female) was inadvertently overwritten. Thus, the analyses reported here derive from 97 participants (Duquesne: 23 women, 23 men; McMaster: 25 women, 26 men). The age

Received July 29, 2009; revised Sept. 17, 2009; accepted Oct. 22, 2009.

This research was supported by grants to D.G. from the National Eye Institute (US) and the Natural Sciences and Engineering Research Council (Canada). We thank Caitlin Hurd and John McIntyre for the finger area and sweat pore measurements, and Raagula Sivayoganathan for help with experiments. We thank Deda Gillespie for assistance with equipment design and construction, and for many fruitful conversations. We thank www.mystring.com for permission to use the hand drawing in Figure 1a.

Correspondence should be addressed to Daniel Goldreich, Department of Psychology, Neuroscience & Behaviour, McMaster University, Hamilton, ON L8S 4K1, Canada. E-mail: goldrd@mcmaster.ca.

DOI:10.1523/JNEUROSCI.3684-09.2009

Copyright © 2009 Society for Neuroscience 0270-6474/09/2915756-06\$15.00/0

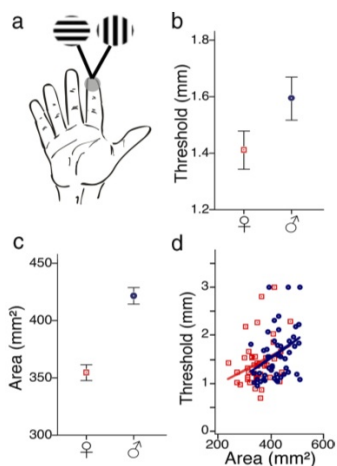


Figure 1. Perceptual data and finger size. *a*, Two-interval forced-choice GOT. An adaptive procedure estimated the width of grooves whose orientation the participant could distinguish with 76% probability (GOT threshold). Hand drawing retrieved from www.mytring.com with permission. *b*, GOT thresholds by sex (means \pm 1 SE). Lower thresholds correspond to better acuity. *c*, Index finger distal phalanx surface area by sex (means \pm 1 SE). *d*, Scatterplot of threshold versus distal phalanx surface area, with female (red) and male (blue) regression lines. Women: red \square ; men: blue \circ .

distributions of these women (mean 20.5 years, SD 1.5 years) and men (mean 20.4 years, SD 1.2 years) were well matched. The young-adult age range of the participants protected the tactile acuity data against variance caused by the detrimental effects of aging (Stevens and Choo, 1996; Goldreich and Kanics, 2003, 2006).

Sensory testing. We used a two-interval forced-choice (2-IFC) grating orientation task (GOT) to assess passive (finger stationary) tactile spatial acuity. The GOT has several advantages over the two-point (calipers) test as a measure of spatial acuity (Johnson and Phillips, 1981; Craig and Johnson, 2000). The testing apparatus and procedure are described in detail in Goldreich et al. (2009). Briefly, grooved surfaces (20 square-wave gratings with groove widths ranging from 0.25 to 3.10 mm, in 0.15 mm increments) rose under computer control to contact the distal pad of the dominant index finger (4 cm/s onset velocity, 1 s duration, 50 g force). In each trial, the finger was contacted twice, with surfaces of identical groove width but orthogonal orientations (perpendicular or parallel to the long axis of the finger, with the order of presentation chosen randomly) (Fig. 1*a*). The participant indicated whether the perpendicular orientation occurred in the first or second interval. Threshold was defined as the width of the grooves whose orientation the participant could discern with 76% probability, corresponding to d -prime = 1 on this 2-IFC task (Gescheider, 1997).

To assess threshold efficiently, we used adaptive procedures, selecting the groove width on each trial according to the participants' previous responses. In the Duquesne experiments, we used a two-down one-up staircase, with 14 reversals per testing block, as described by Goldreich and Kanics (2003). The Duquesne data consisted of two testing blocks per participant, taken from a larger experiment of eight blocks (the two blocks were collected in a lit room with the participant's eyes open, corresponding to the McMaster testing condition; the other blocks, not relevant to the current study, tested different lighting conditions). In the McMaster experiments, we used an adaptive Bayesian procedure, modified from Kontsevich and Tyler (1999) (see supplemental Material, available at www.jneurosci.org). The McMaster data consisted of eight

testing blocks of 40 trials each. Although the Duquesne data were collected by staircase, they were subsequently analyzed with the Bayesian method, so that both data sets yielded the same (76% correct) threshold measure.

Finger measurements. We determined hand dominance by survey (modified from Oldfield, 1971), then scanned the distal index finger of the dominant hand at 300 dpi (Epson Perfection 1260 scanner, Epson Electronics America) for subsequent finger measurements (NIH image 1.63 and ImageJ 1.40; NIH, Bethesda, MD). All finger area and sweat pore measurements were made independently by two observers (not authors) who were blind to the participants' sex and tactile thresholds.

To measure fingertip surface area, we traced the image of each finger from the distal interphalangeal crease to the end of the finger (we refer to this entire distal phalanx area as the "fingertip"). In case of multiple distal interphalangeal creases, we traced the most prominent crease; when two creases were equally prominent, we drew a line parallel to the two creases and equidistant from them (see Fig. 3*a*). Fingertip surface area was measured for every participant. To measure sweat pore density, we recalled 15 participants from the McMaster pool, spanning the ranges of fingertip sizes observed in the study, and coated each participant's distal index finger pad with water-soluble finger paint (Crayola), which settles into the pores, then scanned at high resolution (2400 dpi). Because the spacing between sweat pores within a fingerprint ridge differed from the spacing between pores on adjacent ridges, we separately measured 20 within-ridge and 20 between-ridge pore pair distances per participant, and derived pore density (pores/mm²) from the participant's average within-ridge (w) and between-ridge (b) pore-to-pore spacing (mm): density = $1/(wb)$.

We assessed interobserver reliability in two ways: (1) by Pearson's r , and (2) by calculating, for each participant, the absolute value of the observer 1–observer 2 difference score, divided by the mean of the observer 1 and observer 2 scores. Interobserver agreement was excellent: $r = 0.997$, two-tailed $p < 0.001$ (finger area), $r = 0.882$, two-tailed $p < 0.001$ (sweat pore spacing); average difference score measure = 1% (finger area) and 6% (sweat pore spacing). For each participant, we averaged the two observers' measurements for subsequent analysis.

At Duquesne University, we measured skin compliance as the skin indentation depth produced by a 0.5-inch-diameter surface at 50 g contact force (the same stimulus area and force used in our grating orientation task). We built a laser-based measurement system for this purpose (supplemental Fig. 1, available at www.jneurosci.org as supplemental material). Skin compliance measurements taken on the Duquesne participants showed no significant difference between men and women, nor correlated with GOT threshold. In contrast, fingertip area measurements taken on the same participants did differ significantly by sex and correlate with GOT threshold. Therefore, in our subsequent (McMaster University) experiments, we measured fingertip area only.

Statistical analysis. We performed conventional statistical tests (t tests, correlations, ANCOVA, regression) with SPSS 16, using a significance criterion of 0.05. We report one-tailed p values for all tests, as each of our alternative hypotheses predicted a specific effect direction. We programmed Bayesian analysis (Sivia and Skilling, 2006) in LabVIEW 7.0 (National Instruments). The Bayes factor, B_{12} , comparing models M_1 and M_2 , is a likelihood ratio: $B_{12} = P(D | M_1) / P(D | M_2)$, where $P(D | M)$ is the probability of the data, D , given model M (Kass and Raftery, 1995; Goodman, 1999). For example, a Bayes factor of 10 means that Model 1 predicted the data with 10 times the probability of Model 2. See supplemental Material, available at www.jneurosci.org, for details of the Bayesian method.

Results

We used an automated system (Goldreich et al., 2009) to assess the passive tactile spatial acuity of women and men on a grating orientation task (Fig. 1*a*). The results confirmed the sex difference in tactile acuity (Fig. 1*b*; unpaired $t = 1.79$, $p = 0.038$). In fact, the mean performance difference between the sexes, 0.18 mm, was identical to that reported previously (Goldreich and

Kanics, 2003). We next investigated the cause of this tactile sex difference.

According to Hypothesis 1, women outperform men because women have more compliant fingers. The data refuted this hypothesis, as we found that skin compliance was neither greater in women (unpaired t test, $p = 0.9$) nor predicted tactile acuity (GOT threshold vs compliance correlation, $p = 0.8$). In fact, the data showed a (nonsignificant) trend of greater compliance in male than in female fingers, opposite the direction predicted by Hypothesis 1 (supplemental Fig. 2, available at www.jneurosci.org as supplemental material).

According to Hypothesis 2, women outperform men because women have smaller fingers. As expected, women's fingers were significantly smaller than men's (Fig. 1c) (unpaired $t = 6.72$, $p < 0.001$). To investigate whether this accounted for the better acuity of the women, we performed a sex-by-fingertip-area ANCOVA on the acuity data. Strikingly, and as predicted by Hypothesis 2, this analysis revealed a highly significant main effect of fingertip area ($F_{(1,94)} = 11.7$, $p < 0.001$) but no effect of sex ($F_{(1,94)} = 0.148$, $p = 0.65$). Thus, when finger size was considered, the apparent sex effect on acuity vanished. Indeed, tactile thresholds correlated with finger area not only across the entire participant sample (Pearson's $r = 0.37$, $p < 0.001$) but also within both the male ($r = 0.36$, $p = 0.005$) and female ($r = 0.30$, $p = 0.021$) groups (Fig. 1d). These results strongly support Hypothesis 2: tactile spatial acuity is determined not by sex per se but by finger size.

We independently verified this conclusion by using robust Bayesian analysis to compare four competing models that represented different assumptions about the source(s) of variance in the participants' data (Fig. 2). A null model interpreted participants' thresholds as random samples drawn from a single Gaussian population distribution; a sex model specified separate male and female distributions; a size model interpreted thresholds as a linear function of fingertip area; and a size-and-sex model specified offset male and female functions of fingertip area. The size model emerged the clear winner (size model likelihood: 171, 76, and 6.5 relative to null, sex, and size-and-sex models), supporting the conclusion that finger size, not sex, determines tactile spatial acuity. This model revealed that tactile thresholds increase at a rate of 0.25 mm per cm^2 fingertip surface area (95% confidence interval: 0.11–0.40 mm/cm^2).

The finding that smaller fingers have better acuity suggests an inverse relationship between finger size and the density of Merkel cells, the putative mechanotransducers for statically impressed stimuli (Iggo and Muir, 1969; Ogawa, 1996; Johnson, 2001). Given that Merkel cells cluster around the bases of sweat pores in the deep epidermis (Yamada et al., 1996), we reasoned that sweat pore density would provide a measurable correlate of Merkel cluster density. High-resolution scans revealed that sweat pore density is indeed greater in smaller fingers (Fig. 3) (sweat pore density vs fingertip area, Pearson's $r = -0.50$, $p = 0.028$, $n = 15$), suggesting that Merkel cells pack more densely in smaller fingers.

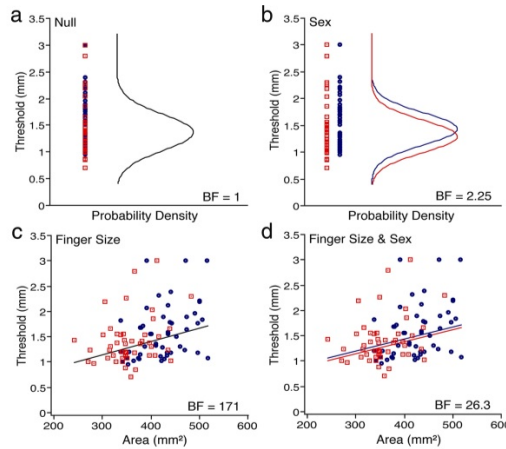


Figure 2. Multivariate Bayesian analysis. Scatterplots and best-fit curves are shown for four models. The data points (participants' GOT thresholds) are identical in the four plots; the models differ in how they consider the data to have been generated. *a*, Null model: the data derive from a single Gaussian population distribution. *b*, Sex model: female and male data (left–right offset for clarity) originate from separate (red and blue) Gaussian populations. *c*, Finger size model: the data derive from a linear trend on fingertip area. *d*, Finger-size-and-sex model. Women: red \square ; men: blue \circ . Bayes factors (BF) are likelihoods relative to the null model.

Discussion

We have confirmed that women possess on average finer passive tactile spatial acuity than men, and we have discovered a surprisingly simple explanation for this: tactile spatial perception improves with decreasing finger size. Indeed, we find that when sex and finger size are both considered in statistical analyses, only finger size predicts tactile acuity. Thus, a man and a woman with fingers of equal size will, on average, experience equal tactile acuity.

Why does finger size affect spatial acuity? The high density of Meissner corpuscles in small fingers (Bolton et al., 1966; Dillon et al., 2001; Nolano et al., 2003) presumably does not improve spatial acuity, because Meissner corpuscles activate rapidly adapting type-I (RA1) afferents that interfere with fine spatial perception (Bensmaïa et al., 2006). In contrast, a high density of Merkel cells could improve spatial acuity.

When a structured surface presses against the skin, it evokes a spatially modulated discharge pattern in the underlying slowly adapting type-I (SA1) afferent axon population (Phillips and Johnson, 1981a). The precision of this neural image depends crucially on SA1 innervation density and receptive field size. The fingertip, for instance, has greater SA1 density (Johansson and Vallbo, 1979), smaller SA1 receptive fields (Schady and Torebjörk, 1983), and correspondingly better spatial acuity than does the finger base (Gibson and Craig, 2002). Anatomical (Güçlü et al., 2008) and physiological (Johansson, 1978) evidence suggests that SA1s branch to innervate several clusters of Merkel cells (Fig. 4a).

We suggest that finger size affects acuity because Merkel cells, like Meissner corpuscles, are distributed more densely in smaller fingers; thus, smaller fingers produce a finer-grained afferent neural image of an impressed tactile stimulus. This interpretation is based on two key assumptions, to be investigated by future

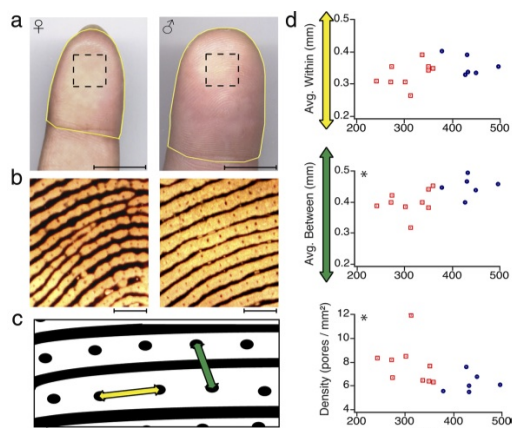


Figure 3. Finger surface microstructure. *a*, Scans from index fingers of a woman (left) and man (right) traced (yellow) for area measurement (scale bar, 1 cm). *b*, Portions of 2400 dpi scans taken from boxed regions in *a* after staining (scale bar, 1 mm). Sweat pores (punctate stain) are more densely distributed in the smaller finger. *c*, Within-ridge (yellow arrow) and between-ridge (green arrow) pore-to-pore measurements were taken from 15 participants. Dots: sweat pores; lines: finger print grooves. *d*, Pore-to-pore within-ridge distance (top), between-ridge distance (middle), and sweat pore density (lower) versus fingertip surface area. Women: red □; men: blue ○. *correlation $p < 0.05$.

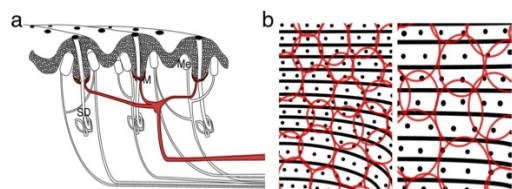


Figure 4. Proposed receptor anatomy and effect of finger size. *a*, Schematic cross-section through finger. An SA1 axon (red) branches to Merkel cell clusters (M) encircling sweat ducts (SD) beneath papillary ridges (stippled). RA1 axons (uncolored) innervate Meissner corpuscles (Me). *b*, We propose that SA1 receptive fields (ellipses) are more densely packed in smaller fingers (left).

anatomical and physiological work: (1) that sweat pore density is a reliable correlate of Merkel cell cluster density, and (2) that the number of Merkel clusters in a typical SA1 receptive field is independent of finger size, so that fingers with more closely spaced Merkel clusters will have more (and smaller) SA1 receptive fields per unit area (Fig. 4*b*).

We recognize that finger size may additionally (or exclusively) correlate with factors other than Merkel cell density to affect tactile spatial acuity. One such factor is Merkel cell depth. If fingers scale uniformly in size such that the relative spacing between components is preserved, then Merkel cells would reside more deeply within the epidermis of larger fingers. In this case, tactile thresholds would be expected to correlate positively with finger size, as we have observed, because the epidermal deformation caused by a stimulus surface diminishes with increasing depth (Phillips and Johnson, 1981*b*; Sripathi et al., 2006).

Other factors that might correlate with finger size to influence tactile spatial acuity include skin thickness, temperature and hydration. We are unaware of studies that have investigated corre-

lations between these factors and finger size, but such correlations are plausible. The stratum corneum, the skin's outermost layer, is slightly thicker in male than in female fingers (Fruhstorfer et al., 2000). A positive correlation between stratum corneum thickness and finger size could account in part for the effect of finger size on acuity. Skin temperature and hydration are also greater in male than in female fingers (Verrillo et al., 1998; see also Lévêque et al., 2000). Skin temperature might plausibly increase with finger size, as larger fingers have smaller surface-to-volume ratios, so should undergo slower heat loss. The effects of small variations in skin temperature and endogenous skin hydration on tactile spatial acuity are unclear, however.

Our statistical analyses indicate that when finger size is considered there is no longer a detectable independent effect of sex on tactile spatial acuity; that is, the sex difference in tactile acuity is fully explained by the effect of finger size. This does not mean, however, that finger size is the only determinant of tactile acuity. Indeed, we note that, even accounting for finger size, much variance in tactile acuity remains unexplained (Fig. 2*c*). Apparently, tactile acuity is influenced by: (1) finger size (which gives rise to the sex difference), and (2) other sources, unrelated to finger size or sex.

What are these other sources of variance in acuity? Three broadly defined processing stages underlie tactile perception, and factors that affect any stage could cause individual differences in tactile spatial acuity. First, a tactile stimulus deforms the skin. Second, mechanoreceptors transform the skin deformation into an afferent population response—a peripheral neural image of the impressed surface.

Third, central neurons interpret this peripheral neural image. We have suggested that finger size, via its influence on receptor density, affects the second stage of processing. Other factors, described below, could affect the first and third stages.

Individual differences in mechanical skin properties might affect the first stage of tactile processing. Two such properties are skin compliance (Woodward, 1993) and conformance (Vega-Bermudez and Johnson, 2004; Gibson and Craig, 2006). A force-controlled stimulus will cause greater skin deformation (strain) when applied to a more compliant or conformant (pliable) finger. SA1 afferents fire at a rate proportional to the compressive (Phillips and Johnson, 1981*b*) or tensile (Sripathi et al., 2006) strain in the epidermis at the depth of the Merkel cells. Therefore, an SA1 afferent in more compliant skin will be more strongly activated by the same fixed-force stimulus. Nevertheless, the variation in skin compliance among our participants was apparently not sufficient to exert measurable effects on tactile acuity, a result consistent with that found by Woodward (1993), and perhaps not surprising in light of the insensitivity of grating orientation

thresholds to increases in skin displacement produced by forces >50 g (Gibson and Craig, 2006). Presumably, as suggested by Gibson and Craig (2006), the afferent spatial image is sufficiently clear at 50 g force that little or no benefit accrues to spatial perception from further increases in skin deformation. The literature on the influence of conformance is mixed, however, and deserves further investigation. Vega-Bermudez and Johnson (2004) report a correlation among young participants between a conformance-associated measure and GOT threshold, whereas Gibson and Craig (2006) report that conformance does not determine acuity on the GOT.

Individual differences in central neural circuitry could affect the third stage of tactile processing. The detailed circuitry that underlies tactile perceptual inference is unknown, but it is clear that the peripheral neural image evoked by a spatially structured surface contains more information than is typically extracted by the brain (Wheat and Goodwin, 2001; Goldreich, 2009). Because central processing is suboptimal in this sense, room for improvement exists. One salient feature of central perceptual areas, known to vary across individuals, is representational size. The representation of the fingertip in the somatosensory homunculus expands with tactile experience (Jenkins et al., 1990; Pascual-Leone and Torres, 1993; Sterr et al., 1999). In addition, cortical neuronal excitability increases following repetitive tactile stimulation (Höfken et al., 2007), and neuronal firing properties are modified by selective tactile attention (Roy et al., 2007). These and other central neural properties presumably account for some individual variation in tactile acuity.

In conclusion, we have shown that finger size variation accounts for the sex difference in passive tactile spatial acuity. We suggest that diminutive digits discern delicate details because within such digits Merkel cell density is high, and consequently SA1 receptive fields are closely spaced and small, resulting in excellent spatial resolution. If the influence of finger size on tactile acuity applies throughout development, then we would expect children to outperform young adults on tactile spatial tasks, as observed in one study (Stevens and Choo, 1996; but see Bleyenheuft et al., 2006). Future research will investigate the extent to which Merkel cell density and other factors—peripheral and central—influence tactile perception throughout development and adulthood.

References

- Bensmaia SJ, Craig JC, Johnson KO (2006) Temporal factors in tactile spatial acuity: evidence for RA interference in fine spatial processing. *J Neurophysiol* 95:1783–1791.
- Bleyenheuft Y, Cols C, Arnould C, Thonnard JL (2006) Age-related changes in tactile spatial resolution from 6 to 16 years old. *Somatosens Mot Res* 23:83–87.
- Bolton CF, Winkelmann RK, Dyck PJ (1966) A quantitative study of Meissner's corpuscles in man. *Neurology* 16:1–9.
- Boulais N, Misery L (2007) Merkel cells. *J Am Acad Dermatol* 57:147–165.
- Craig JC, Johnson KO (2000) The two-point threshold: not a measure of tactile spatial resolution. *Curr Dir Psychol Sci* 9:29–32.
- Dillon YK, Haynes J, Henneberg M (2001) The relationship of the number of Meissner's corpuscles to dermatoglyphic characters and finger size. *J Anat* 199:577–584.
- Fruhstorfer H, Abel U, Garthe CD, Knüttel A (2000) Thickness of the stratum corneum of the volar fingertips. *Clin Anat* 13:429–433.
- Gescheider GA (1997) *Psychophysics: the fundamentals*, 3 Ed. Mahwah, NJ: Lawrence Erlbaum.
- Gibson GO, Craig JC (2002) Relative roles of spatial and intensive cues in the discrimination of spatial tactile stimuli. *Percept Psychophys* 64:1095–1107.
- Gibson GO, Craig JC (2006) The effect of force and conformance on tactile intensive and spatial sensitivity. *Exp Brain Res* 170:172–181.
- Goldreich D (2009) An ideal observer for passive tactile spatial perception. Paper presented at the Conference on Computational and Systems Neuroscience, Salt Lake City, UT, February–March.
- Goldreich D, Kanics IM (2003) Tactile acuity is enhanced in blindness. *J Neurosci* 23:3439–3445.
- Goldreich D, Kanics IM (2006) Performance of blind and sighted humans on a tactile grating detection task. *Percept Psychophys* 68:1363–1371.
- Goldreich D, Wong M, Peters RM, Kanics IM (2009) A tactile automated passive-finger stimulator (TAPS). *J Vis Exp* 28. pii: 1374. [Free Full Text].
- Goodman SN (1999) *Toward evidence-based medical statistics. 2: The Bayes factor*. *Ann Intern Med* 130:1005–1013.
- Güçlü B, Mahoney GK, Pawson LJ, Pack AK, Smith RL, Bolanowski SJ (2008) Localization of Merkel cells in the monkey skin: an anatomical model. *Somatosens Mot Res* 25:123–138.
- Höfken O, Veit M, Knossalla F, Lissek S, Bliem B, Ragert P, Dinse HR, Tegenthoff M (2007) Sustained increase of somatosensory cortex excitability by tactile coactivation studied by paired median nerve stimulation in humans correlates with perceptual gain. *J Physiol* 584: 463–471.
- Iggo A, Muir AR (1969) The structure and function of a slowly adapting touch corpuscle in hairy skin. *J Physiol* 200:763–796.
- Jenkins WM, Merzenich MM, Ochs MT, Allard T, Guic-Robles E (1990) Functional reorganization of primary somatosensory cortex in adult owl monkeys after behaviorally controlled tactile stimulation. *J Neurophysiol* 63:82–104.
- Johansson RS (1978) Tactile sensibility in the human hand: receptive field characteristics of mechanoreceptive units in the glabrous skin area. *J Physiol* 281:101–125.
- Johansson RS, Valbo AB (1979) Tactile sensibility in the human hand: relative and absolute densities of four types of mechanoreceptive units in glabrous skin. *J Physiol* 286:283–300.
- Johnson KO (2001) The roles and functions of cutaneous mechanoreceptors. *Curr Opin Neurobiol* 11:455–461.
- Johnson KO, Phillips JR (1981) Tactile spatial resolution: I. Two-point discrimination, gap detection, grating resolution, and letter recognition. *J Neurophysiol* 46:1177–1192.
- Kass RE, Raftery AE (1995) Bayes factors. *J Am Stat Assoc* 90:773–795.
- Kontsevich LL, Tyler CW (1999) Bayesian adaptive estimation of psychometric slope and threshold. *Vis Res* 39:2729–2737.
- Lévesque JL, Dresler J, Ribot-Ciscar E, Roll JP, Poelman C (2000) Changes in tactile spatial discrimination and cutaneous coding properties by skin hydration in the elderly. *J Invest Dermatol* 115:454–458.
- Nolano M, Provitera V, Crisci C, Stancanelli A, Wendelschafer-Crabb G, Kennedy WR, Santoro L (2003) Quantification of myelinated endings and mechanoreceptors in human digital skin. *Ann Neurol* 54:197–205.
- Ogawa H (1996) The Merkel cell as a possible mechanoreceptor cell. *Prog Neurobiol* 49:317–334.
- Oldfield RC (1971) The assessment and analysis of handedness: the Edinburgh inventory. *Neuropsychologia* 9:97–113.
- Pascual-Leone A, Torres F (1993) Plasticity of the sensorimotor cortex representation of the reading finger in braille readers. *Brain* 116:39–52.
- Phillips JR, Johnson KO (1981a) Tactile spatial resolution. II. Neural representation of Bars, edges, and gratings in monkey primary afferents. *J Neurophysiol* 46:1192–1203.
- Phillips JR, Johnson KO (1981b) Tactile spatial resolution. III. A continuum mechanics model of skin predicting mechanoreceptor responses to bars, edges, and gratings. *J Neurophysiol* 46:1204–1225.
- Roy A, Steinmetz PN, Hsiao SS, Johnson KO, Niebur E (2007) Synchrony: a neural correlate of somatosensory attention. *J Neurophysiol* 98:1645–1661.
- Schady WJ, Torebjörk HE (1983) Projected and receptive fields: a comparison of projected areas of sensations evoked by intraneural stimulation of mechanoreceptive units, and their innervation territories. *Acta Physiol Scand* 119:267–275.
- Sivia D, Skilling J. (2006) *Data analysis: a Bayesian tutorial*, Ed 2. New York: Oxford UP.
- Sripati AP, Bensmaia SJ, Johnson KO (2006) A continuum mechanical model of mechanoreceptive afferent responses to indented spatial patterns. *J Neurophysiol* 95:3852–3864.

Ph.D. Thesis – Peters, RM – Psychology

Peters et al. • Tactile Acuity and Finger Size

J. Neurosci., December 16, 2009 • 29(50):15756–15761 • 15761

- Sterr A, Müller M, Elbert T, Rockstroh B, Taub E (1999) Development of cortical reorganization in the somatosensory cortex of adult braille students. *Electroencephalogr Clin Neurophysiol Suppl* 49:292–298.
- Stevens JC, Choo KK (1996) Spatial acuity of the body surface over the life span. *Somatosens Mot Res* 13:153–166.
- Van Boven RW, Hamilton RH, Kauffman T, Keenan JP, Pascual-Leone A (2000) Tactile spatial resolution in blind braille readers. *Neurology* 54:2230–2236.
- Vega-Bermudez F, Johnson KO (2004) Fingertip skin conformance accounts, in part, for differences in tactile spatial acuity in young subjects, but not for the decline in spatial acuity with aging. *Percept Psychophys* 66:60–67.
- Verrillo RT, Bolanowski SJ, Checkosky CM, McGlone FP (1998) Effects of hydration on tactile sensation. *Somatosens Mot Res* 15:93–108.
- Wheat HE, Goodwin AW (2001) Tactile discrimination of edge shape: limits on spatial resolution imposed by parameters of the peripheral neural population. *J Neurosci* 21:7751–7763.
- Woodward KL (1993) The relationship between skin compliance, age, gender, and tactile discriminative thresholds in humans. *Somatosens Mot Res* 10:63–67.
- Yamada N, Kashima Y, Inoué T (1996) Scanning electron microscopy of the basal surface of the epidermis of human digits. *Acta Anat* 155:242–248.

Chapter 3

3.1 Preface

Having shown that fingertip surface area predicts tactile spatial acuity in young adults, we became interested in fingertip growth over development, and the question of whether or not children have finer acuity than adults. Only two previous studies had measured tactile spatial acuity in children, and they disagreed as to whether children possessed finer acuity than adults. Neither study measured fingertip growth; however, we hypothesized that, when fingertips grow, afferent innervation density decreases as mechanoreceptors embedded in the skin are stretched over an expanding surface.

To test this hypothesis, we measured the tactile spatial acuity of children, and combined this with various measurements of fingertip size (surface area, volume, and sweat pore spacing), as well as skin surface temperature. Our results demonstrate, for the first time, that fingertip growth from childhood into adulthood predicts changes in tactile spatial acuity far more than does age.

3.2 Abstract

Tactile acuity is known to decline with age in adults, possibly as the result of receptor loss, but less is understood about how tactile acuity changes during childhood. Previous research from our laboratory has shown that fingertip size influences tactile spatial acuity in young adults: those with larger fingers tend to have poorer acuity, possibly because mechanoreceptors are more sparsely distributed in larger fingers. We hypothesized that a similar relationship would hold among children. If so, children's tactile spatial acuity might be expected to worsen as their fingertips grow. However, concomitant CNS maturation might result in more efficient perceptual processing, counteracting the effect of fingertip growth on tactile acuity. To investigate, we conducted a cross-sectional study, testing 116 participants ranging in age from 6 to 16 years on a precision-controlled tactile grating orientation task. We measured each participant's grating orientation threshold on the dominant index finger, along with physical properties of the fingertip: surface area, volume, sweat-pore spacing, and temperature. We found that, as in adults, children with larger fingertips (at a given age) had significantly poorer acuity, yet paradoxically acuity did not worsen significantly with age. We propose that finger growth during development results in a gradual decline in innervation density as receptive fields reposition to cover an expanding skin surface. At the same time, central maturation presumably enhances perceptual processing.

3.3 Introduction

In touch, as in other senses, an individual's perceptual acuity is not static throughout life. Among adults, many studies have shown a consistent decline with age in passive tactile spatial acuity, the ability to perceive the fine structure of a stimulus surface pressed against the stationary fingertip (Stevens & Choo, 1996; Goldreich & Kanics, 2003; 2006; Manning & Tremblay, 2006; Wong et al., 2011). This age-associated decline in tactile acuity may result from peripheral mechanoreceptor loss (Cauna, 1964; Bruce, 1980) and/or changes in central perceptual circuits. When a structured surface contacts the fingertip, it evokes a spatially modulated discharge pattern in the population of underlying mechanoreceptors, a peripheral *neural image* of the stimulus. This neural activity image is transmitted to the CNS, where it is sequentially processed within brainstem and thalamic nuclei, the primary somatosensory cortex, and areas beyond, ultimately resulting in a conscious percept. Clearly, accurate perception depends on both peripheral and central processes, but the fidelity of the initial neural image necessarily sets an upper limit on perceptual accuracy. Thus, the receptor density in a skin region ultimately constrains the spatial acuity achievable with that region, and any decrease in receptor density will result in a decline in acuity.

The decline in tactile acuity with age has been well characterized among adults, but less is known about how tactile perception develops in childhood. Indeed, the literature is somewhat conflicting even on the basic question of

whether tactile acuity improves, declines, or remains unchanged with age early in life (Stevens & Choo, 1996; Bleyenheuft et al., 2006; Guclu & Oztek, 2007; Bleyenheuft et al., 2010). During childhood, both peripheral (body growth) and central (maturation of perceptual circuits) factors could plausibly cause age-related tactile acuity changes. Two previous studies from our laboratory implicated finger size as a predictor of tactile spatial acuity among young adults. We found that index finger tactile spatial acuity improved progressively with diminishing fingertip surface area (Peters et al., 2009) and that fingertip surface area set a limit on the tactile spatial acuity that could be achieved through training (Wong et al., 2013). Together with histological data (Cauna, 1964; Bolton et al., 1966; Dillon et al., 2001; Nolano et al., 2003), these findings supported the hypothesis that cutaneous mechanoreceptors are more closely spaced in smaller fingers. If adults with smaller fingers have better tactile spatial acuity, would the tactile spatial acuity of children be even better than that of adults, and would tactile acuity decline with age as children's fingers grow?

We hypothesized that fingertip growth during development would increase tactile receptor spacing (Cauna, 1964; Bolton et al., 1966), with consequent reduction in the fidelity of the peripheral neural image. However, whether tactile spatial acuity would decline with age was unclear, because concomitant CNS maturation might result in more efficient perceptual processing. To investigate, we assessed the tactile spatial acuity of participants aged 6-16 years, and measured each participant's dominant index fingertip surface area, volume, sweat-pore

spacing, and temperature. Sweat pore spacing was of interest because Merkel cell mechanoreceptors tend to cluster around the bases of the sweat ducts (Yamada et al., 1996; Guclu et al., 2008). Skin temperature was of interest because it is known to affect vibrotactile perception (Verrillo et al., 1998), and might plausibly vary with fingertip size. We found that children's tactile spatial acuity indeed worsened with increasing fingertip size; nevertheless, and intriguingly, tactile spatial acuity did not decline with age. These findings suggest that during childhood, tactile spatial perception is challenged by fingertip growth but simultaneously benefits from CNS maturation.

3.4 Methods

All procedures were approved by the McMaster University Research Ethics Board. Because the participants in these experiments were minors, the participant's parent provided signed informed consent, and the participant provided signed assent.

Participants

We tested 116 children ranging from 6 to 16 years of age (57 girls, 59 boys). Participants were free of cuts, calluses or scars on their dominant index finger, as well as conditions that might affect their sense of touch, such as diabetes, cognitive impairment, dyslexia, or neurological disorders. We assessed each participant's hand dominance using a modified version of the Edinburgh Handedness Inventory (Oldfield, 1971). We eliminated the data of 14 children (7 girls and 7 boys) from analysis due to their poor concentration scores (see

Qualification criterion below). The data of another two participants (one 6-year-old boy and one 11-year-old boy) were eliminated as they withdrew from the study prior to completion of their sensory testing. Thus, the data reported here are from 100 participants, 50 boys and 50 girls (Table 1).

Sensory Testing

Participants' passive (finger stationary) tactile spatial acuity was estimated by means of the grating orientation task (GOT)(Johnson & Phillips, 1981; Van Boven & Johnson, 1994; Craig, 1999). The participant was seated comfortably with the distal pad of the dominant index finger resting over a tunnel in a table through which the tactile stimuli emerged from below. A fully automated tactile stimulator, described in detail in (Goldreich et al., 2009), was used to apply the stimuli and record the participant's responses. Acetyl stimulus pieces (0.5” diameter; milled in-house) with parallel grooves varying from 0.25 to 3.1 mm (in steps of 0.15 mm) were pressed gently onto the participant’s dominant index fingertip (contact force 50 g; contact duration 1 s; onset velocity 4 cm/s). We defined “vertical” gratings as those with grooves aligned parallel to the long-axis of the finger, and “horizontal” gratings as those with grooves aligned perpendicular to the long axis of the finger. Small plastic barriers were affixed on either side of the participant’s finger to prevent lateral scanning movement during testing blocks, and a force sensor was placed on the fingernail to monitor upward and downward finger movement. A computer-generated voice alerted the participant if any finger movement was detected, and such trials were

automatically discarded from analysis.

Prior to sensory testing, the participant completed 20 practice trials with auditory feedback. The sensory test consisted of 4 blocks of 40 trials each. The computer program paused to require the participant to rest for at least 15 seconds after every 20 trials (halfway through each testing block), for at least 1 minute between blocks, and for at least 5 minutes at the halfway point of the experiment (after the second testing block). Sensory testing occurred via either a two-interval forced-choice (2-IFC) procedure (initial 55 participants tested) or a single-interval yes-no procedure (final 61 participants tested). The switch from the 2-IFC protocol to the single-interval protocol was made when it became apparent that young children were struggling to qualify (see Results), and we thought a single-interval protocol with feedback might be simpler for children. In the 2-IFC procedure, participants discriminated the order of two successive grating stimuli of equal groove width but orthogonal orientation (1 s inter-stimulus interval; stimulus order chosen randomly). The participants indicated the perceived stimulus order (vertical grating first or second) by pressing one of two response buttons with the non-dominant hand. No auditory feedback was given during 2-IFC testing. In the single-interval procedure, participants were randomly presented with either a vertical or horizontal grating, and were asked to identify its orientation with a button press using the non-dominant hand. Auditory feedback (one of two computer tones) was provided following each trial in the single-interval procedure, to signal whether the participant had answered correctly or

incorrectly. In addition, a visual label was placed on the response button box to identify the vertical and horizontal grating response buttons; no such labels were present for participants tested with the 2-IFC procedure.

For both the 2-IFC and the single-interval tasks, groove width was adaptively varied using a modified version of the Bayesian adaptive ψ -method (Kontsevich & Tyler, 1999; Goldreich et al., 2009). Briefly, we modeled the participant's discriminability, d -prime, as a power function of groove width, and the participant's sigmoidal psychometric function (proportion correct responding as a function of groove width, x), $\Psi_{a,b,\delta}(x)$, as a mixture of a cumulative normal curve and a lapse rate term:

$$d' = \left(\frac{x}{a}\right)^b \quad P_{correct}(x) = \left(\frac{\delta}{2}\right) + (1 - \delta) \frac{1}{\sqrt{2\pi}} \int_{-\infty}^{\frac{d'}{\sqrt{2}}} \exp\left(-\frac{y^2}{2}\right) dy$$

The psychometric function is characterized by three unknown shape parameters, which are initially specified by uniform prior probability densities: a (position), b (slope), and δ (lapse rate). The lapse-rate term accounts for the realistic possibility of occasional attention lapses, resulting in 50% correct response probability, regardless of groove width. The algorithm, which we programmed in LabVIEW for Macintosh (National Instruments) adaptively adjusted groove width from trial to trial, presenting the grating stimulus expected to yield the greatest information regarding the participant's psychometric function shape parameters (expected entropy minimization). We defined the participant's

GOT threshold as the groove width whose orientation the participant could correctly discriminate with 76% probability. This corresponds to $x = a$, at which d -prime equals 1 for the 2-IFC task (Gescheider, 1997), and at which d -prime equals 1.35 for the single-interval task. The algorithm returned the best-fitting psychometric function as well as a posterior probability distribution function (PDF) over the a -parameter (Figure 1).

For the analysis, we combined the responses from all testing blocks on which the participant was clearly not guessing (see Qualification criterion), and from these combined responses we computed the participant's joint (a, b, δ) posterior PDF. For the 2-IFC task data, we marginalized the joint posterior PDF over the b and δ parameters to obtain the participant's a -parameter PDF; we took the mean of the a -parameter PDF as the participant's groove width threshold estimate. For the single-interval task, we equivalently derived the groove width at which d -prime = 1; this is the 69% correct threshold value for the single-interval procedure (Gescheider, 1997). To do this, we marginalized each participant's joint posterior PDF over the δ -parameter, plotted the best-fit psychometric function for each (a, b) pair, and interpolated to find the groove width corresponding to 69% correct performance. We then averaged this groove width across the (a, b) posterior PDF, and took this as the participant's threshold estimate.

Qualification criterion

Consistent performance on a psychophysical task demands sustained concentration. We screened participants for concentration by assessing the

probability that their performance could have resulted from guessing on each trial, relative to the probability that it could be described by a cumulative normal psychometric function. We call the ratio of these two probabilities the Guessing Bayes Factor (GBF), which we compute as:

$$GBF_t = \frac{0.5^t}{\int_a \int_b \int_\delta P(r_1, r_2, \dots, r_t | \Psi_{a,b,\delta}) P(\Psi_{a,b,\delta}) d_a d_b d_\delta}$$

where r_i refers to the participant's response (correct or incorrect) on the i^{th} trial, t is the total number of non-discarded trials in the testing block, and $P(\Psi_{a,b,\delta})$ is the prior probability density over the psychometric function characterized by parameters a , b , and δ .

We chose a criterion value of $GBF = 0.5$ as the cut-off above which we considered a participant not to be concentrating during a given testing block. Thus, only if we were at least twice as confident that a participant was concentrating than randomly pressing buttons did we accept the participant's data from that testing block for further analysis. We applied this criterion on a block-by-block basis. We performed a sensitivity analysis to investigate the effect of different choices of qualification criterion on the statistical results (Table 2).

Physical Skin Measurements

We measured the surface area, volume, temperature, and sweat-pore spacing of the dominant index fingertip of each participant.

To determine fingertip surface area, we scanned the distal portion of the

participant's dominant index finger with a flatbed scanner (Epson Perfection 1260). This scanning procedure is identical to that used by Peters et al., 2009. The participant placed their hand on a glass scanning surface in prone position, and the distal finger pad, from the tip of finger to the distal inter-phalangeal crease, was optically imaged at 400 dpi. Fingertip surface area was digitally measured from these images using ImageJ v10.2 (National Institutes of Health). Fingertip surface area was measured by two naive observer (P.S. and S.P.); we report the average of the observers' measurements.

To measure index finger volume, we determined how much water the fingertip displaces when submerged up to the distal inter-phalangeal crease in a plastic 20 mL graduated cylinder. The cylinder was filled to the top with room-temperature water; insertion of the finger caused a volume of water to spill out that was equal to the volume of the fingertip. We then used a USB microscope with a polarized 30X lens (ProScope HR; Bodelin Technologies) to image the waterline after the finger was withdrawn. These measurements were made digitally using GraphClick v3.0 to define the graduated cylinder tick marks above and below the water line and to measure the water line's linear position (at its lowest point) between the bracketing tick marks. To improve visibility of the water line in the ProScope images, red food colouring was added to the water and a blank piece of white paper was held against the side of the graduated cylinder opposite to the ProScope lens. This measurement was repeated 4 times and the resulting fingertip volume measurements were averaged together for use in the

analysis.

To measure skin surface temperature, we used a thermistor (ON-408-PP, Omega Engineering, USA). These temperature-dependent resistors are designed for accurate skin surface temperature measurement within +/- 0.1 °C. We made three separate temperature measurements: once before sensory testing began, once at the halfway point (after completion of testing block 2), and once upon completion of the sensory testing; these three measurements were averaged together for use in the analysis.

To measure sweat-pore density, we coated participants' dominant index fingertip with water-based paint (Crayola Water Colours) and optically imaged the distal pad at 2400 dpi with a flatbed scanner (EPSON Perfection, 1260). We measured center-to-center sweat-pore spacing from these scans using ImageJ. Because we previously found that sweat-pore spacing between adjacent fingerprint ridges differed from sweat pore spacing within individual ridges (Peters et al., 2009), we estimated average between-ridge (μ_b) and within-ridge (μ_w) sweat-pore spacing separately, from 20 measurements of each. Two observers performed these measurements, an author (RMP) and a naive observer (AB), and we averaged their measurements. We estimated sweat pore density, ρ (pores/mm²), as:

$$\rho = \frac{1}{\mu_b \mu_w}$$

Statistical Analyses

All statistical analyses were conducted using SPSS version 20 for Mac (IBM Corporation) with an alpha level of 0.05. For ANCOVA, we used type III sum of squares. Reported p-values are two-tailed unless otherwise stated. For analyses of the effect of age on fingertip size metrics, and of fingertip size metrics on tactile threshold, we used one-tailed p-values, because we had directional alternative hypotheses. Specifically, we predicted that fingertips would grow with age, and that tactile thresholds would increase with fingertip size. For other analyses, including the effect of age on skin temperature and on tactile thresholds, we used two-tailed p-values, because we had no strong prediction regarding the direction of these effects.

We log transformed participants' tactile thresholds prior to analysis, because the measured thresholds, as well as the standardized residuals from linear regressions with measured threshold as the dependent variable, were non-normally distributed as indicated by the Kolmogorov-Smirnov (KS) test [tactile thresholds ($p < 0.001$); residuals from linear regressions between thresholds and fingertip surface area ($p < 0.001$), volume ($p = 0.004$), temperature ($p = 0.002$), between-ridge sweat-pore spacing ($p = 0.001$), within-ridge sweat-pore spacing ($p = 0.001$), sweat-pore density ($p < 0.001$), age ($p = 0.001$)]. Log-transformation greatly improved normality, with KS tests revealing no significant violations of normality [log thresholds ($p = 0.07$); residuals from linear regressions between log thresholds and fingertip surface area ($p = 0.096$), volume ($p = 0.2$), temperature ($p = 0.085$), between ridge sweat-pore spacing ($p = 0.2$), within ridge sweat-pore

spacing ($p = 0.124$), sweat-pore density ($p = 0.065$), age ($p = 0.181$)]. In one analysis (see Results), we aggregated the data from the current study with those from Peters et al. (2009); for that purpose, we first log-transformed the thresholds from Peters et al. (2009), which improved the normality of the residuals for those data as well.

We performed multiple linear regressions on log tactile thresholds with age and physical fingertip metrics as predictor variables. Because fingertip metrics were correlated with age (see Results), we calculated variance inflation factors (VIF) (Montgomery & Runger, 2010) to assess whether collinearity was not problematically high. All VIF were less than 2.3, indicating that the degree of collinearity among independent variables was well within acceptable limits (Montgomery & Runger, 2010).

3.5 Results

Participant concentration and task difficulty

We found that the youngest participants were much more likely to struggle with the sensory testing. A chi-squared test revealed that the proportion of participants eliminated due to poor concentration (see Methods) was significantly greater than zero among 6 year olds ($X^2 = 6.471$, $p = 0.011$) and 7 year olds ($X^2 = 4.000$, $p = 0.046$) (Figure 2A). Although we had hoped that the single-interval stimulus procedure would prove easier for the younger participants, a chi-squared test revealed that the proportion of participants who failed to qualify on the 2-IFC task did not differ significantly from the proportion who failed to qualify on the

conceptually simpler single-interval task ($X^2 = 0.186$, $p = 0.667$) (Figure 2B). Furthermore, among qualifying participants, the mean tactile threshold on the 2-IFC experiments (1.63 mm; SD = 0.60 mm) did not differ significantly from that on the single-interval experiments (1.45 mm, SD = 0.52 mm) (Figure 2C). An ANCOVA with testing protocol and sex as between subject factors, age as a covariate, and log threshold as the dependent variable revealed no significant effects of any factor (testing protocol, $p = 0.117$; age, $p = 0.544$; sex, $p = 0.462$). Therefore, for subsequent analyses we used the aggregate data from the two protocols.

Fingertip growth during development

To characterize the physical changes in the fingertip that occur during development, we conducted separate linear regressions between participant age and the six fingertip metrics collected in this study. These revealed significant positive relationships between participant age and fingertip surface area ($r = 0.744$, one-tailed $p < 0.001$; slope 14.560 mm²/year), volume ($r = 0.709$, one-tailed $p < 0.001$; slope 0.195 mL/year), between-ridge sweat-pore spacing ($r = 0.572$, one-tailed $p < 0.001$; slope 0.010 mm/year), and within-ridge sweat-pore spacing ($r = 0.555$, one-tailed $p < 0.001$; slope 0.006 mm/year). There was a significant negative relationship between age and estimated sweat-pore density ($r = -0.652$, one-tailed $p < 0.001$; slope -0.316 pores/mm²/year). Thus, fingertips enlarged and sweat pore spacing increased with age. Fingertip temperature did not correlate significantly with age ($p = 0.529$) or with fingertip surface area ($p =$

0.145), volume ($p = 0.093$), or surface-to-volume ratio ($p = 0.158$) (Figure 3).

The effects of age and fingertip characteristics on tactile spatial acuity

Next, we addressed the primary questions of this study: do age and/or fingertip characteristics significantly influence tactile spatial acuity among children? To investigate the effect of age, we first conducted a simple linear regression between age and log tactile threshold; this showed no significant effect of age on tactile spatial acuity among our participant sample ($p = 0.403$). We next conducted separate multiple linear regressions between each of the six physical fingertip metrics along with age (independent variables) and log tactile thresholds (dependent variable). These analyses revealed significant effects of fingertip surface area ($r = 0.206$, one-tailed $p = 0.031$) and volume ($r = 0.230$, one-tailed $p = 0.016$), and a marginally significant effect of between-ridge sweat-pore spacing ($r = 0.182$, one-tailed $p = 0.055$) (Figure 4). Age did not significantly predict tactile acuity in these analyses ($p > 0.3$ in all cases), although interestingly the beta weights for age were consistently negative, suggesting a non-significant trend for acuity to improve a function of age (see Table 2). Thus, among participants 6 to 16 years old, greater fingertip size was associated with significantly poorer tactile spatial acuity, whereas the effect of age was not significant.

Aggregate analysis with the data of Peters et al. (2009).

To further investigate whether tactile spatial acuity changes with age from childhood into early adulthood, we aggregated the data from the 100 qualifying children in the present study with that of 97 young adults whom we had tested in a

previous GOT study (Peters et al., 2009) (Figure 5). When considered alone, age again failed to predict tactile spatial acuity (Figure 5A). A univariate linear regression revealed no significant effect of age on log tactile thresholds in the aggregated dataset ($p = 0.590$). The results were distinct, however, when we considered age along with fingertip surface area (the sole fingertip size metric recorded for all participants by Peters et al. (2009)). A multiple regression on the aggregated log thresholds revealed significant effects of both age ($t = -2.490$, $p = 0.014$) and fingertip area ($t = 4.042$, one-tailed $p < 0.001$), with opposite directionality (Figure 5C, D). Tactile spatial acuity improved significantly with age (rate = 0.017 log mm threshold decrease/year; $\beta = -0.245$) and worsened significantly with increasing fingertip area (rate = 0.002 log mm threshold increase/mm² surface area; $\beta = 0.397$). This finding is consistent with the intriguing hypothesis that two concomitant effects are at play during development: a progressive worsening of acuity as fingertips grow, and a progressive improvement in acuity as the CNS becomes more efficient at tactile processing; together, these factors tend to cancel the effect of age – considered alone – on tactile spatial acuity during development.

3.6 Discussion

In this cross-sectional study, we found that tactile spatial acuity among children worsens with increasing fingertip size, as reported previously in young adults (Peters et al., 2009). Additionally, by combining the data from the present and a previous study, we discovered that fingertip size and age exert opposite

effects on tactile acuity when both variables are considered together. Statistically, at a given age, acuity worsens with increasing fingertip size; at a given fingertip size, acuity improves with increasing age. These findings suggest that two factors act concomitantly during development to influence tactile spatial acuity: fingertip growth results in a gradual decline in mechanoreceptor density, and CNS maturation results in more efficient sensory processing.

Technical considerations in testing young children

Some methodological observations from our experiences testing young children may prove useful to other researchers who are considering psychophysical studies with young participants.

With the GBF, we were able to detect participants who were unable to concentrate consistently on the task. We found that only the 6 and 7 year old groups significantly exceeded criterion, suggesting that they were struggling to perform the task. Based on this observation, we recommended against testing such young children on the GOT and similarly demanding tactile tasks, unless the GBF is also measured.

After testing 55 participants using a 2-IFC procedure, we modified our protocol in an effort to make the experiment as easy as possible to understand and perform. We tested another 61 participants using a single-interval stimulus procedure, providing auditory feedback on every trial, and identifying the response buttons with visual vertical and horizontal gratings. Despite these modifications, we found no significant differences in tactile acuity as measured on

the two tasks. In light of this equivalence in performance, and because the 2-IFC procedure is robust against criterion effects (Gescheider, 1997), we recommend that researchers use the 2-IFC procedure in future GOT studies with children, as with adults.

Effect of fingertip size on tactile spatial acuity in childhood

We found that fingertip size is a significant predictor of tactile spatial acuity in childhood, as shown previously in young adulthood (Peters et al., 2009). This result is consistent with the hypothesis that cutaneous mechanoreceptors become more widely spaced as the finger grows. This change in spacing would maintain sensory coverage throughout the surface of the fingertip. However, the consequent reduction in receptive field density and probable increase in receptive field size would cause a decline in tactile spatial acuity. In addition, it is conceivable that receptor depth increases with finger growth. Receptors deeper beneath the skin surface would experience less strain from a tactile stimulus (Phillips & Johnson, 1981; Sripathi et al., 2006), with consequent reduction in the quality of the peripheral neural image leading to diminished acuity.

Merkel cell mechanoreceptors convey the fine spatial information that underlies performance on passive tactile spatial tasks such as the GOT (Johnson, 2001; Maricich et al., 2009). Therefore, the most probable neural explanation for the decline in tactile acuity with increasing fingertip size is that the Merkel cells become more widely spaced as fingers grow. To our knowledge, no anatomical evidence currently exists regarding the change in density of Merkel cells in

humans with age. However, several studies have reported that the relatively easily visualizable Meissner's corpuscles, which mediate low-frequency vibration perception (Johnson, 2001), are more sparsely distributed in larger fingers (Bolton et al., 1966; Dillon et al., 2001; Nolano et al., 2003). In a cross-sectional anatomical study, Bolton et al. (1966) further showed that the density of Meissner's corpuscles, measured in the little finger, declined with age from childhood through adulthood. Bolton et al. (1966) propose that the decline in Meissner density during childhood is due to finger growth; they note that the continuing (yet slower) decline during adulthood is of unclear cause.

We found that between-ridge sweat-pore spacing was a marginally significant predictor of acuity, whereas within-ridge sweat-pore spacing was not. Between ridge sweat-pore spacing may be more tightly linked to average afferent receptor spacing and receptive field size. Pare et al. (2002) showed that in the distal pads of non-human primates, about 80% of Merkel cells form clusters of 30 - 70 μm in diameter that stud the basal layer of intermediate ridges; the remaining 20% of Merkel cells do not cluster together but rather form chain-like arrangements that are 300 - 500 μm in length. A β afferents can branch to up to three adjacent intermediate ridges (Iggo & Andres, 1982), however, within each intermediate ridge, A β afferents can branch to a Merkel cell cluster surrounding the adjacent sweat duct or to a cluster or chain-like Merkel cell arrangement between adjacent sweat ducts (Pare et al., 2002; Guclu et al., 2008). Thus, the diversity of innervation targets within an intermediate ridge likely renders our

within-ridge sweat-pore spacing a poorer proxy than our between-ridge sweat-pore spacing for receptive field spacing and size, and therefore, a poorer predictor of tactile spatial acuity.

The effects we have observed of fingertip size on tactile spatial acuity, while significant, are weaker than those observed previously among young adult participants (Peters et al., 2009). Clearly, fingertip size is not the sole determinant of tactile spatial acuity; central factors must also play a role. In particular, while studies of conduction latencies suggest that somatosensory axon diameter and myelination become adult-like around the ages of 5 to 7 years (Eyre et al., 1991; Muller et al., 1994), central somatosensory processing circuits and cognitive circuits are presumably maturing throughout much of the age range that we have tested. Future research is needed to better-understand central contributions to the development of tactile spatial acuity.

Effect of age on tactile spatial acuity in childhood and adulthood

Age did not significantly affect tactile spatial acuity among the children tested in the present study, nor did tactile acuity correlate with age alone when the data from the present study were aggregated with those from the young adults tested in Peters et al. (2009). However, we uncovered a beneficial effect of age on tactile spatial acuity when we analyzed the aggregated data set with a multiple regression that included age along with finger size. Our findings suggest that, as fingertips grow during childhood, afferent receptor density declines, diminishing the fidelity of the peripheral neural image that is transmitted into the CNS for

perceptual processing; at the same time, however, as CNS pathways and circuits mature, central perceptual processing likely improves with age. Because of these opposing effects, the influence of age, considered alone, is weak. The beneficial effect of age on tactile spatial acuity becomes apparent once finger size is controlled.

To our knowledge, only two other research groups have investigated age-related tactile spatial acuity change in children. Using a grating orientation task, Bleyenheuft et al. (2006) reported that tactile spatial acuity improved with age, specifically 10 to 16 year old participants outperformed 6 to 9 year olds. Similarly, Bleyenheuft et al. (2010) found that acuity improved from ages 4 to 17 years. Using a gap-detection task, Stevens & Choo (1996) reported that tactile spatial acuity worsened with age, specifically 8 to 14 year old participants outperformed young adults (18 to 28 years old). Because of the different age ranges considered, these studies are not necessarily in disagreement; rather, taken together, the studies suggest a non-monotonic effect of age on tactile acuity, with acuity initially improving and then worsening with increasing age. Indeed, previous research from our laboratory and others shows that during adulthood tactile spatial acuity consistently worsens with age (Stevens & Choo, 1996; Goldreich & Kanics, 2003; 2006; Manning & Tremblay, 2006; Wong et al., 2011), perhaps because of progressive loss of mechanoreceptors (Cauna, 1964; Bruce, 1980).

Conclusion

Our results support the hypothesis that two opposing influences act on tactile spatial perception during childhood: fingertip growth diminishes the fidelity of the peripheral neural image, but CNS maturation enhances perceptual processing. We note that the perceptual data show large individual variability (Figures 4 and 5), and indeed much variance remains unexplained (see R-squared values in Table 2). Future research will continue the important search for the sources of individual variability in tactile perception. Meanwhile, given the results of the present study, we recommend that not only age but also fingertip size be taken into account when tactile spatial acuity is compared across individuals.

3.7 References

- Bleyenheuft Y, Cols C, Arnould C & Thonnard JL (2006). Age-related changes in tactile spatial resolution from 6 to 16 years old. *Somatosensory and Motor Research*. 23: 83-87.
- Bleyenheuft Y, Wilmotte P & Thonnard JL (2010). Relationship between tactile spatial resolution and digital dexterity during childhood. *Somatosensory and Motor Research*. 27: 9-14.
- Bolton CF, Winkelmann RK & Dyck PJ (1966). A quantitative study of Meissner's corpuscles in man. *Neurology*. 16: 1-9.
- Bruce MF (1980). The relation of tactile thresholds to histology in the fingers of elderly people. *Journal of Neurology, Neurosurgery, and Psychiatry*. 43: 730-734.
- Cauna N (1964). The effects of aging on the receptor organs of the human dermis, in *Advances in Biology of Skin*, ed. W. Montagna. (Elmsford, N.Y: Pergamon Press): 63–96.
- Craig JC (1999). Grating orientation as a measure of tactile spatial acuity. *Somatosensory and Motor Research*. 16: 197-206.
- Dillon YK, Haynes J & Henneberg M (2001). The relationship of the number of Meissner's corpuscles to dermatoglyphic characters and finger size. *Journal of Anatomy*. 199: 577-584.
- Eyre JA, Miller S & Ramesh V (1991). Constancy of central conduction delays during development in man: investigation of motor and somatosensory

pathways. *Journal of Physiology*. 434: 441-452.

Gescheider GA (1997). *Psychophysics: the fundamentals*. Mahwah, N.J.; London: L. Erlbaum Associates.

Goldreich D & Kanics IM (2003). Tactile acuity is enhanced in blindness. *The Journal of Neuroscience*. 23: 3439-3445.

Goldreich D & Kanics IM (2006). Performance of blind and sighted humans on a tactile grating detection task. *Perception and Psychophysics*. 68: 1363-1371.

Goldreich D, Wong M, Peters RM & Kanics IM (2009). A tactile automated passive-finger stimulator (TAPS). *Journal of Visualized Experiments*. 28: doi: 10.3791/1374.

Guclu B, Mahoney GK, Pawson LJ, Pack AK, Smith RL & Bolanowski SJ (2008). Localization of Merkel cells in the monkey skin: an anatomical model. *Somatosensory and Motor Research*. 25: 123-138.

Guclu B & Oztek C (2007). Tactile sensitivity of children: effects of frequency, masking, and the non-Pacinian I psychophysical channel. *Journal of Experimental Child Psychology*. 98: 113-130.

Iggo A & Andres KH (1982). Morphology of cutaneous receptors. *Annual Review of Neuroscience*. 5: 1-31.

Johnson KO (2001). The roles and functions of cutaneous mechanoreceptors. *Current Opinion in Neurobiology*. 11: 455-461.

Johnson KO & Phillips JR (1981). Tactile spatial resolution. I. Two-point

discrimination, gap detection, grating resolution, and letter recognition.

Journal of Neurophysiology. 46: 1177-1192.

Kontsevich LL & Tyler CW (1999). Bayesian adaptive estimation of psychometric slope and threshold. *Vision Research*. 39: 2729-2737.

Manning H & Tremblay F (2006). Age differences in tactile pattern recognition at the fingertip. *Somatosensory and Motor Research*. 23: 147-155.

Maricich SM, Wellnitz SA, Nelson AM, Lesniak DR, Gerling GJ, Lumpkin EA & Zoghbi HY (2009). Merkel cells are essential for light-touch responses. *Science*. 324: 1580-1582.

Montgomery DC & Runger GC (2010). Multiple linear regression, in *Applied Statistics and Probability for Engineers*. John Wiley & Sons: 449-512.

Muller K, Ebner B & Homberg V (1994). Maturation of fastest afferent and efferent central and peripheral pathways: no evidence for a constancy of central conduction delays. *Neuroscience Letters*. 166: 9-12.

Nolano M, Provitera V, Crisci C, Stancanelli A, Wendelschafer-Crabb G, Kennedy WR & Santoro L (2003). Quantification of myelinated endings and mechanoreceptors in human digital skin. *Annals of Neurology*. 54: 197-205.

Oldfield RC (1971). The assessment and analysis of handedness: the Edinburgh inventory. *Neuropsychologia*. 9: 97-113.

Pare M, Smith AM & Rice FL (2002). Distribution and terminal arborizations of cutaneous mechanoreceptors in the glabrous finger pads of the monkey.

Journal of Computational Neurology. 445: 347-359.

- Peters RM, Hackeman E & Goldreich D (2009). Diminutive digits discern delicate details: fingertip size and the sex difference in tactile spatial acuity. *The Journal of Neuroscience*. 29: 15756-15761.
- Phillips JR & Johnson KO (1981). Tactile spatial resolution. III. A continuum mechanics model of skin predicting mechanoreceptor responses to bars, edges, and gratings. *Journal of Neurophysiology*. 46: 1204-1225.
- Sripati AP, Bensmaia SJ & Johnson KO (2006). A continuum mechanical model of mechanoreceptive afferent responses to indented spatial patterns. *Journal of Neurophysiology*. 95: 3852-3864.
- Stevens JC & Choo KK (1996). Spatial acuity of the body surface over the life span. *Somatosensory and Motor Research*. 13: 153-166.
- Van Boven RW & Johnson KO (1994). The limit of tactile spatial resolution in humans: grating orientation discrimination at the lip, tongue, and finger. *Neurology*. 44: 2361-2366.
- Verrillo RT, Bolanowski SJ, Checkosky CM & Mcglone FP (1998). Effects of hydration on tactile sensation. *Somatosensory and Motor Research*. 15: 93-108.
- Wong M, Gnanakumaran V & Goldreich D (2011). Tactile spatial acuity enhancement in blindness: evidence for experience-dependent mechanisms. *The Journal of Neuroscience*. 31: 7028-7037.
- Wong M, Peters RM & Goldreich D (2013). A physical constraint on perceptual

Ph.D. Thesis – Peters, RM – Psychology

learning: tactile spatial acuity improves with training to a limit set by
finger size. *The Journal of Neuroscience*. 33: 9345-9352.

Yamada N, Kashima Y & Inoue T (1996). Scanning electron microscopy of the
basal surface of the epidermis of human digits. *Acta Anatomica (Basel)*.
155: 242-248.

3.8 Table and Figure Legends

Table 1. Participants who qualified for the study ($n = 100$), by age and sex.

Table 2. GBF criterion value sensitivity analysis for multiple regressions between different fingertip metrics together with age (independent variables) and log tactile thresholds (dependent variable). P-values and beta weights (standardized regression coefficients) are reported in order 'fingertip metric, age'. R-squared values indicate the proportion of explained variance. Number participants (n) is indicated for each column. Lowest row: results on the data from the present study aggregated with those reported previously from 97 young adults (Peters et al., 2009).

Figure 1. Bayesian adaptive procedure for threshold groove width estimation. Sensory data for two participants (P) are shown in columns: Left (panels **A-C**) = P1, female, age 15.9 years, fingertip surface area = 362.8 mm²; Right (panels **D-F**) = P13, male, age 16.8 years, fingertip surface area = 519.9 mm². (**A, D**) Each participant's performance plot (+ = correct response, x = incorrect response) on a single testing block. (**B,E**) Corresponding best-estimate psychometric function. (**C,F**) PDF over the a -parameter, the 76%-correct groove width. Note that, compared to P1, P13 has an upward-shifted performance plot, a rightward shifted psychometric function, and a rightward-shifted a -PDF, indicative of poorer performance; given the participants' similar ages, this performance difference is likely due to the large difference between the participants' fingertip sizes.

Figure 2. GBF disqualification analysis and comparison between psychophysical

testing protocols. **(A)** Proportion of participants in each age bracket for whom all four end-of-block GBFs exceeded the criterion value of 0.5. **(B)** Proportion of participants disqualified using the two testing protocols. **(C)** Average thresholds of qualifying participants on the two testing protocols (error bars = 1 SD).

Figure 3. Fingertip growth from childhood into adulthood. **(A – F)**. The six different fingertip metrics **(A)** surface area, **(B)** volume, **(C)** temperature, **(D)** between ridge sweat-pore spacing, **(E)** within ridge sweat-pore spacing, and **(F)** sweat-pore density), plotted against age. Black lines: least-squared linear fits.

Figure 4. Tactile spatial acuity as a function of the six fingertip metrics **(A – F)**. Black lines: best-fit exponential curves from multiple regression together with age.

Figure 5. Tactile spatial acuity from childhood into adulthood. Filled circles: current study; open circles: Peters et al., (2009). **(A and B)** results of simple linear regressions. **(A)** threshold vs. age. **(B)** threshold vs. fingertip surface area. In **(A)** and **(B)**, for plotting purposes only, we have omitted the data point from the oldest participant, a 27.29 year-old from Peters et al., (2009) (threshold 1.22 mm, area-adjusted threshold, 1.30 mm). **(C and D)** results of multiple regression with both age and surface area as independent variables. **(C)** surface area-adjusted threshold vs. age. **(D)** age-adjusted threshold vs. surface area. In **(C)** and **(D)**, thresholds were respectively adjusted to the mean surface area and age of the aggregate participant sample. Black solid curves in all panels: least-squared

exponential fits.

3.9 Tables and Figures

Table 1.

Sex	Age										
	6	7	8	9	10	11	12	13	14	15	16
Girls	2	1	5	5	5	5	5	5	5	5	6
Boys	4	2	5	5	5	5	5	5	5	5	5

Table 2.

GBF Criterion				
Current study	1 (n=103)	0.5 (n=100)	0.1 (n=97)	0.01 (n=93)
Fingertip volume, age	p = 0.025, 0.264 β = 0.277, -0.156 R ² = 0.040	p = 0.016, 0.353 β = 0.304, -0.131 R ² = 0.053	p = 0.033, 0.496 β = 0.263, -0.097 R ² = 0.043	p = 0.094, 0.947 β = 0.196, -0.010 R ² = 0.036
Between-ridge pore spacing, age	p = 0.049, 0.541 β = 0.200, -0.074 R ² = 0.029	p = 0.055, 0.818 β = 0.197, -0.028 R ² = 0.033	p = 0.110, 0.983 β = 0.152, 0.003 R ² = 0.024	p = 0.123, 0.701 β = 0.146, 0.048 R ² = 0.031
Fingertip surface area, age	p = 0.059, 0.362 β = 0.236, -0.137 R ² = 0.026	p = 0.031, 0.405 β = 0.281, -0.124 R ² = 0.042	p = 0.073, 0.610 β = 0.223, -0.078 R ² = 0.030	p = 0.129, 1.000 β = 0.175, 0.000 R ² = 0.031
Including young adults				
	1 (n=200)	0.5 (n=197)	0.1 (n=194)	0.01 (n=190)
Fingertip surface area, age	p < 0.001, 0.008 β = 0.373, -0.265 R ² = 0.067	p < 0.001, 0.014 β = 0.397, -0.245 R ² = 0.079	p < 0.001, 0.028 β = 0.380, -0.219 R ² = 0.074	p < 0.001, 0.035 β = 0.364, -0.210 R ² = 0.069

Figure 1.

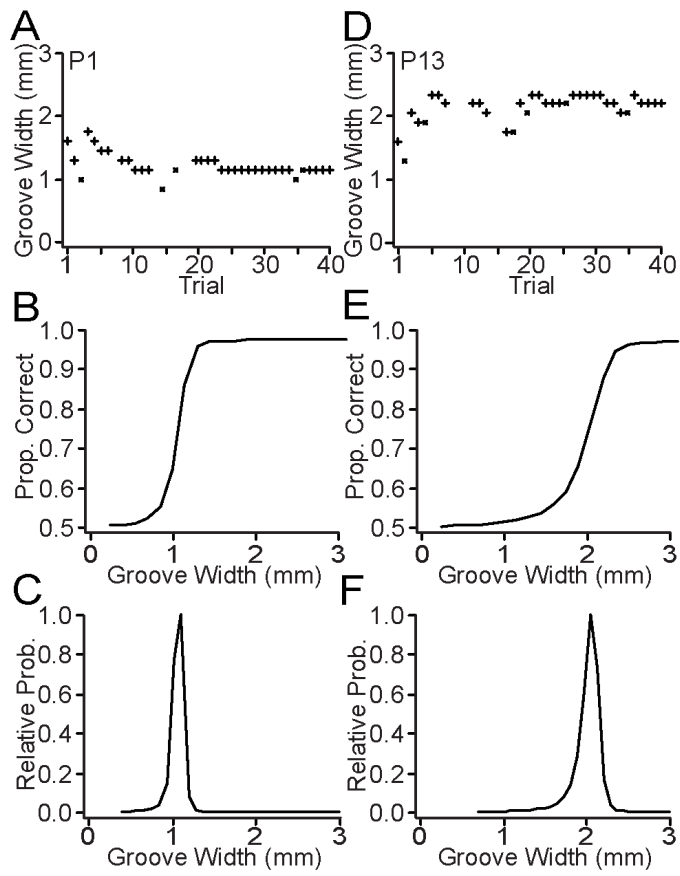


Figure 2.

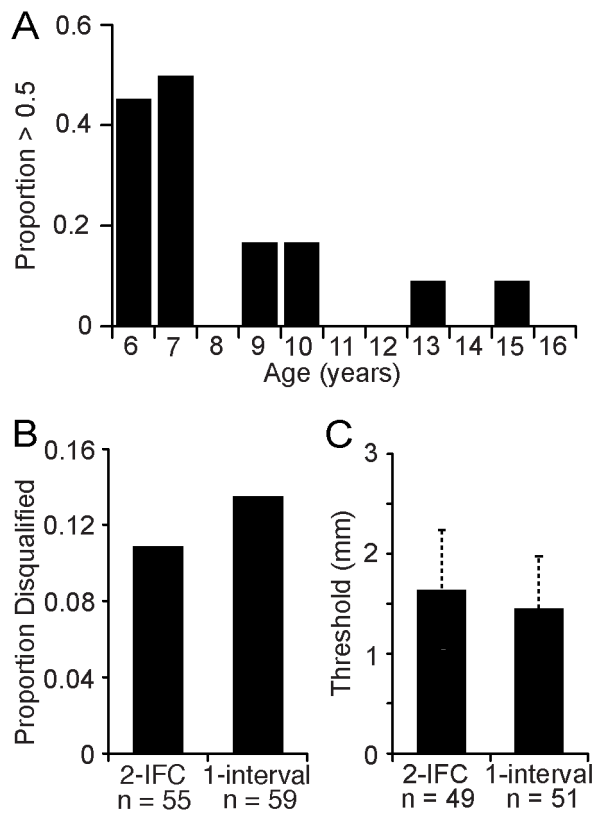


Figure 3.

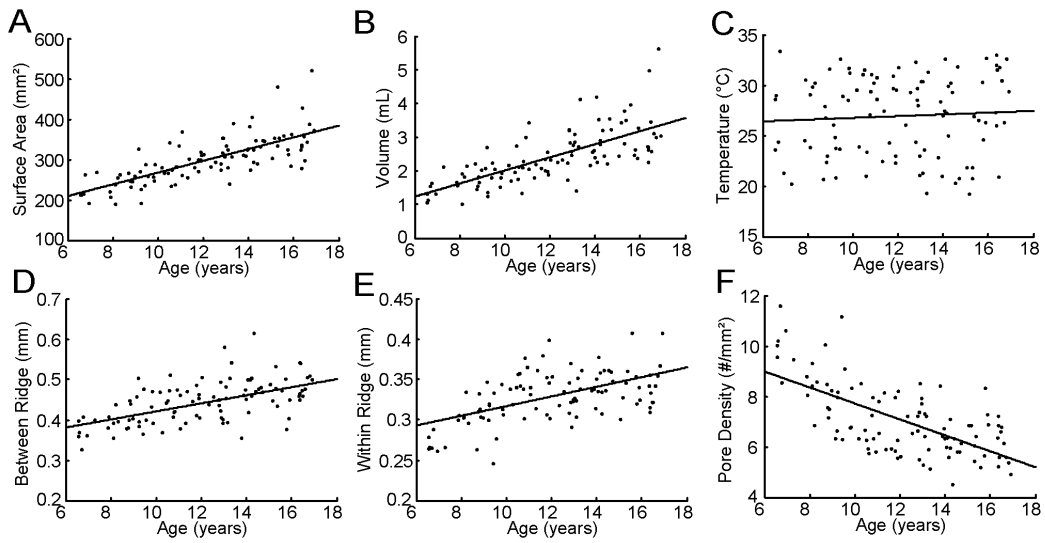


Figure 4.

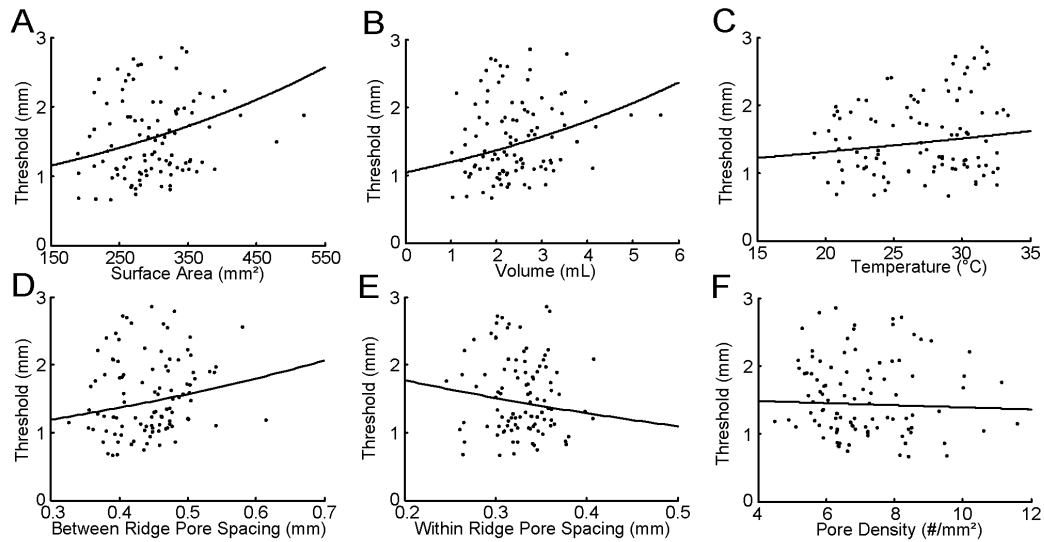
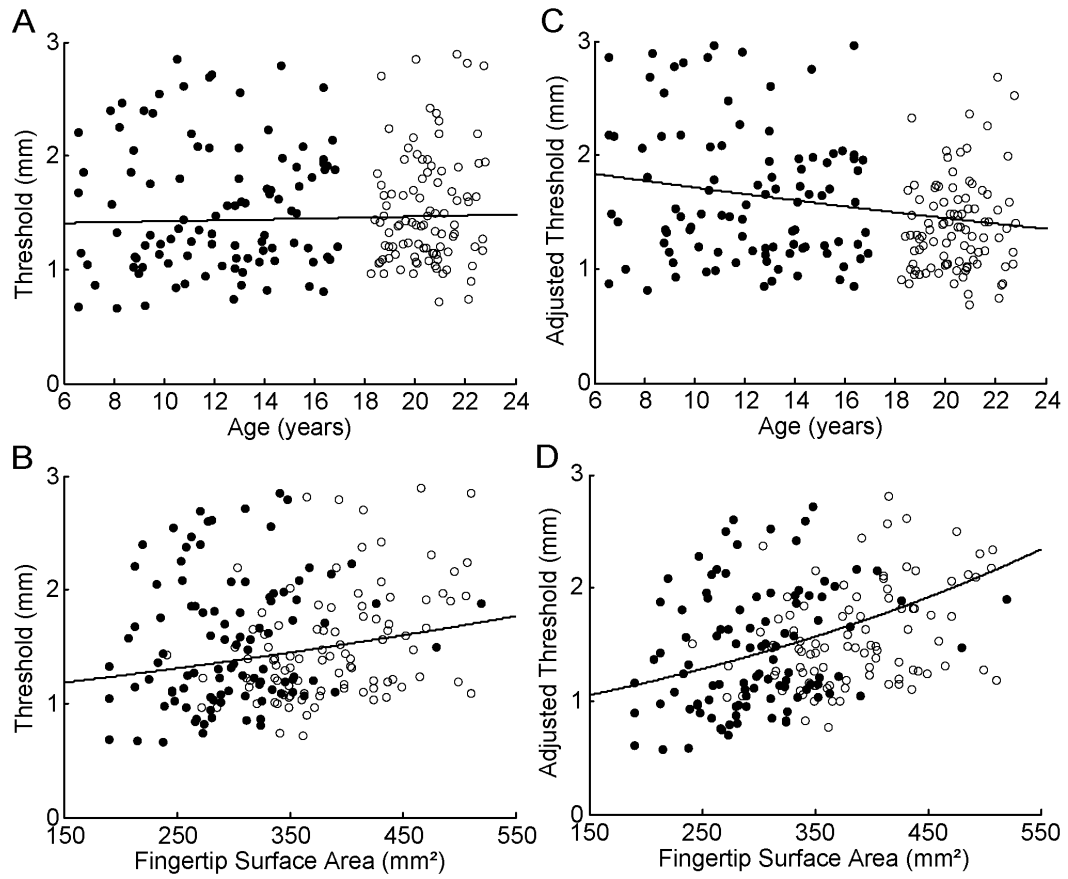


Figure 5.



Chapter 4

4.1 Preface

In this chapter we explore the fingertip size effect on a theoretical and computational basis. Chapters 2 and 3 provide empirical support for the hypothesis that fingertip size significantly predicts tactile spatial acuity. Aggregating the data presented in these two chapters reveals the average fingertip surface area effect on tactile spatial acuity from childhood into young adulthood; it also provides an estimate of the best performance at each fingertip surface area which becomes interesting when comparing human and optimal performance. To explore the fingertip size effect on tactile spatial acuity, we simulate the responses of primate peripheral afferents and somatosensory cortical neurons, and use ideal observer analysis to model performance on the grating orientation task.

We show that average human tactile spatial perception is sub-optimal in that it appears humans do not make use of all the sensorineural information available when making tactile spatial discriminations. We further speculate on biologically plausible sources for this sub-optimality.

4.2 Abstract

We take for granted our ability to perceive the external world, but how does the brain accomplish this remarkable feat? Much is understood about the neural response to physical stimuli, but little about perception (how the brain interprets sensorineural activity to infer the state of the external world). Does human perception make optimal use of the available sensorineural information to form a percept? Here we describe a Bayesian ideal observer model that characterizes the theoretical upper limit of somatosensory perception. Based on the response properties of primate peripheral afferents and somatosensory cortical neurons, described by other laboratories, we simulate neuronal responses to square-wave gratings statically indented into the skin. Our model optimally infers, from this sensorineural activity, the orientation of the grating stimulus, allowing comparison to human performance on the grating orientation task.

The Bayesian ideal observer – when provided access to SA1 firing rates – greatly outperforms average human observers on the grating orientation task. We explore the question of why, specifically, human perception is suboptimal in this sense. We show that the performance of the Bayesian observer worsens as neural firing rates grow noisier, the number of independent neurons is reduced, and stimulus integration time is shortened. We also show that the fingertip size effect emerges only when the ideal observer makes particular sub-optimal assumptions about the afferent responses. Whether and to what degree these limitations characterize human sensory processing remains to be determined.

4.3 Introduction

We sought to synthesize previously collected neurophysiological and anatomical data into a unified (Bayesian) framework, focussing on the processing of cutaneous input originating from the fingertips. With this model, we attempt to better-understand our ability to perceive the orientation of edges indented into the skin, and specifically, to develop a theoretical understanding of the empirically observed effect of fingertip surface area on human tactile spatial acuity (Peters et al., 2009; Wong et al., 2013; Peters & Goldreich, Submitted).

Ideal observers are theoretical devices that enable us to quantify the amount of information available on a given task. They also provide us with a benchmark against which we can compare human performance. The standard of optimality is useful when trying to interpret human perceptual abilities, particularly when constraints imposed on the quality of the information provided to the ideal observer have an anatomical and physiological basis. If human perception is sub-optimal, it becomes interesting to consider the possible source(s) of this sub-optimality; we pursue this idea throughout this chapter. These models have two major components: an *encoding model* (also referred to in the literature as a ‘*generative*’ or ‘*forward*’ model), which simulates the sensorineural response to a given stimulus, and a *decoding model*, which utilizes probability theory to infer the most probable stimulus given the evoked sensorineural response.

The use of ideal observer analysis has a rich history in the study of human visual and auditory perception, dating back to the 1950’s. For instance, Wilson

Geisler and colleagues have elegantly applied ideal observer analysis to study a number of visual phenomena including photon detection and the discrimination of stimuli ranging from dot patterns to complex objects and natural scenes (e.g. Geisler, 1984; Geisler & Davilla, 1985; Geisler, 1989; Geisler & Albrecht, 1997; Geisler et al., 2001). One interesting application – which is the approach we take here – is sequential ideal observer analysis (Geisler, 1989), with the goal being to characterize the transformation of the information content at sequential levels of a given sensory system. Here we wish to extend these ideas to the study of human tactile spatial perception by examining two different levels of the somatosensory system: the SA1 afferent population, and area 3b neurons in the primary somatosensory cortex (S1).

It is generally accepted that the slowly-adapting type 1 (SA1) primary afferent population carries the highest-resolution spatial representation of edges in contact with the skin (for review see Johnson, 2001). In the early 1980's, Phillips and Johnson (Johnson & Phillips, 1981a; Phillips & Johnson, 1981a; 1981b) demonstrated that the SA1 afferent population has greater spatial modulation in its response profile than any other receptor type when bars and gratings are indented into the distal finger pads of macaque monkeys. Furthermore, Phillips and Johnson (Johnson & Phillips, 1981a; Phillips & Johnson, 1981a; 1981b) demonstrated that only the SA1 afferents could account for human psychophysical performance. For this reason, and for simplicity, here we limit our analysis to the SA1 population response. Rapidly-adapting type 1 (RA1) primary afferents –

which are the only other receptor class possessing small enough RFs and high enough innervation density to resolve details on the order of 1 mm – likely contribute less information to spatial perception, and may in fact interfere with, and reduce the high-resolution spatial signal sent through the SA1 afferents (Bensmaia et al., 2006; 2008b).

To simulate the primary afferent population response, we use a continuum mechanics model of the skin. We implement the model described by Sripati et al., (2006b), which generalizes the original continuum mechanics model proposed by Phillips and Johnson (1981b), allowing the stimulus to vary over two-dimensions rather than only one. This model simulates the strain profile resulting within the skin in response to indented spatial patterns (see Figure 1A). SA1 afferents are activated by strain applied to the region of their receptor end organs, Merkel cell-neurite complexes. SA1 responses are well-predicted by a linear translation of the strain value sampled at the depth of the receptor end organs (Phillips & Johnson, 1981b; Sripati et al., 2006). The model requires assumptions to be made about the composition of the skin (that it is a homogeneous and isotropic elastic medium, and that it is infinite in extent from the receptor's point of view); nevertheless, it accurately predicts single-unit firing rates to a wide range of tactile stimuli (mean Pearson's $r = 0.87$; Sripati et al., 2006b).

In addition to modeling the peripheral representation of grating stimuli, we also model the responses of neurons in somatosensory cortex (area 3b). Similar to the early stages of visual processing, a sub-population of area 3b cells have RFs

consisting of an excitatory central region and one or more flanking inhibitory regions (DiCarlo et al., 1998; DiCarlo & Johnson, 2000; Sripati et al., 2006a; Bensmaia et al., 2008b). Just like V1 simple-cells, the receptive fields of orientation selective S1 neurons are well-characterized by oriented Gabor spatial filters (Bensmaia et al., 2008b). Previous ideal observer modelling based on the responses of single neurons in S1 indicates that human bar orientation perception can be accounted for by the spike counts of the most orientation selective neurons (Bensmaia et al., 2008b). Here we attempt to characterize the area 3b population response to the square-wave grating stimuli commonly used to test human tactile spatial acuity, and also extend this analysis beyond the single-cell, to a population code. To simulate the response of area 3b neurons, we use Gabor spatial filters that are fit directly to spike counts recorded from area 3b neurons in response to indented bar stimuli (courtesy of Dr. Sliman Bensmaia).

4.4 Methods

197 undergraduate participants (95 men, 102 women; age range = 6.6 to 27.9; mean age = 16.2; SD = 4.8) tested in two previous studies (Peters et al., 2009; Peters & Goldreich, 2013) were used to test the predictions of the ideal observer model. All sensory testing methods are described in detail in Chapters 2 and 3.

Stimulus encoding models

We aim to characterize the information content of SA1 afferent, and S1 (area 3b) sensorineural population responses. Figure 1 provides a schematic

depiction of the SA1 and S1 encoding models used in our ideal observer analysis. This section describes how we simulated stimulus-epoch spike counts based on previously reported neurophysiological data.

Peripheral afferent encoding model

To model the peripheral afferent population, we begin by defining a receptor grid (the black dots in Figure 1C). To do this, we draw a 10 mm by 10 mm square grid with a given receptor (node) spacing. To avoid having the receptor grid occasionally align perfectly with the grating edges, and to more realistically simulate SA1 sampling positions in the skin (e.g., see Figure 6 from Johansson & Vallbo, 1980), we added Gaussian jitter to the x and y coordinates of each node in the square grid. The SA1 receptor x - y sampling positions are also defined in terms of their depth within the simulated elastic medium (i.e. their position within the basal layer of the epidermis), z . According to the continuum mechanics model, the strain profile dampens and becomes less spatially modulated with increasing depth (because the skin acts as a low-pass mechanical filter).

Following Sripati et al., (2006b), we modeled the expected firing rate of each SA1 afferent, $f_{SA1}(S)$, given the stimulus, S , as a positive-rectified linear transformation of the strain value sampled at each afferent's x - y - z position,

$$\varepsilon_{xyz} ,$$

$$f_{SA1}(S)=[a(\varepsilon_{xyz}-b)]^+ . \quad (\text{Equation 1})$$

Here the constants a and b represent the best-fit sensitivity (slope) and threshold (intercept) of the simulated SA1 afferents, respectively.

To generate realistic firing rates however, we need to take into account the noise present in all neural responses. The noise inherent in SA1 firing rates is remarkably low, and will be characterized here by a Gaussian probability distribution function,

$$P(r_{SA1}|f_{SA1}(S)) = \frac{1}{\sigma_{SA1} \sqrt{2\pi}} \exp\left(-\frac{(r_{SA1} - f_{SA1}(S))^2}{2\sigma_{SA1}^2}\right), \quad (\text{Equation 2})$$

where $P(r_{SA1}|f_{SA1}(S))$ is the conditional probability of observing the firing rate, r_{SA1} , given the expected firing rate, $f_{SA1}(S)$. Furthermore, the relationship between SA1 noise magnitude, σ_{SA1} , and the expected firing rate of an SA1 afferent, $f_{SA1}(S)$, is well-approximated by (Vega-Bermudez & Johnson, 1999),

$$\sigma_{SA1} = 0.45 f_{SA1}(S)^{0.21}. \quad (\text{Equation 3})$$

This SA1 noise relationship was determined empirically by Vega-Bermudez & Johnson (1999) for a 200 ms stimulus duration; thus, for the simulations reported here (see Fig 2), we derived the relationship between the mean and standard deviation of SA1 afferent firing rates over a 50 ms temporal interval, given as:

$$\sigma_{SA1} = 0.3 f_{SA1}(S)^{0.21} \sqrt{n} \quad (\text{Equation 4})$$

where n is the number of 50 ms intervals in the total stimulus duration (i.e., if the

total duration is 1000 ms, then $n = 20$). We chose not to show SA1 noise model curves for stimulus durations longer than 100 ms, because the model already far-surpassed human performance at this point. Therefore, to simulate the firing rate of an individual SA1, r_{SA1} , we randomly sampled from the Gaussian density function given in Equation 2, with the standard deviation given by Equation 4. SA1 noise was added in this manner to each afferent firing rate, r_{SA1}^i (which will here on be indexed by superscript, i). We represent the final population response with the vector, \mathbf{r}_{SA1} , which contains the responses of all activated SA1 afferents.

Finally, we recognize that the neural representation relevant to perception is probably not the peripheral afferent population response. Neural responses in the cortex tend to have much greater variability: the variance in firing rate is nearly equal to the expected firing rate (characteristic of a Poisson process; Sripathi et al., 2006a). In our analysis, we consider the possibility that cortical neurons responsible for making perceptual decisions simply have direct access to the peripheral afferent representation (i.e. implying 1:1 mapping of peripheral RFs to cortical RFs), but that the noise on their spike counts is generated by a homogeneous Poisson process, where,

$$P(r_{SA1} | f_{SA1}(S)) = \frac{e^{-f_{SA1}(S)} f_{SA1}(S)^{r_{SA1}}}{r_{SA1}!} \quad . \quad (\text{Equation 5})$$

Primary somatosensory cortex encoding model

The cortical representation we consider here is that of area 3b of S1. We adopt a linear spatial filter approach for generating cortical spike counts: a commonly used method for modelling neural responses of V1 simple cells (Daugman, 1988). Here we assume that area 3b RF properties are static with respect to time, although, the time course of excitation and inhibition in these neurons is known (DiCarlo et al., 1998, DiCarlo & Johnson, 2000, Sripathi et al., 2006a); how temporal dynamics in RF structure affect information content is an interesting question for future modelling efforts.

We generate S1 responses by creating a 10 x 10 mm image of the grating strain profile, \mathbf{S} , obtained from the continuum mechanics model (Sripathi et al., 2006b), and model the cortical response as a positive-rectified linear transformation of the dot product between each neuron's RF and \mathbf{S} . Therefore, the expected firing rate of neuron i is,

$$f_{SAI}^i = \left[\alpha \left[e^{\frac{-u^2 + y^2 v^2}{2\sigma^2}} \cos\left(\frac{2\pi \cdot u}{\lambda} + \phi\right) \right] \cdot \mathbf{S} + \beta \right]^+ \quad (\text{Equation 6})$$

where,

$$u = (x - x_c) \cdot \cos(\theta) + (y - y_c) \cdot \sin(\theta) \quad , \quad (\text{Equation 7})$$

and

$$v = -(x - x_c) \cdot \sin(\theta) + (y - y_c) \cdot \cos(\theta) \quad . \quad (\text{Equation 8})$$

Here, x_c and y_c are the x and y components of the center position for each modeled neuron. The parameters of the Gabor function (in Equation 6)

are the wavelength of the sinusoidal factor, λ , the orientation of the filter, θ , the phase offset, ϕ , the standard deviation of the Gaussian envelope, σ , and the spatial aspect ratio of the Gabor, γ , which determines the ellipticity of the Gabor bands. Once again, Poisson firing rate noise was added to the expected response (i.e., $f_{SI}(S)$) as per Equation 4. Because it is unclear how many neurons are used by the CNS to represent a grating stimulus, the question of how sparse to make this representation becomes highly relevant. We know there are diminishing returns to the accuracy of inference as the number of neurons on which the inference is based increases. As the number of neurons in the representation increases, performance of an unbiased estimator will asymptotically approach the Cramer-Rao lower bound (Paradiso, 1988; Dayan & Abbott, 2001), the theoretical apex of performance given the constraint of tuning curve shape. However, perceptual decisions may rely on the activity of only a few highly selective neurons (Geisler, 1997; Olshausen & Field, 2004; Bensmaia et al., 2008b). To investigate this, here we parametrically vary the area 3b population size.

Fitting the encoding models to neurophysiological data

To fit the peripheral afferent model we created custom LabVIEW fitting programs that determined the set of parameters that provided the least-squared fit between the simulated SA1 afferent responses and the average SA1 modulation index reported over a range of grating groove widths (Phillips & Johnson, 1981a;

we fit their Figure 8 for the static phase of indentation – middle panel). The spatial modulation index (MI) is a measure of how sensitive SA1 afferents are to edges, and is calculated as:

$$MI = \left(\frac{r_{max} - r_{min}}{r_{max} + r_{min}} \right) \quad (\text{Equation 9})$$

In this equation, r_{max} and r_{min} correspond to the maximum and minimum observed firing rates, respectively, for a given SA1 afferent when a square-wave grating is stepped in 0.2 mm increments across the afferent's RF, indenting the grating at each step. Due to the enhanced edge sensitivity of SA1 afferents, r_{max} will occur when an edge is indented into the afferent's hotspot (skin site of maximum excitability), and r_{min} will occur when a groove (i.e. no edge) overlies the afferent's hotspot. Phillips & Johnson (1981a) recorded the average SA1 modulation index for groove widths ranging from 0 (smooth) to 3 mm; however, we only fit from 0.5 to 2 mm because this provided better fits in the region that matters most (the observer's threshold is always less than 2 mm for the simulations reported here).

For the peripheral afferent model, the parameters that we fit were receptor depth, sensitivity, and threshold, as well as the relative weighting of maximum compressive to maximum tensile strain. We took the weighted average between maximum compressive and maximum tensile strain as the candidate strain component that model SA1s transduced, because this provided better fits to the neurophysiology than using either strain component independently. Previously,

Phillips & Johnson (1981b) favoured maximum compressive strain, and Sripathi et al., (2006b) favoured maximum tensile strain; thus, both strain components are strong candidates according to the literature. Seeing as there is no reason to think that only one of these strain components must be involved, we took the weighted average between maximum compressive and maximum tensile strain as the candidate strain component here. The best fit parameters were: indentation depth = 1200, sensitivity = 190, threshold = 0.0055, max. compressive-to-max. tensile weight = 0.85. With this set of parameters, the model fits the average SA1 modulation index during the static phase of indentation well (Max. rate fit: Pearson's $r = 0.982$; Min. rate fit: Pearson's $r = 0.598$; Mean Pearson's $r = 0.79$). It is also important to note the large error bars on the mean values shown in the original figure from Phillips & Johnson (1981a; see their Figure 8).

For the cortical encoding model, we used macaque (*Macaca mulatta*) area 3b receptive fields provided to us by Dr. Sliman Bensmaia (University of Chicago). The responses of cortical neurons to single bars indented at various orientations and positions relative to the RF center were fit with Gabor spatial filters (Bensmaia et al., 2008b). This fitting was done with custom MATLAB programs written by Dr. Bensmaia and colleagues. Because these Gabor RFs were derived from recordings made while indenting single bars, not grating stimuli, and we wanted to generalize our model to gratings as well as other spatially-structured stimuli like points or embossed letters, we decided to use the strain profile as input to the Gabor (rather than use a binary image of the stimulus, as in Bensmaia

et al., 2008b). Our reasoning was that the strain profile might better capture non-linear changes that occur due to skin mechanics when more than one bar is indented (i.e. a square-wave grating or the letter A). To do this, we adjusted the response of the Gabors using strain profiles of a bar as input (new method) such that it best-matched the response of the Gabors using binary images of a bar as input (original method); to accomplish this, we found the scale factor to apply to the output of the new method, that provided the least-squared fit to the output of original method. Again using custom LabVIEW fitting software, we found that a scale factor of 0.09 gave the best fit. When we apply this scale factor to the response of the Gabor using grating strain images as the input, we get stimulus-epoch spike counts that agree well with empirically observed spike counts (Burton & Sinclair, 1994; Sinclair et al., 1996; Personal communications with Dr. Sliman Bensmaia).

Stimulus decoding models

To examine information at different levels of the somatosensory system we analyze the performance of Bayesian decoding models that are provided with either peripheral afferent or cortical responses. Optimal performance is obtained by making decisions based on evaluation of the likelihood function or competing model likelihoods, which provides an unbiased estimate of latent stimulus parameters (Green & Swets, 1966; Dayan & Abbott 2001). Here we analyze the performance of three decoding models, each differing in terms of the assumptions made about the sensorineural data.

Decoder One (Optimal)

We begin with a decoder that “knows” everything (e.g., with the SA1 encoding model it knows the receptor x - y - z positions, thresholds and sensitivities, as well as the stimulus indentation depth, and duration). This is equivalent to stating that Decoder One knows the stimulus-response function for each of its neurons, a common assumption made in previous probabilistic population code models (e.g., Jazayeri & Movshon, 2006; Gold & Shadlen, 2007). To determine the probability of each grating orientation for each trial, we calculate the probability of observing the population response, \mathbf{r} , given each possible grating orientation. This was calculated for the case of Gaussian noise as,

$$P(\mathbf{r}|f_i(S)) = \prod_i P(r_i|f_i(S)) = \prod_i \frac{1}{\sigma_{SA1} \sqrt{2\pi}} \exp\left(-\frac{(r_i - f_i(S))^2}{2\sigma_{SA1}^2}\right) \quad (\text{Equation 10})$$

and for the case of Poisson noise as,

$$P(\mathbf{r}|f_i(S)) = \prod_i P(r_i|f_i(S)) = \prod_i \frac{e^{-f_i(S)} f_i(S)^{r_i}}{r_i!} \quad (\text{Equation 11})$$

where, $P(r_i|f_i(S))$ is the likelihood for the i -th neuron in the population,

$f_i(S)$ is the stimulus-response function of that particular neuron, and r_i is the observed firing rate.

To simulate the grating orientation task we indented a horizontal grating (of variable spatial frequency and randomized phase) 1 mm into the simulated skin, and had the ideal observer determine whether the sensorineural data (i.e., the afferent population response during the static phase of indentation, \mathbf{r}) was

more probable given a horizontal or a vertical grating orientation. These two hypotheses about orientation (vertical and horizontal) are really compound statistical models, not simply hypotheses, because an optimal inference regarding grating orientation needs to incorporate sub-hypothesis for all the possible grating spatial frequencies and phases, and needs to marginalize over these so-called “*nuisance parameters*” (parameters other than grating orientation in this case). Accordingly, we computed the likelihood of the horizontal orientation model (M1) as,

$$P(\mathbf{r}|M1) = \sum_{GW} \sum_{\phi} \prod_i P(r_i|GW, \phi, M1) P(GW, \phi|M1) \quad , \quad (\text{Equation 12})$$

and the likelihood of the vertical orientation model (M2) as,

$$P(\mathbf{r}|M2) = \sum_{GW} \sum_{\phi} \prod_i P(r_i|GW, \phi, M2) P(GW, \phi|M2) \quad . \quad (\text{Equation 13})$$

Finally, to compare models, we computed the likelihood ratio (LR) between them,

$$LR = \frac{P(\mathbf{r}|M1)}{P(\mathbf{r}|M2)} \quad . \quad (\text{Equation 14})$$

which is equivalent to the posterior odds, given that we applied a uniform prior over the models. If this ratio is greater than 1, the observer has correctly identified the horizontal grating orientation; this same decision variable was used for all simulations. GW and ϕ correspond to all possible grating groove widths (0.5 to 2 mm, in 0.5 mm steps), and all possible grating phases (from 0 to $2 \times GW$, in steps of 0.2 mm), respectively.

Decoder Two (“Knows” it is uncertain regarding receptor location)

The next decoder we simulated is uncertain about the x - y position of each of its neurons, and “knows” this to be the case. To deal with its uncertainty, Decoder Two marginalizes over a square grid of hypothesized positions for each receptor (with a fixed 0.1 mm node spacing), centered on each receptor's actual position. To parametrically vary the strength of Decoder Two's assumption, we varied the hypothesized ranges for possible receptor locations (the size of the square hypothesized receptor grids) from ± 0.3 to 0.9 mm. This marginalization should recover much of the information not provided to Decoder Two (i.e., the actual receptor positions); thus, little difference should be observed between the performance of Decoders One and Two.

For Decoder Two, the model likelihoods are calculated as (note the additional sum over possible receptor locations),

$$P(\mathbf{r}|M) = \sum_{xy} \sum_{GW} \sum_{\phi} \prod_i P(r_i|xy, GW, \phi, M) P(xy, GW, \phi|M) \quad .$$

(Equation 15)

Decoder Three (Mistaken about receptor location)

The final decoder we consider is incorrect about the x - y position of each of its neurons. Sub-optimally, Decoder Three assumes fallacious receptor x - y positions drawn from 2D Gaussians, each centered on the actual receptor grid positions used to generate the population response. To parametrically vary the strength of Decoder Three's assumption in a manner similar to varying the range

of possible receptor positions for Decoder Two, we varied the SD of these 2D Gaussians from 0.3 to 0.9 mm. (in 0.2 mm steps; the various curves are depicted in Figure 4A and 4B). The likelihood computation is therefore identical to that of Decoder One; however, Decoder Three is just slightly-mistaken about the position of each neuron's RF center, and thus, slightly-mistaken about the response to expect.

Decoding model assumptions

We did not implement prior expectation for any particular grating orientation, groove width, or phase – uniform priors were used over these stimulus parameters. All three decoders assumed that the stimulus-epoch spike counts of different neurons within the population were conditionally independent, given the stimulus. The decoders also “knew” the structure of the noise to be Gaussian or Poisson (i.e., Equation 2 or 5).

Model simulations

All simulations were carried out using LabVIEW 11 (National Instruments). To quantify each decoding model's performance, we used the method of constant stimuli and linearly interpolated the groove width resulting in 69% correct performance (where $d\text{-prime} = 1$ for the single interval version of the grating orientation task simulated here). The human thresholds used for comparison also correspond to performance where $d\text{-prime} = 1$ (Peters et al., 2009; Peters & Goldreich, Submitted). We estimated the ideal observer's proportion correct with the method of constant stimuli. For the peripheral afferent

encoding model, we simulated 1000 yes-no trials for each groove width (grating phase randomized across trials), under each parameter setting (e.g., stimulus duration). For the cortical encoding model, we attempted to more closely capture the real-world scenario where each observer deploys a particular set of cortical neurons, and bases its decisions on that particular set of neurons throughout testing. Accordingly, we reduced the number of trials to 50 per groove width and repeated the interpolation 20 times – each time with a unique Gabor population; in the results, we report the mean threshold estimate across the 20 blocks, as well as +/- 1 standard error. Because human perception might integrate only a portion of the evoked sensorineural information to reach decisions (e.g., 100 ms worth of spiking activity, even though 1000 ms worth was available), we varied the duration of the stimulus integration window from 50 to 1000 ms.

4.5 Results

First, we investigate performance of the three decoding models using the peripheral afferent encoding model, and attempt to capture the previously reported effect of fingertip size (Peters et al., 2009; Peters & Goldreich, Submitted). Then we examine Decoder One's (optimal) performance when basing its decisions on cortical (area 3b) responses, rather than peripheral afferent responses.

The effect of fingertip size on human tactile spatial acuity

By aggregating the data from two previous studies involving a total of 197 participants (Peters et al., 2009; Peters & Goldreich, Submitted; Figure 2A), and calculating the average groove width threshold in 50 mm²-wide fingertip surface

area bins, we obtain an estimate of the average effect of fingertip size on human tactile spatial acuity (Figure 2A blue curve), as well as an estimate of the best possible performance in each fingertip size bin (Figure 2B diamonds). A linear regression on the fingertip size bin averages revealed a significant effect of fingertip surface area ($r = 0.88$, one-tailed $p = 0.004$; slope = 0.15 mm/cm^2 ; 95% CI = 0.06 mm/cm^2 to 0.24 mm/cm^2); an additional linear regression on the best thresholds in each fingertip size bin also revealed a significant effect of fingertip surface area ($r = 0.91$, one-tailed $p = 0.002$; 0.16 mm/cm^2 ; 95% CI = 0.08 mm/cm^2 to 0.25 mm/cm^2). Thus, it is quite clear that a relationship exists between fingertip surface area and tactile spatial acuity, but under what circumstances would an ideal-observer predict this?

From the aggregate data (Peters et al., 2009; Peters & Goldreich, Submitted; Figure 3A), we derived a theoretical relationship between human fingertip surface area and average SA1 afferent spacing. Given that we know the average index fingertip surface area was 346.87 mm^2 , and that an estimate of mean SA1 receptor spacing at the fingertip is 1.2 mm (Johansson & Vallbo, 1979), and if we assume that SA1 receptor number is actually fixed between individuals (an extreme statement of the fingertip size hypothesis), then the average SA1 density at the fingertip is,

$$\frac{1}{(1.2 \text{ mm}/SAI)^2} = 0.694 \text{ SAIs/mm}^2 \quad (\text{Equation 16})$$

and thus, the estimated total number of SA1 afferents in the average fingertip is,

$$346.86 \text{ mm}^2 \times 0.694 \text{ SAIs/mm}^2 \approx 241 \text{ SAIs} \quad . \quad (\text{Equation 17})$$

If we assume that the number of SA1 afferents is conserved between individuals, then we can estimate an individual's SA1 density at the fingertip as,

$$\text{Estimated SA1 Density} = \frac{241}{\text{Fingertip Surface Area}} \quad (\text{Equation 18})$$

and estimate their SA1 spacing at the fingertip as,

$$\text{Estimated SA1 Spacing} = \frac{1}{\sqrt{\text{SA1 Density}}} \quad (\text{Equation 19})$$

Using the above equations, we took the entire range of aggregated fingertip surface areas (191.61 to 516.77 mm²), and converted that to a range of corresponding estimated SA1 spacings at the fingertip (0.89 to 1.46 mm). We then plugged this range (0.9 to 1.5 mm in 0.3 mm steps) of estimated fingertip SA1 spacings into the model to see if it would evoke the fingertip size effect reported previously (0.15 mm/cm² – Peters et al., 2009; Peters & Goldreich, Submitted).

Decoder One – Peripheral Afferent Responses

It is clear that the optimal decoder – regardless of using peripheral (Gaussian) or cortical (Poisson) noise, and regardless of reductions in the window of sensorineural integration (i.e., the stimulus duration) – appears to be affected very little by changes in fingertip size. For all the curves depicted in Figure 3, the average slope of the linear regression line was just a 0.02 mm threshold increase / cm² surface area, a much shallower slope than the effect of fingertip size on human tactile spatial acuity reported previously (Peters et al., 2009; Peters &

Goldreich, Submitted). For the various Poisson noise model curves (Figure 3, grey scale lines), reducing the stimulus integration window caused a gradual upward curve shift; however, the slope remained essentially flat (mean slope = 0.02 mm/cm²). The closest-to-human regression slope was obtained with Poisson noise and an integration window of 50 ms (0.04 mm/cm²); however, this slope still falls below the 95% confidence interval for the human regression slope (0.06 to 0.24 mm/cm²). Results of the Poisson noise model do suggest the tantalizing possibility that the very best human performance might in fact be optimal (as seen by the close correspondence between Decoder One's curves and the best performance in each fingertip size bin in Figure 3).

Decoder Two – Peripheral Afferent Responses

Next we wanted to simulate a decoder that can optimally deal with uncertainty in receptor location, and recover performance levels similar to that of the optimal Decoder One. We did this by having Decoder Two make hypotheses about each afferent's x - y position; for each afferent, Decoder Two set up a square grid of hypothesized locations, which was always centered on the true afferent location, but ranged in size +/- 0.3 mm to +/- 0.9 mm (with a constant 0.1 mm grid step size). Decoder Two then marginalized over all possible afferent locations (as well as grating phases and groove widths), to find the probability of each grating orientation (see Methods). Figure 5 shows 100 ms stimulus duration model curves when the size of the square grids of hypothesized receptor locations was increased from +/- 0.3 mm to +/- 0.9 mm (grey scale curves). It is clear that

Decoder Two attains the performance level of Decoder One, and there is very little effect of changing the range of hypothesized locations. The average slope for the curves shown in Figure 4 was 0.04 mm/cm^2 . As we expanded the range of the possible receptor positions to $\pm 0.9 \text{ mm}$, the slope of the regression line approached the human regression slope (0.11 mm/cm^2); the average regression slope for the remaining three curves shown in Figure 4 was 0.02 mm/cm^2 .

Decoder Three – Peripheral Afferent Responses

Having shown that Decoder Two was able to recover much of information it was not provided (i.e., the actual receptor positions) by marginalizing over a grid of possible receptor positions, we wanted to simulate one final decoder that was simply mistaken about the x - y positions of its neurons. Due to this, Decoder Three was also mistaken about the stimulus-epoch spike count to expect from each neuron, given the tactile stimulus – distorting its ability to decode the peripheral afferent response. To vary the amount by which Decoder Three was mistaken, we varied the SD of the 2D Gaussians, centered on the actual receptor x - y positions, from which the fallacious x - y positions were drawn (see Figure 5A and 5B; curves generated using SDs of 0.3 mm to 0.9 mm, in 0.2 mm steps). The different panels of Figure 5 were generated using 1000 ms (Figure 5A) and 100 ms (Figure 5B), respectively. Increasing the SD had a pronounced effect on the model's threshold, elevating the curves into the range of average human performance on the grating orientation task. The average slope for the 1000 ms model curves (Figure 5A) was 0.03 mm/cm^2 , which was shallower than the

average effect of finger size; thus, when Decoder Three integrated spikes over a 1000 ms window, the effect of increasing error in receptor position elevated the model thresholds, but failed to replicate the fingertip size effect. For the 100 ms model curves (Figure 5B), the average slope was 0.13 mm/cm^2 , and ranged from 0.05 mm/cm^2 with an SD of 0.3 mm, up to 0.26 mm/cm^2 with an SD of 0.9 mm; thus, when Decoder Three integrates spikes over a 100 ms window, the effect of increasing error in receptor position reproduced the average fingertip size effect, and even approximately replicated the 95% confidence interval for the human regression slope value when the SD is varied from 0.3 to 0.9 mm (the various curves in Figure 4B). Based on this analysis, it appears that the effect of fingertip size on tactile spatial acuity might be the by-product of two sources of sub-optimality on behalf of human observers: 1) a limited (e.g., 100 ms) temporal stimulus integration window, and 2) slight error in the CNS's ability to know the exact skin region covered by each of its afferent RFs (i.e., receptor position).

Decoder One – Cortical Neuron Responses

Lastly, we examined performance of the optimal decoder when it based its decisions on the responses of area 3b cortical neurons, rather than SA1 afferents. When modelling the cortical responses, the question quickly becomes: on how many cortical neurons does the CNS base its decisions? As the number of neurons in the representation increases, performance of an unbiased estimator asymptotically approaches the Cramer-Rao lower bound (Paradiso, 1988; Dayan & Abbott, 2001); to show this, we considered a range of neuronal population sizes

(see Figure 6), increasing the population size until performance saturated at what is likely the Cramer-Rao lower bound for the area 3b cortical model described here (Figure 6B). Due to the inhomogeneity of tuning curves used in our model (because we used actual area 3b RFs, not idealized Gaussian envelopes), we could not readily derive the Cramer-Rao lower bound analytically, and increasing the population size much beyond 1225 neurons led to memory allocation issues; however, performance appears to converge around 0.6 mm. We note that Paradiso (1988) simulated up to 10,000 neurons in a cortical hyper-column model for visual orientation discrimination, and performance still did not asymptote entirely. Just how many neurons are required to form a perception remains a mystery, but by determining the population size that results in average human performance given the 100 ms stimulus-epoch spike counts simulated here (Figure 6A), we estimate the number to be around 200 independent neurons. The exact number of neurons will depend on the stimulus integration window used by the observer, as well as the degree of correlated firing between neurons within the population.

4.6 Discussion

Throughout evolution, nervous systems have devised myriad ways of converting energy impinging on the body into neural activity. A major challenge the nervous system faces is decoding this neural activity to reconstruct the external world (perception). An increasingly popular viewpoint of the way nervous systems solve this problem – often called ‘the inverse problem’ – lies within the framework of probability theory. Population responses may represent

probability distributions over sensory variables within the CNS, and this information might be passed along to sequential processing centers in a hierarchical structure. The optimal way of manipulating probability distributions is Bayesian inference: this has led to its resurgence in modern neuroscience (Knill & Richards, 1996; Doya et al., 2008). How probabilistic computations could be implemented in biological systems remains an interesting and open question, although plausible theories do exist (e.g. Rao, 2004; Averbek et al., 2006; Jazayeri & Movshon, 2006; Gold & Shadlen, 2007; Deneve, 2008; George & Hawkins, 2009).

Sources of sub-optimality in human perception

Unlike the combination of multiple sources of sensory information (e.g., visual and haptic), which humans appear to do optimally (Ernst & Banks, 2002; Ernst & Bühlhoff, 2004), the utilization of sensorineural information within each given sensory modality does not appear to be entirely optimal. An interesting question arises at this point: what is the source(s) of this sub-optimality? Here we show that performance of the model worsens as neural noise is increased (e.g., Gaussian vs. Poisson noise), as the number of independent neurons is decreased, and as the temporal window of sensorineural integration is reduced.

How well do these factors characterize human perception? An increase in noise certainly occurs in the somatosensory system, from the periphery (where noise is well-approximated by a narrow Gaussian distribution: Vega-Bermudez & Johnson, 1999) to area 3b (where noise becomes Poisson, or Poisson-like: Sripati

et al., 2006a). In terms of neuronal population size, whether one considers afferent receptor density or the number of neurons used for neural decoding in the CNS, reducing the size of the population conveying information about the stimulus results in degraded performance. Finally, the temporal window of integration is another factor that could limit human perception; although we indented grating stimuli for 1000 ms, it is likely that the central neural decoder only based its decisions off a fraction of the total sensorineural data. There is converging evidence in vision as well as olfaction that the window of temporal integration might be around 200 to 300 ms (for review, see Uchida et al., 2006). Limited research has attempted to determine the temporal window of integration for the sense of touch, and never before has this been investigated for human grating orientation task performance. Interestingly, 200 to 300 ms is in close agreement with the findings of Bensmaia et al., (2008a), who showed a slight decrement in performance on a tactile bar orientation discrimination task when the stimulus duration was reduced from 400 ms to 100 ms. Contrary to this 200 to 300 ms window, Craig (1980) has shown that performance on a tactile pattern recognition task only begins to worsen at stimulus duration below about 50 ms, suggesting the 50 ms is the temporal integration window. Ultimately, the temporal window of stimulus integration might be tightly linked to natural exploration strategies (e.g., saccade duration for vision or possibly contact time during haptic exploration for touch), and could depend on various factors including task difficulty or a cognitive emphasis on performance speed or accuracy, as well as biological

constraints such as adaptation, leaky integration of sensory information, and correlated neural activity (see Uchida et al., 2006). To determine the temporal window for the grating orientation task, future researchers should use progressively shorter stimulus durations in experiments with human participants until performance worsens significantly, indicating that the true temporal window of stimulus integration is being impinged upon.

Emergence of the fingertip size effect on human tactile spatial acuity

The modelling results presented here suggest that the previously observed effect of fingertip size on human tactile spatial acuity (Peters et al., 2009; Peters & Goldreich, 2013) is the byproduct of sub-optimal decoding on behalf of the CNS. Only when we introduced error into the expected response of the modelled neurons did the ideal observers' performance approach that of average human observers. Furthermore, only when we reduced the stimulus duration from 1000 ms to 100 ms did a positive slope occur for the model curves which approximates the previously reported relationship between fingertip size and tactile spatial acuity (Peters et al., 2009; Peters & Goldreich, Submitted). Recently, sub-optimality in human perception has been linked to the inability of the neural decoder to precisely read out probabilities from its likelihood function (Putzeys et al., 2012). Here our decoders optimally read out from their likelihood functions; however, whether the fingertip size effect would appear when a sub-optimal likelihood read-out function is used (Putzeys et al., 2012), should be investigated in future modelling efforts.

We note that, although we introduced error in the expected response by making the decoder slightly mistaken about the location of its RFs, this could have been done in other ways. For instance, the decoder could equivalently be mistaken about the anatomical depths, sensitivities and/or mechanical thresholds of its afferents. Exactly what information the neural decoder has, or could possibly have access to is a crucial question for future researchers to consider. Though it is often assumed that the neural decoder has access to the tuning functions of every neuron (e.g., Jazayeri & Movshon, 2006; Gold & Shadlen, 2007), exactly how this is possible is unclear.

Does the timing of individual spikes matter?

We limit our analysis exclusively to a stimulus-epoch spike count code, even though additional information is presumably available if the ideal observer takes spike timing into account (Rieke et al., 1999). There is evidence that perception of vibrotactile amplitude relies on a firing rate code in primary somatosensory cortex (Harvey et al., 2013), and here we show that a firing rate code sufficiently accounts for human discriminability on the grating orientation task. Some researchers have proposed that the perception of vibrotactile frequency also relies on a firing rate code (Luna et al., 2005); however, there is emerging evidence that the frequency of vibrotactile stimulation is coded in a spike timing reliant manner, and that the neural code used in somatosensory cortex is multiplexed, with vibration amplitude coded by firing rate at long time scales, and vibration frequency coded by spike timing at short time scales (Mackevicius et al.,

2012; Harvey et al., 2013). Interestingly, first spike latency alone has been shown to accurately encode the direction of forces applied to the skin (Johansson & Birznieks, 2004), though the extent to which first spike latency could accurately encode spatial structure (e.g., grating orientation) is not known. We do not rule out the relevance of spike timing in decisions based on surface microgeometry (e.g., discriminating between fabrics), which is a spatial property that cannot be resolved with an SA1 spatial code; this can be illustrated quite clearly by our inability to discriminate between fabrics when they are statically pressed against the skin – only when we scan our fingertips over fabrics are they discriminable. Scanning of fabrics elicits a unique spectral signature of vibration across the the skin surface (Bensmaia & Hollins, 2005; Manfredi et al., 2012), which is likely captured primarily by RA2 (a.k.a. Pacinian channel, PC) afferents in the precise timing of action potentials (Mackevicius et al., 2012). However, for the static grating task modelled here, a spatially modulated spike count code seems appropriate. Indeed, spike count decoders become spike timing decoders as the temporal resolution of the decoder is increased sufficiently, allowing only a single spike to occur in each time step (e.g. see Rieke et al., 1999); thus, our modelling framework could readily be extended to consider models of primary afferent spike timing (e.g. see Dong et al., 2013). A fundamental question in neuroscience remains for future research: what is the temporal window over which sensorineural integration occurs and is it task-dependent?

Conclusions

Here we present an ideal-observer for the study of human tactile spatial acuity. Over the years, a plethora neurophysiological data has been collected detailing the neural response to tactile stimuli; with this work, we sought to synthesize this data into a unified model. Over 30 years ago, Phillips & Johnson (1981b) expressed the need for such a modelling framework (i.e., one that enables examination of “the spatial neural representation of complex stimuli when receptor spacings and sensitivities are not uniform”; p. 1202). Although here we have chosen, out of simplicity, to use uniform receptor sensitivities, the model we present offers a scaffolding upon which progressively more complex, and biologically realistic models of tactile perception may be built.

Our ideal-observer model suggests that human tactile spatial acuity is sub-optimal in that all the sensorineural information available appears not to be utilized. Future work is needed to pin-down what information is actually used in perceptual decisions and to test predictions of this model; for example, how does human performance on the grating orientation task degrade when stimulus duration is reduced, or how does adaptation of particular human and model neurons within the population alter perception?

4.7 References

- Averbeck BB, Latham PE & Pouget A (2006). Neural correlations, population coding and computation. *Nature Reviews Neuroscience*. 7: 358–366.
- Bensmaia S & Hollins M (2005). Pacinian representations of fine surface texture. *Perception & Psychophysics*. 67: 842–854.
- Bensmaia SJ, Craig JC & Johnson KO (2006). Temporal factors in tactile spatial acuity: evidence for RA interference in fine spatial processing. *Journal of Neurophysiology*. 95: 1783–1791.
- Bensmaia SJ, Denchev PV, Dammann III JF, Craig JC & Hsiao et al. (2008b). The representation of stimulus orientation in the early stages of somatosensory processing. *The Journal of Neuroscience*. 28: 776–786.
- Bensmaia SJ, Hsiao SS, Denchev PV, Killebrew JH & Craig JC (2008a). The tactile perception of stimulus orientation. *Somatosensory and Motor Research*. 25: 49–59.
- Burton H & Sinclair RJ (1994). Representation of tactile roughness in thalamus and somatosensory cortex. *Canadian Journal of Physiology and Pharmacology*. 72: 546–557.
- Craig JC (1980). Modes of vibrotactile pattern generation. *Journal of Experimental Psychology: Human Perception and Performance*. 6: 151-166.
- Daugman J (1988). Complete Discrete 2-D Gabor Transforms by Neural Networks for Image Analysis and Compression. *IEEE Transactions on*

Acoustics, Speech, and Signal Processing. 36: 1169–1179.

- Dayan P & Abbott LF (2001). Theoretical neuroscience: computational and mathematical modeling of neural systems. London: *MIT Press*.
- Deneve S (2008). Bayesian Spiking Neurons I: inference. *Neural Computation*. 20: 91–117.
- DiCarlo JJ, Johnson KO & Hsiao SS (1998). Structure of receptive fields in area 3b of primary somatosensory cortex in the alert monkey. *The Journal of Neuroscience*. 18: 2626–2645.
- DiCarlo JJ & Johnson KO (2000). Spatial and temporal structure of receptive fields in primate somatosensory area 3b: effects of stimulus scanning direction and orientation. *The Journal of Neuroscience*. 20: 495–510.
- Dong Y, Mihalas S, Kim SS, Yoshioka T, Bensmaia S & Niebur E (2013). A simple model of mechanotransduction in primate glabrous skin. *Journal of Neurophysiology*. 109: 1350–1359.
- Doya K, Ishii S, Pouget A & Rao RPN (2007). Bayesian brain: probabilistic approaches to neural coding. London: *MIT Press*.
- Ernst MO & Banks MS (2002). Humans integrate visual and haptic information in a statistically optimal fashion. *Nature*. 415: 429–433.
- Ernst MO & Bühlhoff HH (2004). Merging the senses into a robust percept. *TRENDS in Cognitive Sciences*. 8: 162–169.
- Geisler WS (1984). Physical limits of acuity and hyperacuity. *Journal of the Optical Society of America*. A: 775–782.

- Geisler WS (1989). Sequential ideal-observer analysis of visual discriminations. *Psychological Review*. 96: 267–314.
- Geisler WS & Albrecht DG (1997). Visual cortex neurons in monkeys and cats: detection, discrimination, and identification. *Visual Neuroscience*. 14: 897–919.
- Geisler WS & Davila KD (1985). Ideal discriminators in spatial vision: two-point stimuli. *Journal of the Optical Society of America*. A: 1483–1497.
- Geisler WS, Perry JS, Super BJ & Gallogly DP (2001). Edge co-occurrence in natural images predicts contour grouping performance. *Vision Research*. 41: 711–724.
- George D & Hawkins J (2009). Towards a mathematical theory of cortical micro-circuits. *PLoS Computational Biology*. 5: 1–26.
- Gold JI & Shadlen MN (2007). The neural basis of decision making. *Annual Review of Neuroscience*. 30: 535–574.
- Green, D. M., & Swets, J. A. (1966). Signal detection theory and psychophysics. New York: *Wiley*.
- Harvey, M.A., Saal, H.P., Dammann, J.F., & Bensmaia, S.J. (2013). Multiplexing stimulus information through rate and temporal codes in primate somatosensory cortex. *Public Library of Science Biology*. 11: e1001558.
- Hsiao SS, Lane J & Fitzgerald P (2002). Representation of orientation in the somatosensory system. *Behavioural Brain Research*. 135: 93–103.
- Jazayeri M & Movshon JA (2006). Optimal representation of sensory information

by neural populations. *Nature Neuroscience*. 9: 690–696.

Johansson RS & Birznieks I (2004). First spikes in ensembles of human tactile afferents code complex spatial fingertip events. *Nature Neuroscience*. 7: 170–177.

Johansson RS & Vallbo ÅB (1979). Tactile sensibility in the human hand: relative and absolute densities of the four types of mechanoreceptive units in glabrous skin. *Journal of Physiology*. 286: 283–300.

Johansson RS & Vallbo ÅB (1980). Spatial properties of the population of mechanoreceptive units in the glabrous skin of the human hand. *Brain Research*. 184: 353–366.

Johansson RS, Vallbo ÅB (1983). Tactile sensory coding in the glabrous skin of the human hand. *Trends in Neurosciences*. 6: 27–32.

Johnson KO (2001). The roles and functions of cutaneous mechanoreceptors. *Current Opinion in Neurobiology*. 11: 455–461.

Johnson KO & Phillips JR (1981). Tactile spatial resolution. I. Two-point discrimination, gap detection, grating resolution, and letter recognition. *Journal of Neurophysiology*. 46: 1177–1191.

Knill DC & Richards W (2001). Perception as Bayesian inference. New York: Cambridge University Press.

Luna R, Hernandez A, Brody CD & Romo R (2005). Neural codes for perceptual discrimination in primary somatosensory cortex. *Nature Neuroscience*. 8: 1210–1219.

- Mackevicius EL, Best MD, Saal HP & Bensmaia SJ (2012). Millisecond precision spike timing shapes tactile perception. *The Journal of Neuroscience*. 32: 15309–15317.
- Manfredi LR, Baker AT, Elias DO, Dammann III JF, Zielinski MC, Polashock VS & Bensmaia SJ (2012). The effect of surface wave propagation on neural responses to vibration in primate glabrous skin. *Public Library of Science ONE*. 7: e31203.
- Olshausen BA & Field DJ (2004). Sparse coding of sensory inputs. *Current Opinion in Neurobiology*. 14: 481–487.
- Paradiso MA (1988). A theory for the use of visual orientation information which exploits the columnar structure of striate cortex. *Biological Cybernetics*. 58: 35–49.
- Peters RM & Goldreich D (Submitted). The development of tactile spatial acuity from childhood into adulthood.
- Peters RM, Hackeman E & Goldreich D (2009). Diminutive digits discern delicate details: fingertip size and the sex difference in tactile spatial acuity. *The Journal of Neuroscience*. 29: 15756-15761.
- Phillips JR & Johnson KO (1981a). Tactile spatial resolution. II. Neural representation of bars, edges, and gratings in monkey primary afferents. *Journal of Neurophysiology*. 46: 1192–1203.
- Phillips JR & Johnson KO (1981b). Tactile spatial resolution. III. A continuum mechanics model of skin predicting mechanoreceptor responses to bars,

edges, and gratings. *Journal of Neurophysiology*. 46: 1204–1225.

Putzeys T, Bethge M, Wichmann F, Wagemans J & Goris R (2012). A new perceptual bias reveals suboptimal population decoding of sensory responses. *Public Library of Science Computational Biology*. 8: e1002453.

Rao RPN (2004). Bayesian Computation in Recurrent Neural Circuits. *Neural Computation*. 16: 1–38.

Rieke F, Warland D, de de Ruyter van Steveninck R & Bialek W (1999). Spikes: exploring the neural code. London: *MIT Press*.

Sinclair RJ, Pruett Jr., JR, & Burton H (1996). Responses in primary somatosensory cortex of rhesus monkeys to controlled application of embossed grating and bar patterns. *Somatosensory and Motor Research*. 13: 287–306.

Sinclair RJ, Sathian K & Burton H (1991). Neuronal responses in ventroposterolateral nucleus of thalamus in monkeys (*Macaca mulatta*) during active touch of gratings. *Somatosensory and Motor Research*. 8: 293–300.

Sripati AP, Bensmaia SJ & Johnson KO (2006b). A continuum mechanical model of mechanoreceptive afferent responses to indented spatial patterns. *Journal of Neurophysiology*. 95: 3852–3864.

Sripati AP, Yoshioka T, Denchev P, Hsiao SS & Johnson KO (2006).

Spatiotemporal receptive fields of peripheral afferents and cortical area 3b

Ph.D. Thesis – Peters, RM – Psychology

and 1 neurons in the primate somatosensory system. *The Journal of Neuroscience*. 27: 2101–2114.

Uchida N, Kepecs A & Mainen ZF (2006). Seeing at a glance, smelling in a whiff: rapid forms of perceptual decision making. *Nature Reviews Neuroscience*. 7: 485–491.

Vallbo ÅB & Johansson RS (1984). Properties of cutaneous mechanoreceptors in the human hand related to touch sensation. *Human Neurobiology*. 3: 3–14.

Wong M, Peters RM, Goldreich D (2013). A physical constraint on perceptual learning: tactile spatial acuity improves with training to a limit set by finger size. *The Journal of Neuroscience*. 33: 9345–9352.

4.8 Figure Legends

Figure 1. Stimulus encoding models. **(A)** The 2D continuum mechanics model (Sripati et al., 2006b), in which the grating stimulus is defined as a series of indented point loads that together cause a spatially modulated profile of strain within a simulated elastic medium. **(B)** The Gabor spatial filter model for S1 responses (Bensmaia et al., 2008b). To simulate S1 responses, we took the dot product between each neuron's RF (Gabor) and the grating strain profile. **(C)** Neuronal sampling grids. For the 2D continuum mechanics model, strain profiles are sampled at each afferent's x - y - z position (black dots) in the fingertip. For the S1 model, we centered Gabors on each neuron's location (only two Gabors shown for illustration). **(D)** The response of each neuron is then linearly scaled to find the expected firing rate, and noise is added to the expected firing rate that is characteristic of either peripheral afferents (Vega-Bermudez & Johnson, 1999), or cortical neurons (Sripati et al., 2006a).

Figure 2. The effect of fingertip size on tactile spatial acuity, from childhood into young adulthood. **(A)** Aggregated human grating orientation task performance data reported in two previous studies from our lab (Peters et al., 2009; Peters & Goldreich, Submitted). Solid line is the least-squares fitting line for the young adult dataset (Peters et al., 2009), and the dashed line is the least-squares fitting line for the child dataset (Peters & Goldreich, Submitted). **(B)** By discretizing fingertip surface area into 50 mm²-wide bins, we obtained an estimate of the mean (dotted blue curve), and best (diamonds) human performance at each finger size.

The blue shaded region denotes ± 1 SD.

Figure 3. Decoder One – Peripheral afferent responses. Human data from Figure 2B are overlaid on model curves for visual comparison. The two red curves depict SA1 noise simulations using 100 ms (solid), and 50 ms (dashed) stimulus durations. The grey scale curves depict Poisson noise simulations using a range of stimulus integration windows: 1000 ms (black), 500 ms, 250 ms, 100 ms, and 50 ms (lightest grey) windows shown.

Figure 4. Decoder Two – Peripheral afferent responses. Human data from Figure 2B are overlaid on model curves for visual comparison. Shown here are model simulations using a 100 ms stimulus integration window. The grey scale curves depict Poisson noise simulations, each generated using a different range of hypothesized receptor x - y locations centered on the actual location: ± 0.3 mm (black), to 0.9 mm (lightest grey), in 0.2 mm steps.

Figure 5. Decoder Three – Peripheral afferent responses. Human data from Figure 2B are overlaid on model curves for visual comparison. Shown separately are model stimulations using two different stimulus integration windows: 1000 ms (**A**), and 100 ms (**B**). The grey scale curves depict Poisson noise simulations, each generated using a different standard deviation for the 2D Gaussian distributions from which the fallacious receptor x - y locations are drawn: 0.3 mm (black), to 0.9 mm (lightest grey), in 0.2 mm steps.

Figure 6. Decoder One – S1 responses. (**A**) Psychometric functions from model simulations using different populations sizes. Grey scale curves depict the various

population sizes used. The number of neurons used is listed above each curve. **(B)**

Interpolated 69% correct groove width threshold as a function of the number of neurons. Note the diminishing returns on increasing population size.

4.9 Figures

Figure 1

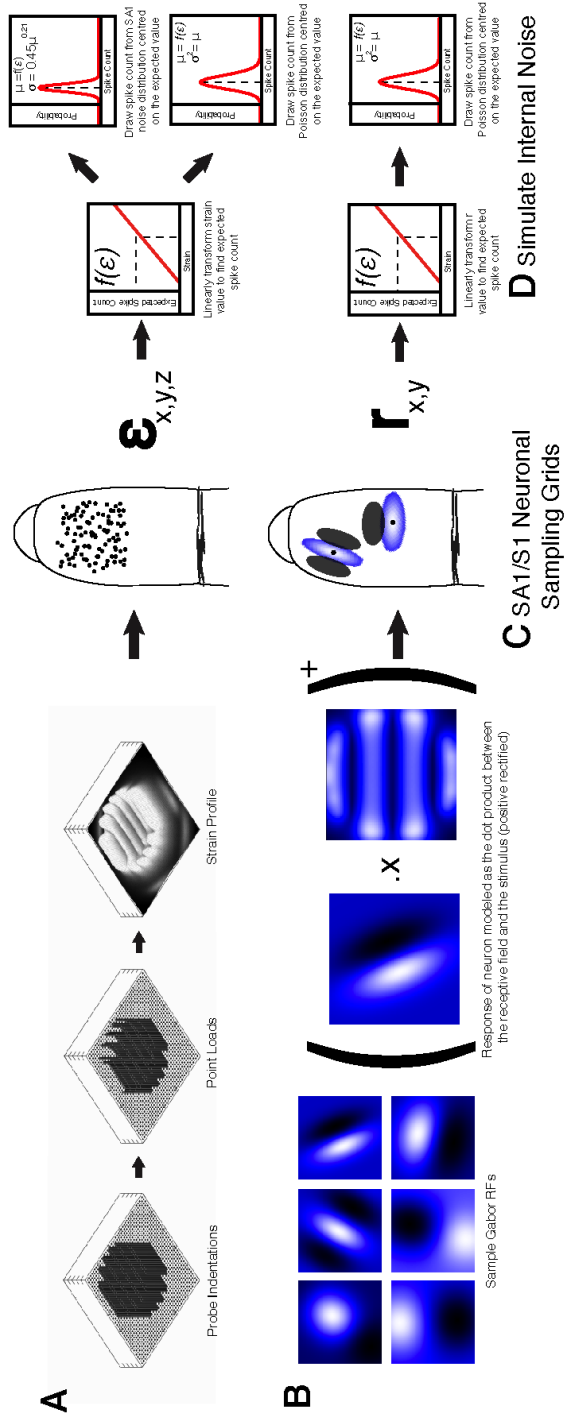


Figure 2

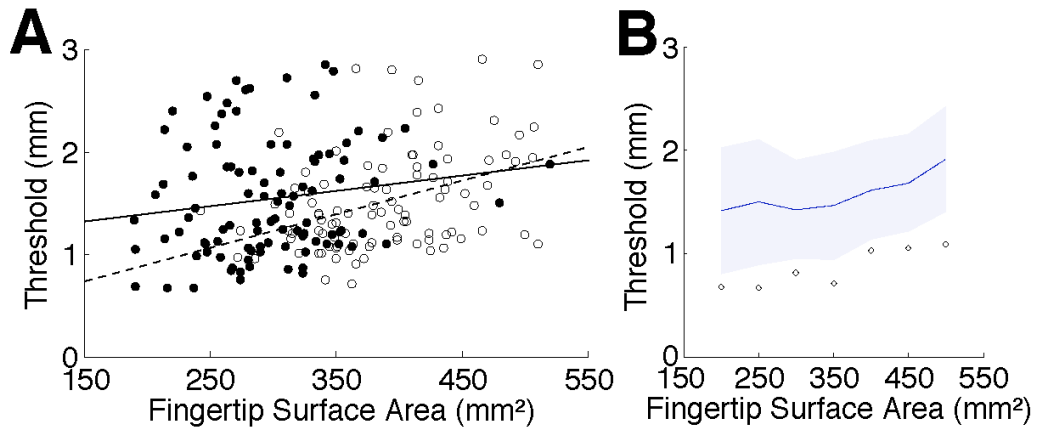


Figure 3

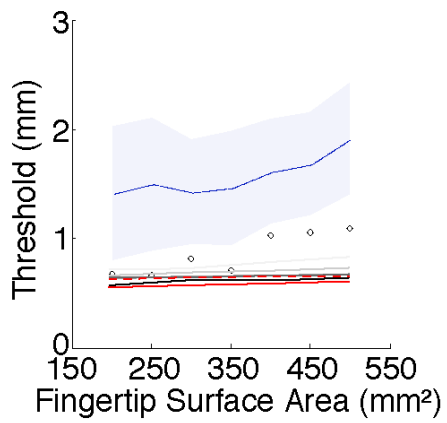


Figure 4

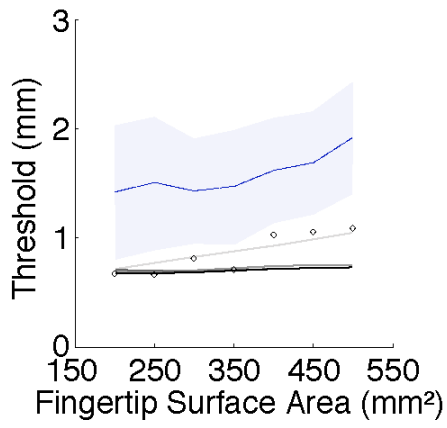


Figure 5

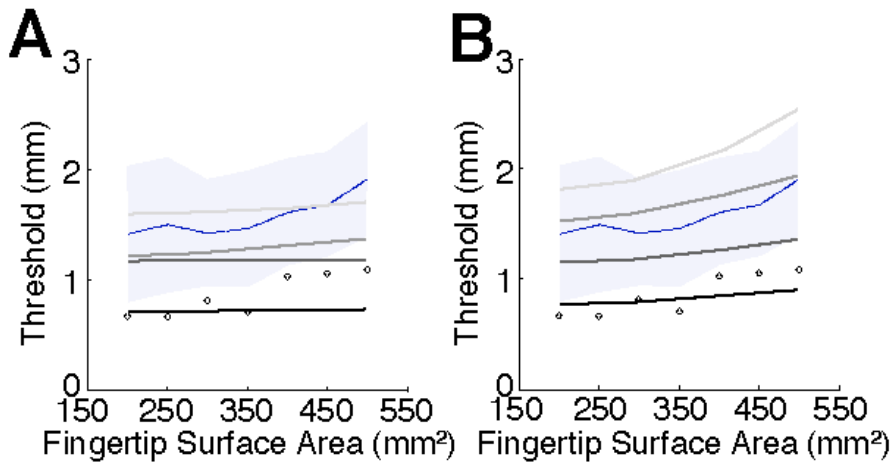
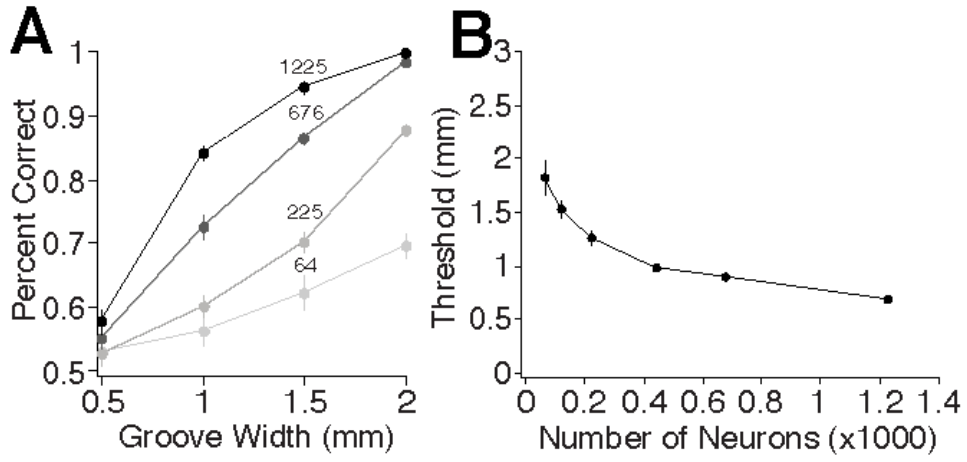


Figure 6



Chapter 5

General discussion

5.1 Summary of studies

The empirical and theoretical work presented herein is an accumulation of support for a novel source of variability in the sense of touch, namely, fingertip size. In Chapter 2, we first showed that fingertip size predicted tactile spatial acuity, and when included as a covariate, fully-explained the previously reported sex difference on the grating orientation task. In Chapter 3, we showed that this effect extends back into childhood, as fingertips grow to become their adult size. The introduction of fingertip size into the analysis in Chapter 3 also helped clarify the previously debated effect of age on tactile spatial acuity during childhood. We showed that when age was considered independently of fingertip size, it failed to predict tactile spatial acuity; however, when age was included together with fingertip size, age predicted a gradual improvement in acuity from childhood into young adulthood. Taken together, Chapter 3 argues for two concomitant influences on tactile spatial acuity during development: a gradual decline in acuity as fingertips grow, along with a simultaneous improvement in spatial acuity into young adulthood. We suggest that the degradation in tactile spatial acuity with fingertip growth is the result of a gradual reduction in peripheral afferent innervation density, as RFs span-out over an expanding surface area. Furthermore,

we suggest that the improvement in tactile spatial acuity with age is the result of enhanced processing efficiency in the CNS, likely through ongoing myelination of the somatosensory pathways (Sato et al., 1991), and experience dependent plasticity (Wong et al., 2011; Wong et al., 2013). Finally, in Chapter 4, we provide a theoretical basis for the fingertip size effect, and we show that this effect appears to be the by-product of sub-optimal decoding in human perception. We speculate on biologically plausible sources for this sub-optimality, and conclude that performance of the ideal-observer approaches human levels when neural responses grow more noisy, stimulus duration is reduced, and error is introduced into the ideal-observer's ability to “know” the neural response to expect, given the stimulus, which we accomplished by making the decoder slightly mistaken about the x - y positions of its neurons. Whether, and to what extent these factors limit real-world human perception remains to be determined empirically.

5.2 The neural basis of human tactile spatial acuity

5.2.1 Peripheral factors limiting acuity

Serving as our primary physical interface with the environment, the skin, our largest sensory apparatus, shapes the initial response of our nervous system to tactile stimuli. Information about tactile events occurring on the skin's surface gets extracted from the resulting spatiotemporal pattern of stress and/or strain within the tissue by specialized receptor end organs; thus, the skin plays a critical role in filtering peripheral afferent responses prior to sensory transduction. Several different mechanical models of the skin reveal that its viscoelastic properties

make it a spatial low-pass mechanical filter (Phillips & Johnson 1981c; Srinivasan & Dandekar, 1996; Gerling & Thomas, 2005; Gerling, 2006; Sripati et al., 2006; Gerling & Thomas, 2008; Lesniak & Gerling, 2009; Gerling, 2010), meaning the fine spatial detail in tissue stress and strain profiles caused by skin indentation becomes increasingly blurred at greater skin depths.

Excellent reviews exist detailing the roles and functions of the four cutaneous mechanoreceptive afferents (Johnson, 2001; Johnson, 2002), so I will only briefly review the role of SA1 afferents here, as they are the most relevant to performance on the grating orientation task. Several lines of evidence suggest that SA1 afferents provide the highest resolution spatial information, and subserve tactile form and texture perception for spatial details with periods larger than 200 microns (Johnson, 2001; Johnson, 2002; Hollins & Bensmaia, 2007). In the early 1980's, John Phillips and Kenneth Johnson (Johnson & Phillips, 1981; Phillips & Johnson, 1981a,b) demonstrated that SA1 afferents have greater spatial modulation in their responses than any other afferent type to bars and square-wave gratings indented into the fingertips of macaques (*Macaca nemestrina*). Phillips and Johnson also demonstrated that only the SA1 afferents could account for human psychophysical performance when discriminating spatially structured stimuli like edges and gratings; this is facilitated by the enhanced edge sensitivity of SA1 afferents (Phillips & Johnson, 1981a,b). Around the same time, Johansson et al., (1982) confirmed that human SA1 afferents are the most sensitive afferent type to edges indented into the skin; however, methodological differences

between the studies of Phillips & Johnson (1981a) and Johansson et al., (1982) made their results difficult to compare.

Anatomically, an SA1 afferent consists of an $A\beta$ primary afferent fiber, that ramifies 500 microns below the epidermis to innervate spatially distributed clusters and chain-like arrangements of 5 to 10 Merkel cells (Iggo & Andres, 1982; Lacour et al., 1991; Guinard et al., 1998; Gülçü et al., 2008; see Fig 1). Synaptic transmission remains to be demonstrated within these so-called Merkel cell-neurite complexes; however, intricate biomolecular transduction mechanisms that have been proposed are currently under investigation (e.g., see Lumpkin & Caterina, 2007). Whether or not Merkel cells are the actual transducers of tissue deformation is the topic of current debate in several recent articles and reviews (Mills & Diamond, 1995; Ogawa, 1996; Tachibana & Nawa, 2002; Boulais & Misery, 2007; Lucarz & Brand, 2007; Lumpkin & Caterina, 2007; Haeberle & Lumpkin, 2008; Lumpkin et al., 2010).

The main hypothesis put forth in this thesis – that fingertip size sets receptor density, and therefore predicts tactile spatial acuity – relies on the assumption that Merkel cell-neurite complexes are present with higher density in smaller fingertips. While this is true for Meissner's corpuscles (Dillon et al., 2001; Nolano et al., 2003), which are the receptor end organs for RA1 afferents, whether or not Merkel-cell neurite complexes pack more densely into the fingers of those with diminutive digits remains to be determined. Unlike Meissner's corpuscles which are easily visualized with light microscopy, Merkel cell-neurite complexes

are difficult to image anatomically, requiring immunofluorescent labelling to distinguish Merkel cells from other epidermal cells, and 3D reconstruction to track immunofluorescently labeled $A\beta$ primary afferent fibers, across serial sections. While 3D reconstructions of this sort have been accomplished previously with confocal imaging of individual human Merkel-cell neurite complexes from the fingertip (Guinard et al., 1998), never before have anatomists directly measured SA1 afferent innervation density in this fashion, much less tried to relate it to an individual's fingertip size. An estimate of the number of Merkel cells in fingertip epidermis exists: about 83 per mm^2 of skin surface (Lacour et al., 1991). Yet, no attempt has ever been made to relate these estimates to the underlying density of afferent fiber innervation. To directly measure SA1 density would require 3D reconstruction of the entire population of SA1 afferents, all the $A\beta$ afferents and the Merkel cells they innervate; however, this will likely prove technically challenging. Thus, our approach of using human psychophysics and computational modelling could prove the closest that neuroscience will come for some time to approximating the true relationship between body growth and SA1 afferent density.

5.2.2 Central factors limiting acuity

The central hypothesis of this thesis regards a peripheral source of individual variability in the sense of touch; however, the CNS's ability to process sensorineural information must also determine acuity to some extent.

Convergence and divergence of afferent inputs likely occurs to a certain

degree in the dorsal column nuclei (Pubols & Pubols, 1973), ventral posterior nuclear complexes of the thalamus (Mountcastle et al. 1969; Sinclair et al. 1991; Weiss et al. 2008), and in areas 3b and 1 of somatosensory cortex (Iwamura et al. 1983, Pei et al. 2009). Although the precise amount of convergence or divergence in these brain regions for humans remains unknown, one observation has consistently been reported in humans and other vertebrates: afferent type-specific pooling. This means that the afferent inputs converging onto the same post-synaptic neurons within the different sub-cortical nuclei all tend to be of the same mechanoreceptor receptor type (i.e. SA1 afferents with adjacent receptive fields tend to converge onto the same post-synaptic targets, RA1 afferents onto their own targets, and so on for the other afferent types). This type of convergence leads to the continued propagation of parallel somatosensory pathways, each subserved by its own mechanoreceptor type. Convergence of the different pathways onto the same post-synaptic targets is thought to first occur in cortex (Sripati et al. 2006; Hsiao & Yau, 2008; Pei et al., 2009).

The anatomical projections of mechanoreceptive thalamic neurons terminate predominantly in areas 3b and 1, and to a lesser extent in S2 (Hsiao & Yau, 2008; Pei et al., 2009). Unlike sub-cortical nuclei, the majority of neurons in S1 (areas 3b and 1) have both SA- and RA-type responses, most likely resulting from convergence of the largely independent “labelled lines” originating in SA and RA primary afferent populations (Pei et al., 2009). RFs of area 3b neurons for the finger representation of S1 occupy a single digit, with estimates of RF area

ranging from around 10 to 70 mm² (DiCarlo & Johnson, 1998; Sripati et al., 2006). Cutaneous information from areas 3b and 1 is passed along to S2, where RFs become larger, often spanning multiple digits (Fitzgerald et al., 2004; Fitzgerald et al., 2006b), and where RFs are modulated by selective attention much more than in S1 (Hyvärinen et al., 1980; Hsiao et al., 1993; Burton et al., 1997; Burton & Sinclair, 2000; Chapman & Meftah, 2005). From S2, cutaneous information gets passed along to the insular cortex, a frontal lobe region believed to be involved in higher order cognition and motor planning, as well as to area 7b, a parietal lobe region believed to be involved in visuotactile integration (Hsiao & Yau, 2008).

The prevailing viewpoint of early somatosensory processing is that of stimulus feature extraction. To accomplish the decomposition of multifaceted tactile events, early sensory areas deploy a diverse set of filters – each optimized to extract specific stimulus features, while remaining relatively insensitive to other stimulus features. For example, neuronal tuning in somatosensory cortex has been demonstrated for features such as the frequency of skin vibration (Mountcastle et al., 1969; Luna et al., 2005; Mackevicius et al., 2012; Harvey et al., 2013), the orientation of bars and edges (Bensmaia et al., 2008; Hsiao et al., 2002; Fitzgerald et al., 2006a), the roughness of surfaces (Burton & Sinclair, 1994; Sinclair et al., 1996), and the direction of motion (Pei et al., 2010; Pei et al., 2011). Furthermore, these tuning properties appear robust to changes in other stimulus parameters. For example, the orientation tuning of S1 neurons remained

the same regardless of whether single bar stimuli were scanned across, or indented into the skin (Bensmaia et al., 2008); similarly, the directional tuning of S1 neurons remained the same regardless of whether the tactile stimuli scanned across the skin were bars, dot patters, or random-dot stimuli (Pei et al., 2010).

For the case of spatial processing, it is interesting to note that a hallmark of early sensory areas is a transformation from a neural representation of the stimulus that is largely isomorphic (i.e. the spatial pattern of activation in somatosensory peripheral afferent and retinal ganglion cell populations resembles the encoded stimulus), into an increasingly abstract representation where patterns of activation might represent the (log) probabilities of stimulus parameters (Rao, 2004; Jazayeri & Movshon, 2006; Gold & Shadlen, 2007) in a multi-dimensional space. To encode many variables simultaneously, cortical sensory processing might utilize a sparse coding strategy, wherein only neurons that are particularly sensitive to a given stimulus parameter are harnessed for decision making (Olshausen & Field, 2004; Bensmaia et al., 2008; Jacobs, 2009). By honing-in on the most informative neurons for a given task through perceptual learning, the neural decoder will enhance its performance (Jacobs, 2009).

The results of Chapter 3 suggest that once fingertip growth is accounted for, the effect of age from childhood into young adulthood is that of a gradual improvement in tactile spatial acuity. We speculate that this improvement with age is likely the byproduct of increased efficiency on behalf of the CNS to process sensorineural information. Based on what little is known about somatosensory

processing, there are a number of potential neural mechanisms by which spatial acuity might improve during development. For instance, the myelination process is known to continue into puberty (Sato et al., 1991); thus, when myelination is incomplete, synchronous transmission of an isomorphic neural image supplied by the peripheral afferents will be disrupted due to large differences in conduction velocity between fibers. Additionally, neurons in S1, for example, might be more broadly tuned to crucial (i.e., ecologically relevant) stimulus parameters in childhood; only through experience-dependent plasticity occurring over age might they reach an adult level of tuning sharpness, reducing the disruptive effect of internal noise inherent in neural responses.

Improvements in tactile spatial acuity could be effected by increased processing efficiency of the neural decoder, enhancing its ability to utilize more of the sensorineural information available (for a discussion of efficiency within the context of ideal observer analysis, see Geisler, 2003). At an information processing level, this may involve an enhancement of central signal strength (Gold et al., 1999), a reduction of noise (Doshier & Lu, 1998), or both. More research is needed to tease apart these competing hypothesis regarding the neural basis of improvement in tactile spatial acuity occurring from childhood into young adulthood.

5.3 Implications & Future Directions

The measurement of tactile spatial acuity can be traced back about 180 years to Weber's first empirical work in 1834; since then, researchers have used

tactile spatial acuity to probe a wide variety of topics ranging from neurological disorders (Grant et al., 1999; 2005; Wingert et al., 2008), to the development of tactile spatial acuity in children, and its relation to manual dexterity (Bleyenheuft et al., 2006; 2010), to tactile perceptual learning (Sathian & Zangaladze, 1997; Wong et al., 2013), and the enhanced tactile acuity of blind individuals (Goldreich & Kanics, 2003; Wong et al., 2011). One broad implication of the research presented in this thesis is that, had tactile researchers making comparisons between different participant groups controlled for fingertip size along with age as covariates, they would have been able to make stronger comparisons. Another is that, however alluring, differences in perceptual abilities between the sexes need to be considered in light of simple anatomical differences that vary continuously (e.g., fingertip size), prior to concluding that sex alone is causing the effect.

Future directions for the research presented here include: 1) the investigation of still more potential sources of variability in the sense of touch, as unaccounted variability persists even after taking into account fingertip size and age, 2) the longitudinal measurement of tactile spatial acuity and fingertip growth in the same children, to further examine the relationship between these variables during childhood, 3) the direct anatomical measurement of innervation density for the four different afferent classes innervating the body surface, and the amount of variability between different individuals, and lastly, 4) the further development and empirical validation of the Bayesian modelling framework presented in Chapter 4.

5.4 Conclusion

In conclusion, we have provided consistent support for the effect of fingertip size on tactile spatial acuity. This insight has helped us to understand the nature of the previously reported sex difference in tactile spatial acuity, as well as the influence of age on tactile spatial acuity from childhood into young adulthood.

5.5 References

- Bensmaia SJ, Denchev PV, Dammann III JF, Craig JC & Hsiao et al. (2008). The representation of stimulus orientation in the early stages of somatosensory processing. *The Journal of Neuroscience*. 28: 776–786.
- Bleyenheuft Y, Cols C, Arnould C, & Thonnard JL (2006). Age-related changes in tactile spatial resolution from 6 to 16 years old. *Somatosensory and Motor Research*. 23: 83–87.
- Bleyenheuft Y, Wilmotte P & Thonnard JL (2010). Relationship between tactile spatial resolution and digital dexterity during childhood. *Somatosensory and Motor Research*. 27: 9–14.
- Boulais N & Misery L (2007). Merkel cells. *Journal of the American Academy of Dermatology*. 57: 147–165.
- Burton H & Sinclair RJ (1994). Representation of tactile roughness in thalamus and somatosensory cortex. *Canadian Journal of Physiology and Pharmacology*. 72: 546–557.
- Burton H, Sinclair RJ, Hong SY, Pruett Jr. JR & Whang KC (1997). Tactile-spatial and cross-modal attention effects in the second somatosensory and 7b cortical areas of rhesus monkeys. *Somatosensory & Motor Research*. 14: 237–267.
- Burton H & Sinclair RJ (2000). Tactile-spatial and cross-modal attention effects in the primary somatosensory cortical areas 3b and 1-2 of rhesus monkeys. *Somatosensory & Motor Research*. 17: 213–228.

- Chapman CE & Meftah E (2005). Independent controls of attentional influences in primary and secondary somatosensory cortex. *Journal of Neurophysiology*. 94: 4094–4107.
- DiCarlo JJ, Johnson KO & Hsiao SS (1998). Structure of receptive fields in area 3b of primary somatosensory cortex in the alert monkey. *The Journal of Neuroscience*. 18: 2626–2645.
- Dillon YK, Haynes J & Henneberg M (2001). The relationship of the number of Meissner's corpuscles to dermatoglyphic characters and finger size. *Journal of Anatomy*. 199: 577–584.
- Dosher BA & Lu ZL (1998). Perceptual learning reflects external noise filtering and internal noise reduction through channel reweighting. *Proceedings of the National Academy of Sciences*. 95: 13988–13993.
- Fitzgerald PJ, Lane J, Thakur PH & Hsiao SS (2004). Receptive field properties of the Macaque second somatosensory cortex: evidence for multiple functional representations. *The Journal of Neuroscience*. 24: 11193–11204.
- Fitzgerald PJ, Lane JW, Thakur PH & Hsiao SS (2006a). Receptive field properties of the macaque second somatosensory cortex: representation of orientation on different finger pads. *The Journal of Neuroscience*. 26: 6473–6484.
- Fitzgerald PJ, Lane JW, Thakur PH & Hsiao S (2006b). Receptive field (RF) properties of the macaque second somatosensory cortex: RF size, shape,

and somatotopic organization. *The Journal of Neuroscience*. 26: 6485–6495.

Geisler WS (2003) in *The Visual Neurosciences*, edited by Chalupa LM, Werner JS. MIT Press, Cambridge: 825–838.

Gerling GJ & Thomas GW (2005). The effect of fingertip microstructures on tactile edge perception. In *Eurohaptics Conference and Symposium on Haptic Interfaces for Virtual Environment and Teleoperator Systems. World Haptics 2005*. IEEE: 63–72.

Gerling GJ (2006). The sampling position within, not the undulating geometry of, fingertip skin microstructure may amplify the sensation of edges. In *Haptic Interfaces for Virtual Environment and Teleoperator Systems*. IEEE: 141–145.

Gerling GJ & Thomas GW (2008). Fingerprint lines may not directly affect SA-I mechanoreceptor response. *Somatosensory and Motor Research*. 25: 61–76.

Gerling GJ (2010). SA-I mechanoreceptor position in fingertip skin may impact sensitivity to edge stimuli. *Applied Bionics and Biomechanics*. 7: 19–29.

Gold J, Bennett PJ & Sekuler AB (1999). Signal but not noise changes with perceptual learning. *Nature*. 402: 176–178.

Gold JI & Shadlen MN (2007). The neural basis of decision making. *Annual Review of Neuroscience*. 30: 535–574.

Goldreich D & Kanics IM (2003). Tactile acuity is enhanced in blindness.

Journal of Neuroscience. 23: 3439–3445.

- Gülçü B, Mahoney GK, Pawson LJ, Pack AK, Smith RL & Bolanowski SJ (2008). Localization of Merkel cells in the monkey skin: an anatomical model. *Somatosensory and Motor Research*. 25: 123–138.
- Guinard D, Usson Y, Guillermet C & Saxod R (1998). Merkel complexes of human digital skin: three-dimensional imaging with confocal laser microscopy and double immunofluorescence. *The Journal of Comparative Neurology*. 398: 98–104.
- Grant AC, Zangaladze A, Thiagarajah MC & Sathian K (1999). Tactile perception in developmental dyslexia: a psychophysical study using gratings. *Neuropsychologia*. 37: 1201–1211.
- Grant AC, Henry TR, Fernandez R, Hill MA & Sathian K (2005). Somatosensory processing is impaired in temporal lobe epilepsy. *Epilepsia*. 46: 534–539.
- Haeberle H & Lumpkin EA (2008). Merkel cells in somatosensation. *Chemosensory Perception*. 1: 110–118.
- Harvey MA, Saal HP, Dammann JF & Bensmaia SJ (2013). Multiplexing stimulus information through rate and temporal codes in primate somatosensory cortex. *Public Library of Science Biology*. 11: e1001558.
- Hollins M & Bensmaia SJ (2007). The coding of roughness. *Canadian Journal of Experimental Psychology*. 61: 184–195.
- Hsiao SS, Lane J & Fitzgerald P (2002). Representation of orientation in the

- somatosensory system. *Behavioural Brain Research*. 135: 93–103.
- Hsiao SS, O'Shaughnessy DM & Johnson KO (1993). Effects of selective attention on spatial form processing in monkey primary and secondary somatosensory cortex. *Journal of Neurophysiology*. 70: 444–447.
- Hsiao SS & Yau JM (2008). Neural basis of tactile sensation. In: Human Haptic Perception: Basics and Applications, edited by Grunwald M. *Leipzig, Germany: Birkhäuser Verlag*: 103–112.
- Hyvärinen J, Poranen A & Jokinen Y (1980). Influence of attentive behaviour on neuronal responses to vibration in primary somatosensory cortex of the monkey. *Journal of Neurophysiology*. 43: 870–882.
- Iggo A & Andres KH (1982). Morphology of cutaneous receptors. *Annual Review of Neuroscience*. 5: 1–31.
- Iwamura Y, Tanaka M, Sakamoto M & Hikosaka O (1983). Converging patterns of finger representation and complex response properties of neurons in area 1 of the first somatosensory cortex of the conscious monkey. *Experimental Brain Research*. 51: 327–337.
- Jacobs RA (2009). Adaptive precision pooling of model neuron activities predicts the efficiency of human visual learning. *Journal of Vision*. 9: 1–15.
- Jazayeri M & Movshon JA (2006). Optimal representation of sensory information by neural populations. *Nature Neuroscience*. 9: 690–696.
- Johansson RS, Landström U & Lundström R (1982). Sensitivity to edges of mechanoreceptive afferent units innervating the glabrous skin of the human

hand. *Brain Research*. 244: 27–32.

Johnson KO (2001). The roles and functions of cutaneous mechanoreceptors.

Current Opinion in Neurobiology. 11: 455–461.

Johnson KO (2002). Neural basis of haptic perception. In *Steven's Handbook of Experimental Psychology, 3rd Ed.* Edited by Pashler H & Yantis S. Vol 1: *Sensation and Perception*. New York. Wiley: 537–583.

Johnson KO & Phillips JR (1981). Tactile spatial resolution. I.

Two-point discrimination, gap detection, grating resolution, and letter recognition. *Journal of Neurophysiology*. 46: 1177–1191.

Lacour JP, Dubois D, Pisani A & Ortonne JP (1991). Anatomical mapping of Merkel cells in normal human adult epidermis. *British Journal of Dermatology*. 125: 535–542.

Lesniak DR & Gerling GJ (2009). Predicting SA-I mechanoreceptor spike times with a skin-neuron model. *Mathematical Biosciences*. 220: 15–23.

Lucarz A & Brand G (2007). Current considerations about Merkel cells.

European Journal of Cell Biology. 86: 243–251.

Lumpkin EA & Caterina MJ (2007). Mechanisms of sensory transduction in the skin. *Nature*. 445: 858–865.

Lumpkin EA, Marshall KL & Nelson AM (2010). The cell biology of touch. *The Journal of Cell Biology*. 191: 237–248.

Luna R, Hernandez A, Brody CD & Romo R (2005). Neural codes for perceptual discrimination in primary somatosensory cortex. *Nature Neuroscience*. 8:

1210–1219.

Mackevicius EL, Best MD, Saal HP & Bensmaia SJ (2012). Millisecond precision spike timing shapes tactile perception. *The Journal of Neuroscience*. 32: 15309–15317.

Mills LR & Diamond J (1995). Merkel cells are not the mechanosensory transducers in the touch dome of the rat. *Journal of Neurocytology*. 24: 117–134.

Mountcastle VB, Talbot WH, Sakata H & Hyvarinen J (1969). Cortical neuronal mechanisms in flutter-vibration studied in unanesthetized monkeys: neuronal periodicity and frequency discrimination. *Journal of Neurophysiology*. 32: 452–484.

Nolano M, Provitiera V, Crisci C, Stancanelli A, Wendelschafer-Crabb G, Kennedy WR & Santoro L (2003). Quantification of myelinated endings and mechanoreceptors in human digital skin. *Annals of Neurology*. 54: 197–205.

Ogawa H (1996). The Merkel cell as a possible mechanoreceptor cell. *Progress in Neurobiology*. 49: 317–334.

Olshausen BA & Field DJ (2004). Sparse coding of sensory inputs. *Current Opinion in Neurobiology*. 14: 481–487.

Pei Y, Denchev PV, Hsiao SS, Craig JC & Bensmaia SJ (2009). Convergence of submodality-specific input onto neurons in primary somatosensory cortex. *Journal of Neurophysiology*. 102: 1843–1853.

- Pei Y, Hsiao SS, Craig JC & Bensmaia SJ (2010). Shape invariant coding of motion direction in somatosensory cortex. *Public Library of Science Biology*. 8: e1000305.
- Pei Y, Hsiao SS, Craig JC & Bensmaia SJ (2011). Neural mechanisms of tactile motion integration in somatosensory cortex. *Neuron*. 69: 536–547.
- Phillips JR & Johnson KO (1981a). Tactile spatial resolution. II. Neural representation of bars, edges, and gratings in monkey primary afferents. *Journal of Neurophysiology*. 46: 1192–1203.
- Phillips JR & Johnson KO (1981b). Tactile spatial resolution. III. A continuum mechanics model of skin predicting mechanoreceptor responses to bars, edges, and gratings. *Journal of Neurophysiology*. 46: 1204–1225.
- Pubols LM & Pubols BH (1973). Modality composition and functional characteristics of dorsal column mechanoreceptive afferent fibers innervating the raccoon's forepaw. *Journal of Neurophysiology*. 36: 1023–1037.
- Rao RPN (2004). Bayesian Computation in Recurrent Neural Circuits. *Neural Computation*. 16: 1–38.
- Sato S, Ogihara Y, Hiraga K, Nishijima A & Hidano A (1977). Fine structure of unmyelinated nerves in neonatal skin. *Journal of Cutaneous Pathology*. 4: 1–8.
- Sathian K & Zangaladze A (1997). Tactile learning is task specific but transfers between fingers. *Perception & Psychophysics*. 59: 119–128.

- Sinclair RJ, Pruett Jr., JR, & Burton H (1996). Responses in primary somatosensory cortex of rhesus monkeys to controlled application of embossed grating and bar patterns. *Somatosensory and Motor Research*. 13: 287–306.
- Sinclair RJ, Sathian K & Burton H (1991). Neuronal responses in ventroposterolateral nucleus of thalamus in monkeys (*Macaca mulatta*) during active touch of gratings. *Somatosensory and Motor Research*. 8: 293–300.
- Srinivasan MA and Dandekar K (1996). An investigation of the mechanics of tactile sense using two-dimensional models of the primate fingertip. *Journal of Biomechanical Engineering*. 118: 48–55.
- Sripati AP, Yoshioka T, Denchev P, Hsiao SS & Johnson KO (2006). Spatiotemporal receptive fields of peripheral afferents and cortical area 3b and 1 neurons in the primate somatosensory system. *The Journal of Neuroscience*. 27: 2101–2114.
- Tachibana T & Nawa T (2002). Recent progress in studies on Merkel cell biology. *Anatomical Science International*. 77: 26–33.
- Weber EH (1834). *De tactu*. Koehler, Leipzig.
- Weiss N, Ohara S, Johnson KO & Lenz FA (2009). The human thalamic somatic sensory nucleus [Ventral caudal (Vc)] shows neuronal mechanoreceptor-like responses to optimal stimuli for peripheral mechanoreceptors. *Journal of Neurophysiology*. 101: 1033–1042.

- Wingert JR, Burton H, Sinclair RJ, Brunstrom JE & Damiano DL (2008). Tactile sensory abilities in cerebral palsy: deficits in roughness and object discrimination. *Developmental Medical Child Neurology*. 50: 832–838.
- Wong M, Gnanakumaran V & Goldreich D (2011). Tactile spatial acuity enhancement in blindness: evidence for experience-dependent mechanisms. *The Journal of Neuroscience*. 31: 7028 –7037.
- Wong M, Peters RM, Goldreich D (2013). A physical constraint on perceptual learning: Tactile spatial acuity improves with training to a limit set by finger size. *The Journal of Neuroscience*. 33: 9345–9352.